NASA CONTRACTOR REPORT

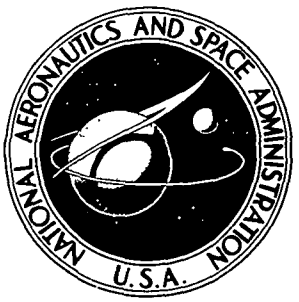

NASA CR-2331

NASA CR-2331

FLUTTER ANALYSIS AND TESTING OF PAIRS OF AERODYNAMICALLY INTERFERING DELTA WINGS

by Richard R. Chipman and Frank J. Rauch

Prepared by
GRUMMAN AEROSPACE CORPORATION
Bethpage, N.Y. 11714
for Langley Research Center

NATIONAL AERONAUTICS AND SPACE ADMINISTRATION • WASHINGTON, D. C. • NOVEMBER 1973

1. Report No. NASA CR-2331	2. Government Accession No.	3. Recipient's Catalog No.
4. Title and Subtitle FLUTTER ANALYSIS AND TESTING OF PAIRS OF AERODYNAMICALLY INTERFERING DELTA WINGS		5. Report Date November 1973 6. Performing Organization Code
7. Author(s) Richard R. Chipman and Frank J. Rauch		8. Performing Organization Report No.
9. Performing Organization Name and Address Grumman Aerospace Corporation Bethpage, N. Y.		10. Work Unit No. 502-32-02-03 11. Contract or Grant No. NAS1-10635-7
12. Sponsoring Agency Name and Address National Aeronautic and Space Administration Washington, D.C. 20546		13. Type of Report and Period Covered Contractor Report 14. Sponsoring Agency Code

15. Supplementary Notes

This is a final report.

16. Abstract

To examine the effect on flutter of the aerodynamic interference between pairs of closely spaced delta wings, several structurally uncoupled 1/80th-scale models were studied by experiment and analysis. Flutter test boundaries run in the NASA Langley 26-in. Transonic Blowdown Wind Tunnel were compared with subsonic analytical results generated using the doublet lattice method. Trends for several combinations of vertical and longitudinal wing separation showed that flutter speeds can be significantly lowered in closely spaced configurations. For some configurations, a new flutter mechanism, characterized by coupling of the flexible modes from both surfaces at a distinctive flutter frequency, was predicted and observed.

17. Key Words (Suggested by Author(s))	18. Distribution Statement
Flutter of interfering delta wings Subsonic and transonic tests Subsonic flutter analysis	Unclassified - Unlimited

19. Security Classif. (of this report)	20. Security Classif. (of this page)	21. No. of Pages	22. Price*
Unclassified	Unclassified	93	Domestic, $3.75 Foreign, $6.25

*For sale by the National Technical Information Service, Springfield, Virginia 22151

FLUTTER ANALYSIS AND TESTING OF PAIRS OF AERODYNAMICALLY INTERFERING DELTA WINGS

By Richard Chipman and Frank Rauch
Grumman Aerospace Corporation

SUMMARY

To examine the effect on flutter of the aerodynamic interference between pairs of closely spaced delta wings, several structurally uncoupled 1/80th-scale models were studied by experiment and analysis. Flutter test boundaries run in the NASA Langley 26-in. Transonic Blowdown Wind Tunnel were compared with subsonic analytical results generated using the doublet lattice method. Trends for several combinations of vertical and longitudinal wing separation showed that flutter speeds can be significantly lowered in closely spaced configurations. For some configurations, a new flutter mechanism, characterized by coupling of the flexible modes from both surfaces at a distinctive flutter frequency, was predicted and observed.

INTRODUCTION

The aerodynamic interaction of lifting surfaces in proximity can create aerodynamic forces sufficient to destabilize surfaces otherwise flutter-free within their flight envelope. This problem on various aircraft designs has stimulated the efforts of several investigators: T-tail flutter was found to be a problem by Stahle (ref. 1). To predict unsteady aerodynamic loads on a T-tail, Stark (ref. 2) subsequently developed a subsonic nonplanar doublet-lattice theory. Similarly, Laschka (ref. 3) extended the so called kernel function method to multiple coplanar surfaces. Experiments reported by Topp et al. (ref. 4) showed a dramatic degradation in the flutter speed of a variable sweep aircraft, due to aerodynamic and structural coupling of the wing, tail, and fuselage. Only by accounting for aerodynamic interference between the wing and tail, could this trend be calculated (ref. 5). Exploring

this phenomenum in depth, Mykytow et al.(ref. 6) conducted flutter tests on a wing-fuselage-tail model and correlated findings with predictions made using both doublet-lattice and kernel function methods developed by Albano and Rodden (ref. 7 and 8). Using structurally coupled modes in the analysis of a similar configuration, Triplett et al.(ref. 9) showed that the flutter mechanism could go entirely undetected if aerodynamic forces were calculated on both the wing and tail without including their aerodynamic interference.

More recently the problem of interference flutter was of concern on fly-back booster space shuttle configurations. Wind tunnel tests conducted by the NASA Langley Research Center on pairs of equally sized low-sweep wings indicated that close proximity could severely affect the flutter boundary (ref. 10).

To determine the effect of close spacing on unequally sized, highly swept delta wings, a joint analytical and experimental study was performed on pairs of 1/80th-scale shuttle wings. Specifically, various delta wing models were designed, fabricated, and analyzed, and were tested at the Langley Research Center's 26-inch Transonic Blowdown Wind Tunnel. For various horizontal and vertical separations of the leading and trailing wings, test flutter boundaries were determined for the Mach number range of 0.6 to 1.4. These were compared for subsonic flow with trends derived from the application of the doublet lattice method (ref. 11), which had been used successfully to predict interference flutter on the aforementioned low-sweep wings (ref. 13). The results of this test program and the comparison with theory are the basis of this report.

Many individuals at Grumman contributed to the work reported herein. The authors wish especially to acknowledge the efforts of Messrs. E. Pasyanos and P. Kelly for assisting in the performance of the analyses, Mr. D. Marco for designing the wings and mounting block, Messrs. M. Shapiro and J. Markowitz for aid in automating the test data reduction process, and Mr. J. Smedfjeld for technical supervision and criticism.

SYMBOLS

a	complex aerodynamic operator matrix, N/m
b	wing semichord, m
b_r	reference semichord of trailing wing, m
c	mean aerodynamic chord of leading wing, m
f	frequency, Hz
g	damping
h	biplanar (vertical) wing separation, m
k	stiffness matrix, N/m
ℓ	streamwise (longitudinal) wing separation, m
m	mass matrix, kg
m_w	mass of wing, kg
M	Mach number
q	dynamic pressure, N/m^2
q_{adj}	dynamic pressure adjusted for deviations in model stiffnesses, N/m^2
v_w	volume of a conical frustum surrounding the wing with its root chord as the base diameter, tip chord as the top diameter, and semispan as the height, m^3
V	free-stream velocity, m/sec
V_f	flutter velocity, m/sec
$V_f(\infty)$	V_f of flutter-critical isolated wing, m/sec
$V_f(h,\ell)$	V_f of a configuration with biplanar and streamwise separations, h and ℓ, m/sec
F.S.I.	flutter speed index = $\dfrac{V_f}{b_r \omega_r \sqrt{\mu}}$

ζ displacement vector of the degrees of freedom

μ mass density $= \dfrac{m_w}{\sigma \rho_{sl} V_w}$

ρ_{sl} air density at sea level, kg/m^3

σ ratio of air density in tunnel to that at sea level

ω_f flutter frequency, rad/sec

ω_r reference frequency, rad/sec

MODELS

General Description and Design Technique

The models used in this investigation were 1/80th-scale semispan plate models based on typical configurations considered during preliminary shuttle studies. The basic design for both the leading (orbiter) and the trailing (booster) wings was a cropped delta with a 60° sweep and an aspect ratio of 0.794. The trailing wing has a fifty percent greater chord and span than the leading wing. As shown in figures 1 and 2, each model consisted of a homogeneous aluminum alloy core plate with cut-outs designed to provide a realistic torsion-to-bending frequency ratio. The core plates had a constant thickness of 1.78mm (0.070 in.) and 2.54mm (0.100 in.) for the leading and trailing wing, respectively. An 8% airfoil profile was obtained by bonding, to each core, end-grain balsa wood with a thin mylar covering. The leading wing was equipped with a full-span control surface with sets of interchangeable hinges of various stiffnesses made of thin strips of beryllium copper. A section of the wing is shown in figure 3. By a simple change of hinges, the control surface could alternately be set at one of two selected stiffnesses: With the first (stiff) set, the leading wing would have a flutter boundary higher in dynamic pressure than that of the isolated trailing wing. With the second (flexible) set, the leading wing boundary would be about the same as that of the trailing wing.

To assure the flutter boundary would be within the tunnel operating range, mode shapes and frequencies were measured on a preliminary set of models (using techniques described below in the section on Ground Vibration Survey) and preliminary flutter analyses were run using these data.

Model Designations

A total of 13 models were used during the investigation -- seven of the orbiter wing and six of the booster wing. The designs for these models were designated by codes, as shown in Table I, identifying the stiffness level of the plate and the spring rate of the control-surface flexures in the case of the orbiter models. Additionally, each individual model was assigned a number. For example, a model designation of 070/032-1 would represent orbiter model #1 with a plate thickness of .070 in. (determining the overall stiffness level) and control surface flexures .032 in. thick (determining spring rate).

Mounting Block

To provide variations in the streamwise and vertical wing separations without introducing structural coupling, a rigid mounting block with various slots was made. The tangs of the wings were clamped into the desired slots and the entire assembly was bolted to a holding block and its affixed splitter plate, which were fastened to the wind tunnel wall. A typical installation is shown in figure 4.

TESTING

Ground Vibration Survey

Prior to wind tunnel installation, one model of each of the three types was subjected to a vibration survey to determine its resonant frequencies and associated mode shapes. The models were mounted on the tunnel mounting block and solidly clamped to a stand, to simulate the root condition of the tunnel installation. To check similarity between subsequent models of each type, a survey of the frequencies and node line locations was made.

To obtain accurate resonant frequencies and distortion-free mode shapes, noncontacting measurement and excitation systems were used. An air shaker consisting of an exponential cone attached to the front of a 10 cm diameter speaker was used to excite the modes. A noncontacting inductance-type pickup, sensitive to the separation between the pickup coil and metallic surface, was used to measure vibration amplitude. Mode shape measurement points are listed in Table II. Figures 5 through 7 present the mode shape data in tabular and graphic form for design 070/032, 070/040 and 100. Mass distributions were calculated for the designs and are given in Table III.

Wind Tunnel

Flutter tests were conducted in the NASA Langley Research Center 26-inch Transonic Blowdown Wind Tunnel for a Mach number range of 0.6 to 1.4. One hundred and ninety tunnel runs were made to obtain flutter boundaries for the pairing of each of the two leading wings with the trailing wing at the various horizontal and vertical separations shown in Table IV. Additionally, boundaries for each of the three isolated wings were obtained.

Instrumentation

Each model was instrumented with eight strain gages grouped in two four-arm bridges, as shown in figures 1 and 2. Through their response to bending and torsional motions, these bridges were used to detect the onset of flutter and to measure flutter frequency. Models with control surfaces were additionally equipped with a solenoid having its coil and core plug on opposite sides of the hinge line to detect elevon rotation. An 18 channel oscillograph was used to record the following items:

(1) Output of model strain gage and magnetic coil circuits
(2) Total test section pressure (P_o)
(3) Total test section temperature (T_o)
(4) Static test section pressure (P_s)
(5) Reference trace used in determining P_o, P_s and T_o trace deflection
(6) Movie camera correlation trace

A high speed movie camera was used to obtain a visual record of model behavior during the tunnel runs.

Test Procedures

Before each tunnel run, the models were visually examined for signs of damage due to previous runs. To confirm model integrity after installation, each model was excited and oscillograph records of the strain gage outputs were monitored to check the frequencies and dampings of the first three modes. These frequencies are presented in Table V.

On the basis of the results of previous runs, a desired tunnel operating path was selected for the run. Appropriate tunnel adjustments were made including:

(1) Setting the gate valve which determines the ultimate desired Mach number for the test run.

(2) Programming the rate of increase of dynamic pressure and Mach number in the test section.

Instrumentation calibrations and checks were performed and the test run begun. The selected path was followed until either the tunnel air supply was exhausted or flutter was detected visually. High speed films were taken during the runs to record any dynamic instability encountered. After the run, the models were inspected and modal frequencies checked to detect any model damage. Several runs following different paths were made on each configuration to determine a boundary of flutter speed vs. Mach number.

Data Reduction and Presentation

Flutter points were initially determined from the oscillograph record and visual observations during the run, and then either confirmed or adjusted by subsequent reduction of the movie data. The flutter point was taken as the point during the run where the model(s) circuit traces indicated a frequency regularity and/or significant increase in the model vibrational amplitude. Tunnel data converted to the parameters Mach number, air density ratio, and dynamic pressures are presented in Table VI.

For each flutter point (or significant stable point), the Mach number and dynamic pressure are presented as coded symbols in figure 8. Since in many cases different sets of models were used to define the flutter boundary of a particular configuration, it was deemed necessary to adjust for the slight stiffness differences between models. Since for these delta wings the modes are highly coupled, the more conventional practice of correcting q based on only the torsional frequency was found to be unsatisfactory. The squares of the first and second modal frequencies are approximately proportional to bending and torsional stiffnesses of the wing; hence, an overall stiffness level correction was assumed to be given by the average of the ratio of each frequency to its respective norm. The dynamic pressure of each test point was adjusted by this assumed stiffness correction:

$$q_{adj} = \tfrac{1}{2}\left[\left(\frac{f_{R1}}{f_{m1}}\right)^2 + \left(\frac{f_{R2}}{f_{m2}}\right)^2\right] q_{test},$$

where f_{m1} and f_{m2} are the first two modal frequencies measured on a model during its pre-run, and f_{R1} and f_{R2} are the nominal values of the first two modal frequencies of that type wing. The nominal (reference) frequencies are recorded in Table I and were chosen for each of the three model types after inspecting the entire set of pre-run frequency checks shown in Table V. For a test run involving paired orbiter and booster wings, two adjustments are possible: one based on the deviation of the orbiter stiffness from the nominal value as revealed through its pre-run modal frequencies and one based on that of the booster. Both adjustments are presented in Table VI for each test point. To avoid confusion from an overabundance of symbols, only the unadjusted dynamic pressures are plotted in figure 8. The test flutter boundaries in this figure, however, are drawn with the adjusted values in mind and, hence, do not always pass through the unadjusted symbols. Furthermore, since two adjustments are possible, two boundaries are presented in configurations where the adjusted values are significantly different from one another - as in figure 8(e).

Using the semichord, mass density, and nominal torsional frequency of the booster as common reference parameters, flutter speed indices were calculated from the adjusted dynamic pressure for each test point. Together with flutter frequency indices and mass density ratios, flutter speed indices are presented in Table VI and plotted as a function of Mach number in figure 9 for each configuration.

In addition to data presented in Table VI and figures 8 and 9, several non-flutter points during each run were studied to determine the tunnel path taken during the run. These paths are plotted in figure 8 to help define the suggested flutter boundaries.

Test Results

Shown in figures 8 (a) - (c) are the dynamic pressures for the three isolated delta wing models. The flutter boundary of each has a relatively shallow transonic dip characteristic of delta wings -- equivalent to 11%, 10% and 6% decrease in flutter speed relative to the flutter speed at M = 0.75 for the 100, 070/040 and 070/032 respectively. A sharp recovery in flutter speed is common to all three wings, and both control-surface models exhibit what appears to be a buzz region at low supersonic Mach numbers. The variation of flutter frequency with M is shown in figures 9 (a) - (c). It is seen that a more pronounced variation is exhibited by the 100 wing.

Testing of the 100 delta, paired with each of the two 070 deltas, was performed for the separations indicated in Table IV. Results are plotted in figures 8 (d) - (m) and 9 (d) - (m). Two types of interference effects were observed. The first was simply the alteration of the flutter speed(s) of one or both surfaces with each surface retaining its unique flutter frequency, while the second was a new mechanism characterized by the coupled flutter of both surfaces at a new, common frequency and an altered flutter speed. Films of this mechanism in one case show the surfaces oscillating 180° out of phase; and upon the flutter destruction of one surface, the other surface can be seen to stabilize.

In figure 10, for each configuration, the ratio of the minimum flutter speed in the transonic dip region to that of the more flutter-critical isolated

wing is plotted as a function of streamwise and vertical separation between wing apexes. For interfering configurations, only the minimum flutter speed of the flutter critical wing could be determined, since wind tunnel excursions much above the boundary of the flutter critical wing could result in its destruction. The Mach number at which the minimum flutter speed occurs is plotted as a function of wing separation in figure 11.

For configurations pairing the 070/032 with the 100 delta wing, figure 10 reveals that the subsonic flutter speed of the flutter critical leading wing is reduced by as much as 15%. In the 070/040 - 100 pairings, the flutter speed of the flutter critical trailing wing is generally increased but only by moderate amounts - 6% maximum. Although not shown on this figure, the flutter speed of the leading wing has decreased.

Further inspection of the 070/032 - 100 flutter data points show (figures 8 (d) - (h)) an interesting phenomenon. Since the Mach number at the transonic dip is not the same for both of these wings and their isolated flutter speeds are almost equal, the flutter boundaries of the paired configurations have two dips. As shown in figure 11, interference lowers the Mach number of both dips -- the leading wing's being lowered more. This double dip is not observable on most 070/040 - 100 pairings since the flutter speeds of these two wings in isolation differ appreciably.

Although no supersonic flutter could be found on the isolated surfaces within tunnel bounds, points of supersonic flutter occurred on both the 070/032, 070/040 and the 100 wing models for several of the interfering configurations. The data is insufficient, however, to determine quantitative trends. Also noticeable is the fact that the recovery of the transonic dip occurred at a higher Mach number for the interfering cases than for the isolated wing.

An anomaly revealed in testing is the occurrence of instances of flutter at a much higher frequency than the norm. Such cases are shown in figures 8(b) and 8(k). These instabilities were not found to be reproducible from tunnel run to run. It is conjectured that a mild instability, sensitive to structural damping, occurred involving vibration modes higher in frequency than are present in the primary flutter mechanism.

ANALYSIS

Method

Unsteady aerodynamic influence coefficients were calculated by the doublet-lattice method described in reference 11. From these coefficients and measured normal modes, generalized aerodynamic forces were then computed. The measured modes and measured modal frequencies were used in conjunction with calculated mass distributions to calculate the generalized masses and stiffnesses. Flutter solutions were determined by the classical V-g method (ref. 13). In obtaining the flutter speeds and frequencies, a nominal structural damping level of 0.02 was assumed.

Shown in Figure 12 is a representative V-g-f plot for the 070/032 and 100 wings without aerodynamic interference. For clarity, only the lowest two modes of each surface are shown; the analysis, however, includes the lowest five modes of each surface. The principal flutter mechanism of each wing is associated with the coalescence of the coupled first bending and coupled first torsion modes (see, for example, the modes in figures 5 (a) - (b) and 7 (a) - (b)). For the orbiter , this first torsional mode consists primarily of torsion and control surface rotation.

Since the present study involves structurally uncoupled components, the equations of motion for the two-component system may be written:

$$\begin{bmatrix} m_{AA} & 0 \\ 0 & m_{BB} \end{bmatrix} \begin{Bmatrix} \ddot{\zeta}_A \\ \ddot{\zeta}_B \end{Bmatrix} + (1 + ig) \begin{bmatrix} k_{AA} & 0 \\ 0 & k_{BB} \end{bmatrix} \begin{Bmatrix} \zeta_A \\ \zeta_B \end{Bmatrix} = \begin{bmatrix} a_{AA} & a_{AB} \\ a_{BA} & a_{BB} \end{bmatrix} \begin{Bmatrix} \zeta_A \\ \zeta_B \end{Bmatrix}, \quad (1)$$

where a_{ij} is the complex aerodynamic operator, $b_{ij}\ \partial/\partial t + V\ c_{ij}\ \partial/\partial x$. If one surface is rigid, a simplified equation can be written:

$$\left[m_{AA}\right] \left\{\ddot{\zeta}_A\right\} + (1 + ig) \left[k_{AA}\right] \left\{\zeta_A\right\} = \left[a_{AA}\right] \left\{\zeta_A\right\} \quad (2)$$

Even in this case, aerodynamic interference is present due to the simple reflection by component B of the perturbations originating on surface A. Figure 13 illustrates the effect of this simple reflection for the 070/032 and a rigid 100 planform with a vertical separation of 0.4 mean chords and 0.0 streamwise separation. By comparing these results with those of figure 12, we see that the flutter speed of the 070/032 is reduced 7% and the frequency $4\frac{1}{2}\%$.

Inclusion of the flexibility of surface B gives the coupled equation (1) and produces the V-g-f plot of figure 14. The reductions in flutter speed and frequency are 12% and $11\frac{1}{2}\%$ in this case -- 1.75 and 2.5 times greater, respectively, than predicted by simple reflection. In fact, the flutter mechanism itself appears to have changed to a coalescence of the 070/032 bending and 100 torsion modes. On the damping plot, the 100 torsion mode appears flutter critical. This is somewhat misleading, however, since aerodynamic coupling changes the character of a mode as airspeed is increased. An inspection of the eigenvector reveals that the flutter critical mode is a combination (in order of importance) of 070/032 torsion, 070/032 bending, and 100 torsion. Similarly, the flutter mode of the noncritical mechanism is found to be a combination of sizable contributions from all four principal normal modes. Consequently, it is apparent that the inclusion of the a_{AB} and a_{BA} coupling terms in equation (1) is essential to the analysis and results in coupled flutter involving undamped motion on both surfaces at a frequency substantially different from that predicted without these terms.

Analytical Results

Flutter analyses were run for each of the three isolated surfaces and for the 100 wing paired first with the 070/032, then with the 070/040 in each of the nine configurations shown in Table IV. Flutter speed and frequency indices were obtained for several values of air density ratio over a range of subsonic Mach numbers. These flutter speed boundaries are shown for the isolated wings in figures 15 (a) - (c). The flutter speed varies little with M until high Mach numbers are reached, where the variation experienced is

strongly dependent on air density. Hence, in detailed correlation with test data, the air density ratio must be matched by analysis.

The analytical flutter boundaries for the paired configurations are typified by those shown in figures 16 (a) and (b), where the 070/032 and the 100 wings are separated vertically by 0.4 mean chords and have no streamwise separation. Figure 16 (a) represents the flutter speeds predicted by the instability branch associated with the orbiter torsion mode, while 16 (b) shows the flutter branch associated with the booster torsion mode (see figure 14). The latter flutter speed trends are similar to those of the isolated booster but are at a slightly higher velocity. The trends of figure 16 (a), however, are markedly different from those of an isolated orbiter. At the higher air densities, the flutter speed increases with increasing M at first. then dips before the Mach 1.0 recovery is approached. The initial increasing flutter speed is associated with moderate coupling between the booster torsion mode and the orbiter bending and torsion modes as shown in figure 17. and is essentially the same velocity as predicted by simple aerodynamic reflection. As higher Mach numbers are approached. the coupling becomes stronger causing the new flutter mechanism described in reference to figure 14. Thus, both the flutter speed and frequency drop appreciably.

For the other configurations analyzed, the flutter boundaries are much the same as those of figure 16. As the separation between the wings is increased, the dip disappears from the orbiter associated branch of the solution, and the flutter trends come to resemble those of the isolated orbiter. If separation is decreased, the dip is accentuated and the flutter speed is reduced further. The booster associated branch defines trends resembling the isolated booster for all separations studied Analysis of the 070/040 - 100 configuration yields nothing qualitatively different from the phenomena described for the 070/032 - 100. Since the flutter speeds of the isolated 070/040 are higher than those of the 070/032, the orbiter associated branch of the solution is higher for the 070/040 - 100 than for the 070/032.

From the analyses at a representative tunnel air density, trends of minimum flutter speed as a function of wing separation were determined and are shown in figure 10, where they are seen to compare well with test data. Inter-

ference, as discussed above, typically lowered the flutter speed branch of the orbiter (leading) wing, while slightly raising that of the booster (trailing) wing. Since the flutter critical wing of the 070/032 - 100 pairing was seen in testing to be the leading wing, the minimum flutter speed of that configuration was lowered by interference. Conversely, on the 070/040 - 100 configurations, the trailing wing was critical and interference caused a slight increase in the minimum flutter speed of the pairing.

For the 070/032 - 100 configuration, the effect of interference diminishes rapidly with both increased streamwise and vertical separations: At a streamwise separation of one mean chord, the flutter speed reduction is less than 3% for all values of h/c shown. For the 070/040 - 100 configuration, the effect of interference is much less, and seems to have a periodic component in both vertical and streamwise separations: In the cases analyzed, the flutter speed is higher at $\ell/c = 0.73$ than at $\ell/c = 0.0$ or 1.45. Also at $\ell/c = 0$, the flutter speed is lower at $h/c = 0.4$ than at either $h/c = 0.2$ or 0.6.

CORRELATION

The correlation between test and analysis was complicated by the nature of the wind tunnel: In a blowdown tunnel the air density is a function of the dynamic pressure and Mach number. Hence, different points on a measured flutter boundary correspond to different air densities, and the effect of compressibility cannot be isolated. To account for differences in air density, the analyses were run for several densities and interpolated to measured tunnel values at various Mach numbers on each boundary.

The analytical boundaries derived by this technique are shown for the isolated wings in figures 9 (a) - (c). Excellent correlation is obtained in the flutter speed of the 100 booster wing: At Mach numbers below the transonic dip, the maximum discrepancy is only 3%. The flutter frequencies predicted for this wing, however, are 12 to 40% larger than measured. On the 070 control surface models, the theoretical flutter speeds are 11 to 19% lower than those occurring in the wind tunnel. while the analytical and test flutter frequencies agree within 5% for the 070/040 and within 12% for the 070/032. The

poorer flutter speed prediction on these wings is probably due to the presence of the control surface and the hinge-line gap. On all three wings there are anomalies in the transonic dip prediction. The measured dip is localized to a small band in Mach number while the theory predicts a gradual, less severe trend. Since linearized aerodynamic theory neglects thickness and hence local Mach number effects, it cannot be expected to accurately predict the transonic dip region.

The discrepancies between test and theory found for the isolated wings are, of course, present in the interfering configurations as well. To appraise the theory's ability to predict interference alone, these discrepancies had to be removed. Consequently, the predicted flutter speed and flutter frequency indices of the interfering configurations were adjusted by the ratios of the test-to-analysis indices of the isolated wings. These adjusted indices are presented for the test configurations in figures 9 (d) - (m). Both adjusted roots are presented -- one associated with the mode which at zero air speed is orbiter torsion, the other with a mode which is originally booster torsion. As has been discussed, however, these roots are highly coupled at flutter so that identification of these roots with flutter on one surface alone is inaccurate in many cases. The test points could be expected to correlate with the critical (lowest in airspeed) root. Except for three areas, the agreement between the flutter speeds of test and analysis is now excellent, indicating that the interference effects have in fact been adequately represented in the analysis.

The first discrepancy is typified by the configuration of figure 9 (d) where the analytical orbiter flutter speed does not show the proper recovery. Apparently, the use of isolated surface measured flutter data to correct the theory empirically is not entirely successful at Mach numbers of 0.9 and greater. One reason may be that the Venturi effect of the wings in the closer configurations causes the local Mach numbers in the region between them to be significantly different from those of the isolated wings.

A second area of poor agreement in flutter speed exists around M = 0.7 on the configuration of figure 9 (e), where a coupled instability occurs 14½% lower than the predicted level. In examining the test data associated with

this flutter point, it was found that the measured structural dampings of the booster wing used in that tunnel run were much lower than the norm. In fact, the damping in the torsion mode was 50% lower. The low damping is insufficient, it is conjectured, to stabilize the marginal instability predicted by theory in figure 18. This V-g-f plot reveals a point of neutral aerodynamic stability 8% lower in air speed than that of the primary mechanism, and is a transition between the aerodynamic damping trends typified in figures 14 and 17. The flutter frequency index calculated for this instability is also reasonable; its value of 0.82 lies between the orbiter and booster flutter frequencies as does the measured value of 0.86.

The third discrepancy is the failure of the theory to predict the shift in the Mach number at which the transonic dip occurs. As shown in figure 11, this point varies with vertical separation and occurs quite low on the 070/032 -100 configuration. Theory predicts no such variation. Once again, the absence of local Mach number effects from the theory is the probable cause of this failing.

CONCLUSIONS

Interference flutter of closely spaced pairs of structurally uncoupled delta wings was studied by experiment and analysis. Significant reductions in the subsonic flutter speed of the leading wings were predicted and observed on configurations with small wing separations. The subsonic flutter boundary of the large trailing wing was slightly increased by interference. Sizable reductions in the supersonic flutter boundary of the wings were encountered in testing.

Except for the difficulty associated with control surfaces, correlation between the flutter speeds of the theory and test in the subsonic range was generally good: The reductions in flutter speed due to aerodynamic interference were calculated within experimental accuracy; however, the shift in Mach number of the transonic dip was not predicted, indicating that local M effects were more important on closely paired wing configurations than on an isolated wing.

Analysis showed that the flexibilities of both surfaces were essential to the flutter mechanism and that predictions made assuming one wing to be a rigid reflecting plane were often inaccurate. Inclusion of flexibility on both wing causes a new flutter mechanism to be predicted wherein the normal modes of both wings aerodynamically couple at a unique flutter frequency. Such coupling was observed in many wind tunnel test runs.

REFERENCES

1. Stahle, C. V.: Transonic Effects on T-tail Flutter. The Martin Company RM-24, 1959, Baltimore, Md.

2. Stark, V. J. E.: Aerodynamic Forces on a Combination of a Wing and a Fin Oscillating in Subsonic Flow: SAAB TN54, Feb. 1964, Linkoping, Sweden.

3. Laschka, B. and Schmid, H: Unsteady Aerodynamic Forces on Coplanar Lifting Surfaces in Subsonic Flow (Wing-Horizontal Tail Interference). Paper presented at the AGARD Structures and Materials Panel Meeting, Sept. 25-27, 1967, Ottawa, Canada.

4. Topp, L. J.; Rowe, W. S.; and Shattuck, A. W.: Aeroelastic Considerations in the Design of Variable Sweep Airplanes. ICAS Paper No. 66-12, Sept. 1966.

5. Sensberg, O.; and Laschka, B.: Flutter Induced by Aerodynamic Interference between Wing and Tail. Journal of Aircraft, Vol. 7, No. 4, July-Aug., 1970, p. 319-324.

6. Mykytow, W. J.; Noll, T. E.; Huttsell, L. J; and Shirk, M. H.: Investigations Concerning the Coupled Wing-Fuselage-Tail Flutter Phenomenon. Journal of Aircraft, Vol. 9, No. 1, Jan., 1972, p. 48-54.

7. Albano, E.; and Rodden, W. P.: A Doublet Lattice Method for Calculating Lift Distributions on Oscillating Surfaces in Subsonic Flow. AIAA Journal, Vol. 7, No. 2, Feb., 1969, pp 279-285.

8. Albano, E.; Perkinson, F; and Rodden, W. P.: Subsonic Lifting Surface Theory Aerodynamics and Flutter Analysis of Interfering Wing/Horizontal Tail Configurations. AFFDL-TR-70-59, Sept. 1970, AFFDL, Wright-Patterson Air Force Base, Ohio.

9. Triplett, W. E.; Burkhart, T. H.; and Birchfield, E. B.: A Comparison of Methods for the Analysis of Wing-Tail Interaction Flutter. AIAA Paper 70-80, presented at Aerospace Sciences Meeting, Jan. 19-21, 1970, N. Y., N.Y.

10. Goetz, R. C.: Lifting and Control Surface Flutter. NASA TM X-52876, Vol. III, July, 1970.

11. Rodden, W. P.; Giesing, J. P.; and Kalman, T. P.: New Developments and Applications of the Subsonic Doublet-Lattice Method for Nonplanar Configurations. AGARD Conference Preceedings No. 80, April 1971.

12. Chipman, R. R.: Interference Flutter on Space Shuttle Configurations. Paper presented at Aerospace Flutter and Dynamics Council Meeting, May 1972, N.Y., N.Y.

13. Bisplinghoff, R. L.; and Ashley, H.: Principles of Aeroelasticity. John Wiley and Sons, Inc., N.Y., N.Y., 1962.

TABLE I. - PHYSICAL PROPERTIES OF MODELS

TYPE	TRAILING (BOOSTER)	LEADING (ORBITER)	LEADING (ORBITER)
Cross-Section	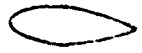		
Designation	100	070.040	070/032
Core - m (in)	0.00254(0.100)	0.00178(0.070)	0.00178(0.070)
Hinge - m (in)	-	0.00102(0.040)	0.00081(0.032)
b - m (in)	0.118(4.63)	0.0784(3.09)	0.0784(3.09)
Aspect Ratio	0.794	0.794	0.794
Leading Edge Sweep	60°	60°	60°
m_w - k_g(slugs)	0.2026(0.0139)	0.0690(0.0047)	0.0690(0.0047)
v_w - m^3(ft^3)	0.00606(0.214)	0.0018(0.0635)	0.0018(0.0635)
Airfoil Designation	NASA0008-64	NASA0008-64	NASA0008-64
f_1 - Hz	104.	129.8	129.5
f_2 - Hz	223.	283.8	261.4

TABLE II

VIBRATION SURVEY MEASUREMENT AND MASS POINT LOCATIONS

ORBITER

POINT	X		Y		POINT	X		Y	
	METERS	INCHES	METERS	INCHES		METERS	INCHES	METERS	INCHES
1	.0173	.68	.0064	.25	13	.0986	3.88	.0455	1.79
2	.0490	1.93	.0064	.25	14	.1420	5.59	.0455	1.79
3	.0986	3.88	.0064	.25	15	.1811	7.13	.0455	1.79
4	.1420	5.59	.0064	.25	16	.2004	7.89	.0455	1.79
5	.1811	7.13	.0064	.25	17	.2256	8.88	.0455	1.79
6	.2004	7.89	.0064	.25	18	.1420	5.59	.0800	3.15
7	.2256	8.88	.0064	.25	19	.1811	7.13	.0800	3.15
8	.0490	1.93	.0254	1.0	20	.2256	8.88	.0800	3.15
9	.0986	3.88	.0254	1.0	21	.1811	7.13	.1024	4.03
10	.1420	5.59	.0254	1.0	22	.2004	7.89	.1049	4.13
11	.1811	7.13	.0254	1.0	23	.2256	8.88	.1049	4.13
12	.0838	3.30	.0455	1.79					

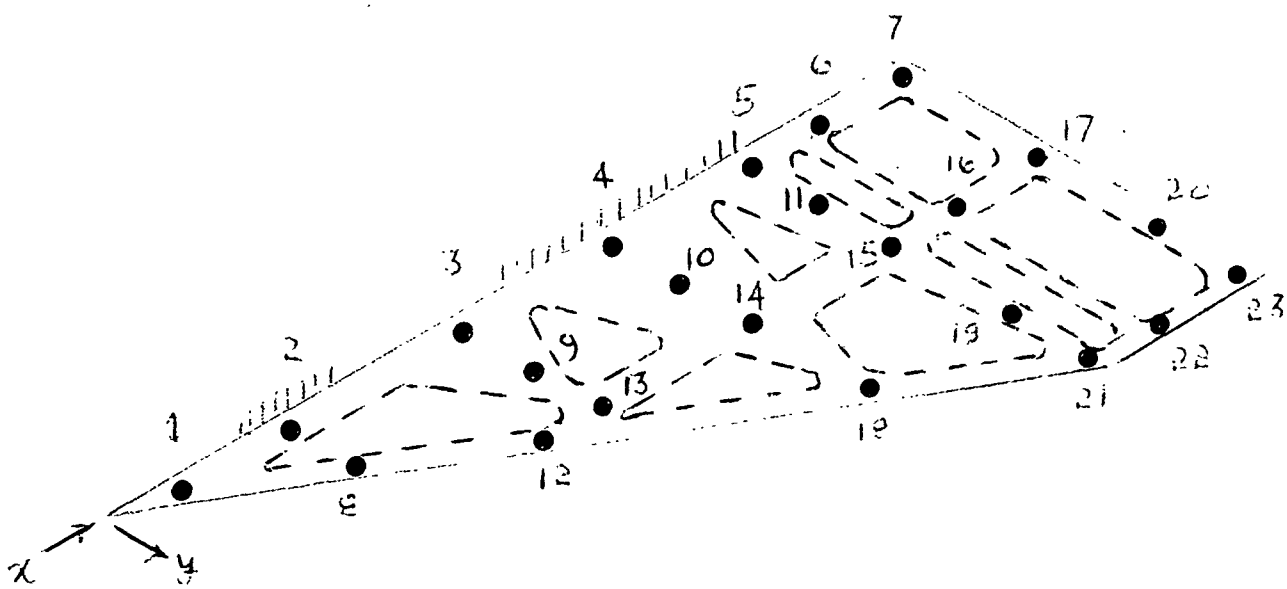

TABLE II. - Continued

BOOSTER

1	.0259	1.02	.0095	.375	13	.1478	5.82	.0683	2.69
2	.0762	3.00	.0095	.375	14	.2134	8.40	.0683	2.69
3	.1478	5.82	.0095	.375	15	.2743	10.80	.0683	2.69
4	.2134	8.40	.0095	.375	16	.3007	11.84	.0683	2.69
5	.2743	10.80	.0095	.375	17	.3383	13.32	.0683	2.69
6	.3007	11.84	.0095	.375	18	.2134	8.40	.1201	4.73
7	.3383	13.32	.0095	.375	19	.2743	10.80	.1201	4.73
8	.0762	3.00	.0381	1.5	20	.0843	3.32	.1201	4.73
9	.1478	5.82	.0381	1.5	21	.2743	10.80	.1537	6.05
10	.2134	8.40	.0381	1.5	22	.3007	11.84	.1575	6.20
11	.2743	10.80	.0381	1.5	23	.3383	13.32	.1575	6.20
12	.1257	4.95	.0683	2.69					

TABLE III

CALCULATED MODEL MASS DISTRIBUTION

POINT	ORBITER		BOOSTER	
	KILOGRAMS	SLUGS $\times 10^{-2}$	KILOGRAMS	SLUGS $\times 10^{-2}$
1	.0019	.0131	.0063	.0432
2	.0025	.0168	.0082	.0560
3	.0084	.0578	.0211	.1445
4	.0058	.0396	.0156	.1066
5	.0036	.0249	.0068	.0466
6	.0018	.0126	.0043	.0292
7	.0007	.0045	.0021	.0143
8	.0018	.0120	.0059	.0404
9	.0071	.0486	.0232	.1592
10	.0072	.0495	.0237	.1622
11	.0017	.0118	.0056	.0385
12	.0014	.0093	.0043	.0292
13	.0013	.0091	.0042	.0289
14	.0071	.0489	.0234	.1604
15	.0037	.0256	.0113	.0774
16	.0024	.0163	.0068	.0466
17	.0010	.0068	.0032	.0221
18	.0039	.0264	.0126	.0861
19	.0012	.0081	.0039	.0270
20	.0018	.0122	.0035	.0239
21	.0009	.0064	.0021	.0146
22	.0012	.0085	.0036	.0249
23	.0005	.0035	.0009	.0059
SUB-TOTAL	.0690	.4720	.2026	1.3877
TANGS	.0208	.1427	.0298	.2038

TABLE IV - CONFIGURATIONS

h/c \ ℓ/c	Fore 0.00	Middle 0.73	Aft 1.45
Upper 0.20	A	A&E	A
Middle 0.40	A&E	A&E	A
Lower 0.60	A&E	A&E	A

A = ANALYSIS PERFORMED

E = EXPERIMENT PERFORMED

TABLE V.

PRE-RUN FREQUENCIES

Run	070/032			070/040			100			Run	070/032			070/040			100			Run	070/032			070/040			100		
	F1	F2	F3	F1	F2	F3	F1	F2	F3		F1	F2	F3	F1	F2	F3	F1	F2	F3		F1	F2	F3	F1	F2	F3	F1	F2	F3
2	---	---	---	140	300	424	---	---	---	74	---	---	---	128	280	390	100	215	325	136	137	264	402	---	---	---	107	228	340
3	---	---	---	140	300	422	---	---	---	75	---	---	---	130	280	390	97	216	307	137	125	270	395	---	---	---	102	216	320
4	---	---	---	139	299	420	---	---	---	76	126	266	390	---	---	---	101	224	317	138	135	270	405	---	---	---	104	215	320
5	---	---	---	140	295	416	---	---	---	77	128	260	404	---	---	---	100	220	315	139	140	265	408	---	---	---	105	215	315
6	---	---	---	136	293	414	---	---	---	78	126	267	390	---	---	---	100	220	317	140	138	262	405	---	---	---	105	215	312
7	---	---	---	137	284	412	---	---	---	79	126	269	384	---	---	---	100	220	320	141	136	272	405	---	---	---	105	214	318
8	---	---	---	137	288	418	---	---	---	80	127	270	385	---	---	---	100	219	314	142	136	269	400	---	---	---	104	212	315
9	---	---	---	135	296	410	---	---	---	81	126	269	385	---	---	---	101	225	320	143	136	267	400	---	---	---	103	214	315
10	---	---	---	140	290	420	---	---	---	82	124	273	385	---	---	---	101	224	320	144	137	267	400	---	---	---	104	213	320
11	---	---	---	135	288	416	---	---	---	83	130	270	395	---	---	---	97	216	310	145	135	268	397	---	---	---	100	221	323
12	---	---	---	134	290	414	---	---	---	84	126	270	385	---	---	---	97	215	305	146	135	267	402	---	---	---	101	227	330
13	---	---	---	---	---	---	100	220	315	85	127	274	390	---	---	---	100	220	319	147	136	269	400	---	---	---	98	223	332
24	---	---	---	135	315	415	---	---	---	86	126	265	390	---	---	---	101	224	320	148	135	266	398	---	---	---	99	220	334
25	---	---	---	134	310	410	---	---	---	87	128	264	390	---	---	---	101	221	318	149	135	266	396	---	---	---	98	219	332
26	---	---	---	133	300	405	---	---	---	88	126	266	390	---	---	---	101	223	319	150	135	268	400	---	---	---	99	220	332
27	---	---	---	131	295	405	---	---	---	89	130	266	396	---	---	---	101	224	317	151	134	264	390	---	---	---	99	220	328
28	---	---	---	130	295	396	---	---	---	90	130	262	390	---	---	---	103	218	312	152	---	---	---	---	---	---	99	220	330
29	---	---	---	---	---	---	106	230	330	91	---	---	---	---	---	---	108	220	330	153	135	260	390	---	---	---	---	---	---
30	---	---	---	---	---	---	111	228	340	92	---	---	---	---	---	---	109	220	335	154	133	260	389	---	---	---	98	223	320
31	---	---	---	---	---	---	105	226	332	93	---	---	---	---	---	---	108	220	335	155	132	263	388	---	---	---	---	---	---
32	---	---	---	---	---	---	102	220	336	94	---	---	---	135	285	411	108	220	328	156	131	265	388	---	---	---	---	---	---
33	---	---	---	---	---	---	102	225	335	95	---	---	---	128	280	385	102	223	320	157	131	265	380	---	---	---	---	---	---
34	---	---	---	---	---	---	102	224	335	96	---	---	---	128	285	385	101	215	326	158	132	264	387	---	---	---	---	---	---
35	---	---	---	---	---	---	100	235	336	97	---	---	---	128	284	385	100	215	328	159	132	263	388	---	---	---	---	---	---
36	129	270	395	---	---	---	---	---	---	98	---	---	---	125	284	394	102	225	326	160	---	---	---	136	293	408	99	221	320
37	127	269	390	---	---	---	---	---	---	99	---	---	---	126	280	388	102	226	327	161	---	---	---	136	286	408	96	220	318
38	129	265	385	---	---	---	---	---	---	100	---	---	---	127	285	387	104	226	330	162	135	273	390	---	---	---	---	---	---
39	130	265	385	---	---	---	---	---	---	101	---	---	---	125	285	386	106	219	330	163	135	270	392	---	---	---	100	220	338
40	130	264	384	---	---	---	---	---	---	102	---	---	---	126	285	389	107	219	330	164	132	270	382	---	---	---	100	220	340
41	130	260	385	---	---	---	---	---	---	103	---	---	---	127	285	386	107	216	330	165	136	266	400	---	---	---	100	220	340
42	130	260	385	---	---	---	---	---	---	104	---	---	---	127	285	389	106	218	330	166	132	265	390	---	---	---	---	---	---
43	130	260	385	---	---	---	---	---	---	105	---	---	---	127	284	389	106	215	330	167	132	266	390	---	---	---	---	---	---
44	129	260	385	---	---	---	---	---	---	106	---	---	---	127	284	385	106	217	330	168	---	---	---	126	280	390	105	225	332
45	129	260	385	---	---	---	---	---	---	107	---	---	---	127	284	386	106	218	330	169	---	---	---	127	286	398	96	210	340
46	129	260	384	---	---	---	---	---	---	108	---	---	---	128	285	389	107	219	335	170	---	---	---	126	285	390	96	221	340
47	129	260	385	---	---	---	---	---	---	109	---	---	---	130	295	404	100	220	320	171	---	---	---	125	285	388	95	220	340
48	129	258	395	---	---	---	---	---	---	110	---	---	---	130	294	404	100	216	320	172	---	---	---	125	286	390	96	216	336
49	130	265	395	---	---	---	---	---	---	111	---	---	---	129	290	404	100	220	324	173	125	257	384	---	---	---	107	225	
50	---	---	---	---	---	---	105	225	330	112	---	---	---	128	290	404	100	220	318	174	130	270	384	---	---	---	105	225	330
51	---	---	---	---	---	---	108	225	334	113	---	---	---	128	290	404	100	219	320	175	129	264	392	---	---	---	106	230	328
52	---	---	---	---	---	---	106	225	346	114	---	---	---	129	290	404	99	220	320	176	136	275	398	---	---	---	105	214	
53	---	---	---	---	---	---	105	226	345	115	---	---	---	129	290	404	99	219	320	177	133	269	396	---	---	---	106	226	332
54	---	---	---	---	---	---	105	222	345	116	---	---	---	128	289	403	99	217	318	178	130	266	396	---	---	---	106	226	343
55	---	---	---	128	295	402	---	---	---	117	---	---	---	126	289	404	105	215	328	179	129	275	396	---	---	---	105	229	339
56	---	---	---	134	306	405	100	223	316	118	---	---	---	126	285	398	105	215	330	180	---	---	---	130	299	410	---	---	---
57	---	---	---	133	305	405	---	---	---	119	---	---	---	125	285	400	105	216	328	181	---	---	---	---	---	---	100	218	332
58	---	---	---	133	306	409	---	---	---	120	---	---	---	129	289	406	104	218	302	182	---	---	---	130	286	400	---	---	---
59	---	---	---	133	306	405	---	---	---	121	---	---	---	128	289	404	103	215	300	183	122	262	398	---	---	---	99	220	328
60	---	---	---	132	299	406	101	220	315	122	---	---	---	129	292	398	108	218	334	184	122	261	390	---	---	---	99	220	322
61	---	---	---	135	300	415	101	220	314	123	---	---	---	127	294	394	105	220	330	185	129	264	392	---	---	---	98	220	323
62	---	---	---	135	300	418	100	217	313	124	---	---	---	127	294	394	105	220	330	186	123	258	386	---	---	---	98	220	330
63	132	267	395	---	---	---	---	---	---	125	---	---	---	126	292	396	106	220	330	187	---	---	---	123	290	400	104	225	322
64	---	---	---	133	290	400	100	214	313	126	---	---	---	128	290	400	105	218	330	188	---	---	---	---	---	---	94	226	320
65	---	---	---	132	290	400	---	---	---	127	---	---	---	126	289	398	98	229	310	189	127	275	390	---	---	---	95	212	320
66	---	---	---	128	285	395	---	---	---	128	---	---	---	127	290	398	97	216	320	190	120	255	384	---	---	---	93	206	310
67	---	---	---	129	278	390	98	220	300	129	132	262	376	---	---	---	100	213	315										
68	---	---	---	130	285	392	100	220	314	130	---	---	---	125	289	393	101	214	320										
69	---	---	---	130	284	390	100	218	314	131	125	270	385	---	---	---	98	215	324										
70	---	---	---	129	284	395	100	220	314	132	132	265	400	---	---	---	98	226	320										
71	---	---	---	131	284	395	100	215	317	133	135	264	400	---	---	---	98	225	318										
72	---	---	---	130	285	396	100	218	315	134	137	260	392	---	---	---	99	225	318										
73	---	---	---	129	281	390	101	219	315	135	137	264	400	---	---	---	107	230	340										

TABLE VI

ORBITER/BOOSTER ADJUSTED FLUTTER TEST PARAMETERS

(a) ISOLATED ORBITER 070/032

RUN NO.	MODELS	MODEL BEHAVIOR	M(TEST)	SIGMA	Q(TEST) (N/M2)	Q(TEST) (PSI)	QADJ (N/M2)	QADJ (PSI)	MU	F.S.I.	FLUT FREQ (HZ)
36- 5	8	FI	0.6450	3.8250	0.854E 05	12.390	0.838E 05	12.160	7.125	0.430	220.0
							0.0	0.0	0.0	0.0	0.0
37- 3	8	FSS	0.7550	2.3950	0.817E 05	11.850	0.810E 05	11.754	11.380	0.423	204.0
							0.0	0.0	0.0	0.0	0.0
38- 4	4	FSS	0.6750	2.8880	0.780E 05	11.310	0.780E 05	11.313	9.437	0.415	208.0
							0.0	0.0	0.0	0.0	0.0
39- 4	4	FSS	0.6420	3.1650	0.752E 05	10.910	0.745E 05	10.803	8.611	0.405	200.0
							0.0	0.0	0.0	0.0	0.0
40- 5	4	FI	0.6090	3.8900	0.804E 05	11.660	0.804E 05	11.660	7.006	0.421	500.0
							0.0	0.0	0.0	0.0	0.0
41- 3	4	FSS	0.8250	1.8620	0.732E 05	10.610	0.739E 05	10.718	14.637	0.404	200.0
							0.0	0.0	0.0	0.0	0.0
43- *4	4	FSS	0.8820	1.9850	0.856E 05	12.420	0.865E 05	12.546	13.730	0.437	208.0
							0.0	0.0	0.0	0.0	0.0
44- 2	4	FSS	1.0020	1.6610	0.923E 05	13.390	0.942E 05	13.662	16.409	0.456	205.0
							0.0	0.0	0.0	0.0	0.0
45- 2	4	FSS	1.0060	1.1760	0.667E 05	9.680	0.681E 05	9.877	23.176	0.387	200.0
							0.0	0.0	0.0	0.0	0.0
46- 2	4	FSS	1.0150	1.2730	0.734E 05	10.650	0.749E 05	10.866	21.410	0.406	196.0
							0.0	0.0	0.0	0.0	0.0
47- 4	4	FSS	0.8980	1.8810	0.849E 05	12.310	0.866E 05	12.560	14.490	0.437	201.0
							0.0	0.0	0.0	0.0	0.0
48- 3	4	FSS	0.7760	2.0070	0.712E 05	10.320	0.733E 05	10.638	13.580	0.402	200.0
							0.0	0.0	0.0	0.0	0.0
49- 5	4	FSS	1.2250	2.0900	0.148E 06	21.460	0.147E 06	21.249	13.041	0.568	232.0
							0.0	0.0	0.0	0.0	0.0
63- *5	4	FSS	0.9580	2.9850	0.137E 06	19.910	0.132E 06	19.137	9.131	0.539	220.0
							0.0	0.0	0.0	0.0	0.0
153- 3	9	FD	0.8570	1.6460	0.711E 05	10.310	0.691E 05	10.026	16.558	0.390	200.0
							0.0	0.0	0.0	0.0	0.0
155- 4	1	FSS	1.1270	1.1660	0.767E 05	11.120	0.752E 05	10.904	23.375	0.407	190.0
							0.0	0.0	0.0	0.0	0.0
156- *6	1	FI	0.7510	2.4670	0.792E 05	11.490	0.777E 05	11.264	11.048	0.414	196.0
							0.0	0.0	0.0	0.0	0.0
157- 4	1	FSS	0.7530	2.4660	0.785E 05	11.390	0.770E 05	11.166	11.052	0.412	198.0
							0.0	0.0	0.0	0.0	0.0
162- 6	1	FI	0.9160	2.6740	0.107E 06	15.570	0.101E 06	14.693	10.193	0.473	200.0
							0.0	0.0	0.0	0.0	0.0
166- 4	1	FSS	0.9250	2.0340	0.948E 05	13.750	0.920E 05	13.348	13.400	0.450	200.0
							0.0	0.0	0.0	0.0	0.0
167- 4	1	FSS	0.9110	2.0500	0.929E 05	13.480	0.893E 05	12.957	13.295	0.444	195.0
							0.0	0.0	0.0	0.0	0.0

1 S - Stable
FI - Intermittent Flutter
FSS - Steady State Flutter
FD - Divergent Flutter
LD - Low Amplitude Damped Instability

* Near Shutdown

TABLE VI - Continued

(b) ISOLATED ORBITER 070/040

RUN NO.	MODELS	MODEL BEHAVIOR	M(TEST)	SIGMA	Q(TEST) (N/M2)	Q(TEST) (PSI)	QADJ (N/M2)	QADJ (PSI)	MU	F.S.I.	FLUT FREQ (HZ)
3- *5	6	S	0.8950	2.4540	0.106E 06	15.360	0.943E 05	13.674	11.106	0.456	0.0
							0.0	0.0	0.0	0.0	0.0
4- *3	6	LD	1.0120	1.9960	0.114E 06	16.560	0.102E 06	14.754	13.655	0.473	210.0
							0.0	0.0	0.0	0.0	0.0
7- 4	6	FI	0.9460	2.5840	0.125E 06	18.070	0.118E 06	17.052	10.548	0.509	214.0
							0.0	0.0	0.0	0.0	0.0
8- *4	6	S	1.1300	2.1500	0.140E 06	20.280	0.128E 06	18.572	12.677	0.531	0.0
							0.0	0.0	0.0	0.0	0.0
9- 3	6	FSS	0.7340	3.0260	0.985E 05	14.290	0.948E 05	13.751	9.007	0.457	215.0
							0.0	0.0	0.0	0.0	0.0
11- 2	7	FSS	0.8490	2.5570	0.103E 06	14.930	0.980E 05	14.220	10.659	0.465	199.0
							0.0	0.0	0.0	0.0	0.0
11- 3	7	S	0.8450	2.6090	0.103E 06	15.010	0.986E 05	14.296	10.446	0.466	0.0
							0.0	0.0	0.0	0.0	0.0
11- 6	7	FSS	0.8830	2.8070	0.111E 06	16.030	0.105E 06	15.267	9.710	0.482	205.0
							0.0	0.0	0.0	0.0	0.0
12- 5	7	FSS	0.9140	2.6610	0.120E 06	17.410	0.114E 06	16.572	10.242	0.502	208.0
							0.0	0.0	0.0	0.0	0.0
12- 6	7	FI	0.9050	2.7580	0.121E 06	17.580	0.115E 06	16.734	9.882	0.504	204.0
							0.0	0.0	0.0	0.0	0.0
12- 7	7	FSS	0.9070	2.8220	0.123E 06	17.900	0.117E 06	17.039	9.658	0.509	207.0
							0.0	0.0	0.0	0.0	0.0
12- 8	7	FD	0.9030	2.8650	0.124E 06	17.940	0.118E 06	17.077	9.513	0.509	207.0
							0.0	0.0	0.0	0.0	0.0
24- 3	4	FSS	0.6760	3.7070	0.101E 06	14.710	0.872E 05	12.641	7.352	0.438	530.0
							0.0	0.0	0.0	0.0	0.0
25- 4	4	FSS	0.8030	2.8950	0.108E 06	15.620	0.961E 05	13.935	9.414	0.460	209.0
							0.0	0.0	0.0	0.0	0.0
26- *5	8	S	0.6830	3.7760	0.102E 06	14.780	0.943E 05	13.680	7.218	0.456	0.0
							0.0	0.0	0.0	0.0	0.0
27- *4	8	S	0.9300	3.4390	0.145E 06	21.050	0.138E 06	20.049	7.925	0.552	0.0
							0.0	0.0	0.0	0.0	0.0
28- 3	8	S	0.9220	3.4510	0.154E 06	22.280	0.148E 06	21.440	7.898	0.571	0.0
							0.0	0.0	0.0	0.0	0.0
55- 4	6	FSS	0.6390	4.3250	0.993E 05	14.400	0.950E 05	13.786	6.302	0.458	220.0
							0.0	0.0	0.0	0.0	0.0
57- *3	4	S	1.2200	2.6900	0.189E 06	27.340	0.173E 06	25.079	10.132	0.617	0.0
							0.0	0.0	0.0	0.0	0.0
58- 3	4	FSS	1.0680	1.6550	0.105E 06	15.170	0.951E 05	13.793	16.468	0.458	218.0
							0.0	0.0	0.0	0.0	0.0
59- 3	4	LD	0.9420	3.2060	0.140E 06	20.330	0.127E 06	18.485	8.501	0.530	220.0
							0.0	0.0	0.0	0.0	0.0
65- 4	6	FSS	1.0110	1.9980	0.109E 06	15.860	0.105E 06	15.244	13.641	0.491	215.0
							0.0	0.0	0.0	0.0	0.0
66- 5	6	S	1.1580	2.6880	0.172E 06	24.920	0.175E 06	25.434	10.139	0.622	0.0
							0.0	0.0	0.0	0.0	0.0
180- 4	8	FD	0.8460	1.9230	0.790E 05	11.460	0.753E 05	10.927	14.173	0.407	195.0
							0.0	0.0	0.0	0.0	0.0
182- *5	1	FI	0.8370	1.8860	0.765E 05	11.090	0.757E 05	10.981	14.451	0.408	200.0
							0.0	0.0	0.0	0.0	0.0

TABLE VI - Continued

(c) ISOLATED BOOSTER 100

RUN NO.	MODELS	MODEL BEHAVIOR	M(TEST)	SIGMA	Q(TEST) (N/M2)	Q(TEST) (PSI)	QADJ (N/M2)	QADJ (PSI)	MU	F.S.I.	FLUT FREQ (HZ)
31- 5			0.6480	3.4560	0.803E 05	11.650	0.0	0.0	0.0	0.0	0.0
	5	FSS					0.787E 05	11.420	7.886	0.417	170.0
33- *5			0.7210	2.4560	0.749E 05	10.860	0.0	0.0	0.0	0.0	0.0
	5	FI					0.757E 05	10.977	11.097	0.408	164.0
34- 3			0.8460	1.5320	0.642E 05	9.310	0.0	0.0	0.0	0.0	0.0
	5	FD					0.655E 05	9.502	17.790	0.380	146.0
50- 7			0.9980	2.6540	0.121E 06	17.510	0.0	0.0	0.0	0.0	0.0
	3	LD					0.118E 06	17.165	10.269	0.511	150.0
50- *8			0.9900	2.6440	0.116E 06	16.830	0.0	0.0	0.0	0.0	0.0
	3	S					0.114E 06	16.498	10.308	0.501	0.0
50-8.1			0.9530	2.6000	0.107E 06	15.550	0.0	0.0	0.0	0.0	0.0
	3	S					0.105E 06	15.244	10.483	0.481	0.0
50- 9			0.9030	2.4560	0.921E 05	13.360	0.0	0.0	0.0	0.0	0.0
	3	FD					0.903E 05	13.097	11.097	0.446	145.0
52- *3			0.5830	4.3250	0.833E 05	12.080	0.0	0.0	0.0	0.0	0.0
	4	S					0.809E 05	11.726	6.302	0.422	0.0
53- 4			0.7810	2.3070	0.803E 05	11.650	0.0	0.0	0.0	0.0	0.0
	4	FSS					0.787E 05	11.420	11.814	0.417	159.0
54- 3			0.8590	1.6620	0.706E 05	10.240	0.0	0.0	0.0	0.0	0.0
	4	FSS					0.699E 05	10.139	16.399	0.393	144.0
91- 4			0.7800	2.2790	0.772E 05	11.200	0.0	0.0	0.0	0.0	0.0
	4	FSS					0.751E 05	10.891	11.959	0.407	155.0
92- 5			0.8320	2.0030	0.769E 05	11.150	0.0	0.0	0.0	0.0	0.0
	4	FI					0.741E 05	10.745	13.607	0.404	150.0
93- 5			1.2140	2.3280	0.148E 06	21.490	0.0	0.0	0.0	0.0	0.0
	4	S					0.144E 06	20.897	11.707	0.564	156.0
152- 10			0.9140	2.1920	0.938E 05	13.600	0.0	0.0	0.0	0.0	0.0
	7	FD					0.998E 05	14.473	12.434	0.469	136.0
181- 2			0.8900	1.2460	0.580E 05	8.410	0.0	0.0	0.0	0.0	0.0
	7	FSS					0.616E 05	8.941	21.874	0.369	125.0
188- 2			0.9170	1.2360	0.603E 05	8.750	0.0	0.0	0.0	0.0	0.0
	7	FSS					0.668E 05	9.690	22.051	0.384	117.0
188- 3			0.9290	1.2500	0.623E 05	9.040	0.0	0.0	0.0	0.0	0.0
	7	S					0.690E 05	10.011	21.804	0.390	0.0
188- 4			0.9980	1.5210	0.843E 05	12.230	0.0	0.0	0.0	0.0	0.0
	7	FSS					0.934E 05	13.544	17.919	0.454	125.0

TABLE VI - Continued

(d) FORWARD MID POSITION 070/032 ~ 100

RUN NO.	MODELS	MODEL BEHAVIOR	M(TEST)	SIGMA	Q(TEST) (N/M2)	Q(TEST) (PSI)	QADJ (N/M2)	QADJ (PSI)	MU	F.S.T.	FLUT FREQ (HZ)
86- 5	4	FSS	0.6430	2.3460	0.582E 05	8.440	0.594E 05	8.622	11.618	0.362	190.0
	5	FSS					0.600E 05	8.705	11.618	0.364	190.0
87- 4	4	FSS	0.7000	1.8460	0.545E 05	7.900	0.551E 05	7.985	14.764	0.348	187.0
	5	S					0.567E 05	8.228	14.764	0.354	0.0
88- 4	4	FSS	0.7660	1.7380	0.591E 05	8.570	0.598E 05	8.673	15.692	0.363	190.0
	5	S					0.609E 05	8.839	15.692	0.366	0.0
89- 4	4	FSS	0.8490	1.5670	0.654E 05	9.480	0.641E 05	9.296	17.393	0.376	186.0
	5	S					0.674E 05	9.778	17.393	0.385	0.0
89- 5	4	FD	0.8490	1.5910	0.662E 05	9.600	0.649E 05	9.414	17.131	0.378	0.0
	5	FD					0.683E 05	9.901	17.131	0.389	160.0
90- 3	6	FSS	0.8280	1.2120	0.492E 05	7.140	0.492E 05	7.140	22.487	0.329	186.0
	3	S					0.507E 05	7.360	22.487	0.334	0.0
90- 4	6	FD	0.8500	1.2200	0.518E 05	7.510	0.518E 05	7.510	22.340	0.339	180.0
	3	FD					0.534E 05	7.741	22.340	0.343	180.0
129- 2	7	FSS	0.9210	1.0780	0.592E 05	8.580	0.580E 05	8.413	25.283	0.358	192.0
	7	S					0.642E 05	9.310	25.283	0.376	0.0
129- 3	7	S	1.0060	1.2040	0.759E 05	11.010	0.744E 05	10.796	22.637	0.405	0.0
	7	S					0.824E 05	11.947	22.637	0.426	0.0
129- 6	7	S	1.0590	1.5830	0.107E 06	15.490	0.105E 06	15.189	17.217	0.480	0.0
	7	FSS					0.116E 06	16.808	17.217	0.505	160.0
129- 7	7	S	1.0340	1.6520	0.106E 06	15.340	0.104E 06	15.042	16.498	0.478	0.0
	7	S					0.115E 06	16.645	16.498	0.503	0.0
129- 9	7	FSS	0.9650	1.6400	0.931E 05	13.500	0.913E 05	13.238	16.619	0.449	220.0
	7	S					0.101E 06	14.648	16.619	0.472	0.0
129- 10	7	FD	0.8820	1.5530	0.752E 05	10.910	0.738E 05	10.698	17.550	0.403	0.0
	7	FD					0.816E 05	11.838	17.550	0.424	184.0
154- 4	1	S	1.1700	2.0900	0.140E 06	20.260	0.138E 06	20.072	13.041	0.552	230.0
	6	S					0.149E 06	21.594	13.041	0.573	0.0
154- 7	1	FSS	1.0080	2.5620	0.126E 06	18.240	0.125E 06	18.071	10.638	0.524	225.0
	6	FSS					0.134E 06	19.441	10.638	0.544	148.0

TABLE VI - Continued

(e) FORWARD LOW POSITION 070/032 - 100

RUN NO.	MODELS	MODEL BEHAVIOR	M(TEST)	SIGMA	Q(TEST) (N/M2)	Q(TEST) (PSI)	QADJ (N/M2)	QADJ (PSI)	MU	F.S.I.	FLUT FREQ (HZ)
76- 3	8	FSS	0.6490	2.6540	0.674E 05	9.770	0.682E 05	9.887	10.269	0.388	206.0
	4	S					0.695E 05	10.077	10.269	0.391	0.0
76- 4	8	FD	0.6610	2.6950	0.705E 05	10.230	0.714E 05	10.353	10.113	0.397	180.0
	4	FD					0.727E 05	10.551	10.113	0.400	180.0
77- 3	4	FD	0.7110	1.7070	0.525E 05	7.610	0.541E 05	7.844	15.967	0.345	198.0
	4	S					0.552E 05	8.011	15.967	0.349	0.0
77- 4	4	FD	0.6900	1.7290	0.504E 05	7.310	0.520E 05	7.535	15.763	0.338	198.0
	4	FD					0.531E 05	7.695	15.763	0.342	192.0
78- 4	7	FSS	0.7790	1.8300	0.656E 05	9.520	0.664E 05	9.634	14.893	0.393	196.0
	4	S					0.691E 05	10.022	14.893	0.390	0.0
79- 4	7	LD	0.8710	1.6990	0.738E 05	10.710	0.740E 05	10.739	16.042	0.404	182.0
	4	FD					0.777E 05	11.274	16.042	0.414	135.0
79- *5	7	FI	0.8670	1.7420	0.750E 05	10.880	0.752E 05	10.909	15.646	0.407	176.0
	4	FD					0.790E 05	11.453	15.646	0.417	130.0
81- 4	7	FSS	0.9340	1.3690	0.679E 05	9.850	0.681E 05	9.877	19.909	0.387	185.0
	5	FI					0.694E 05	10.062	19.909	0.391	114.0
81- *5	7	FSS	0.9550	1.3950	0.718E 05	10.420	0.720E 05	10.448	19.538	0.398	190.0
	5	S					0.734E 05	10.645	19.538	0.402	0.0
82- *5	7	S	1.1450	1.8830	0.117E 06	16.980	0.119E 06	17.257	14.474	0.512	0.0
	5	S					0.121E 06	17.513	14.474	0.516	0.0
83- *7	7	FI	0.6720	2.8590	0.740E 05	10.730	0.719E 05	10.422	9.533	0.398	210.0
	3	S					0.821E 05	11.905	9.533	0.425	0.0
84- 5	7	FD	0.7450	2.2450	0.732E 05	10.610	0.734E 05	10.639	12.140	0.402	205.0
	3	S					0.820E 05	11.890	12.140	0.425	0.0
84-5.1	7	FD	0.7470	2.2730	0.743E 05	10.780	0.745E 05	10.809	11.991	0.405	205.0
	3	FD					0.833E 05	12.080	11.991	0.428	188.0
85- 3	6	FSS	0.8120	1.6460	0.638E 05	9.250	0.621E 05	9.011	16.558	0.370	190.0
	4	S					0.671E 05	9.737	16.558	0.385	0.0
85- 4	6	FD	0.8230	1.6620	0.659E 05	9.560	0.642E 05	9.313	16.399	0.376	190.0
	4	FD					0.694E 05	10.064	16.399	0.391	190.0
163- 3	1	S	0.9110	1.5190	0.708E 05	10.270	0.661E 05	9.588	17.943	0.382	0.0
	7	FI					0.745E 05	10.811	17.943	0.405	120.0
163- *4	1	S	0.9160	1.5520	0.728E 05	10.560	0.680E 05	9.859	17.561	0.387	0.0
	7	S					0.766E 05	11.116	17.561	0.411	0.0
164- 4	1	LD	1.1080	1.6380	0.105E 06	15.190	0.997E 05	14.459	16.639	0.469	209.0
	7	LD					0.110E 06	15.990	16.639	0.493	122.0
164- 6	1	FSS	1.0080	1.8950	0.102E 06	14.760	0.969E 05	14.050	14.383	0.462	229.0
	7	S					0.107E 06	15.538	14.383	0.486	0.0
164- 7	1	S	0.9440	1.9990	0.952E 05	13.810	0.906E 05	13.146	13.634	0.447	218.0
	7	FI					0.100E 06	14.538	13.634	0.470	133.0
164- *8	1	S	0.9430	2.0100	0.956E 05	13.870	0.910E 05	13.203	13.560	0.448	0.0
	7	FI					0.101E 06	14.601	13.560	0.471	120.0
164- 9	1	FSS	0.8640	1.9280	0.799E 05	11.590	0.761E 05	11.032	14.136	0.409	190.0
	7	S					0.841E 05	12.201	14.136	0.431	0.0
165- 3	1	FSS	1.0740	1.3270	0.824E 05	11.950	0.770E 05	11.162	20.539	0.412	204.0
	7	LD					0.967E 05	12.580	20.539	0.437	124.0
165- 7	1	FSS	1.0160	2.4630	0.126E 06	18.320	0.118E 06	17.113	11.066	0.510	235.0
	7	S					0.133E 06	19.285	11.066	0.541	0.0
165- 8	1	FD	0.9580	2.5770	0.119E 06	17.230	0.111E 06	16.095	10.576	0.495	235.0
	7	FD					0.125E 06	18.138	10.576	0.525	150.0

TABLE VI - Continued

(f) MID UPPER POSITION 070/032 - 100

RUN NO.	MODELS	MODEL BEHAVIOR	M(TEST)	SIGMA	Q(TEST) (N/M2)	Q(TEST) (PSI)	QADJ (N/M2)	QADJ (PSI)	MU	F.S.I.	FLUT FREQ (HZ)
173- 5	6	FD	0.6610	2.4550	0.638E 05	9.250	0.678E 05	9.834	11.102	0.387	192.0
	6	S					0.613E 05	8.893	11.102	0.368	0.0
173- 6	6	FD	0.6570	2.4630	0.632E 05	9.170	0.672E 05	9.749	11.066	0.385	192.0
	6	FSS					0.608E 05	8.816	11.066	0.366	152.0
183- *4	5	S	0.8870	1.7030	0.768E 05	11.140	0.819E 05	11.874	16.004	0.425	0.0
	7	FI					0.817E 05	11.855	16.004	0.424	120.0
184- *4	5	LD	0.9890	1.6010	0.860E 05	12.480	0.917E 05	13.302	17.024	0.450	190.0
	7	FI					0.916E 05	13.281	17.024	0.449	120.0
185- *5	5	FI	1.1290	1.2910	0.871E 05	12.630	0.871E 05	12.634	21.111	0.438	209.0
	7	S					0.937E 05	13.590	21.111	0.454	0.0
186- 4	5	FD	0.7320	2.2200	0.701E 05	10.170	0.754E 05	10.929	12.277	0.408	199.0
	7	S					0.754E 05	10.943	12.277	0.408	0.0
186- 5	5	FD	0.7240	2.2350	0.691E 05	10.020	0.742E 05	10.768	12.195	0.404	199.0
	7	FD					0.743E 05	10.782	12.195	0.405	192.0
189- 4	8	FSS	0.7890	1.8970	0.694E 05	10.060	0.676E 05	9.800	14.367	0.386	200.0
	7	S					0.803E 05	11.648	14.367	0.421	0.0
189- 5	8	FD	0.7990	1.9020	0.711E 05	10.310	0.692E 05	10.043	14.330	0.391	200.0
	7	FSS					0.823E 05	11.937	14.330	0.426	180.0
190-2.1	9	S	0.9000	1.4120	0.663E 05	9.620	0.744E 05	10.795	19.302	0.405	0.0
	7	FSS					0.811E 05	11.755	19.302	0.423	125.0

TABLE VI - Continued

(g) MID MID POSITION 070/032 - 100

RUN NO.	MODELS	MODEL BEHAVIOR	M(TEST)	SIGMA	Q(TEST) (N/M2)	Q(TEST) (PSI)	QADJ (N/M2)	QADJ (PSI)	MU	F.S.I.	FLUT FREQ (HZ)
141- 5	1	FI	0.6680	3.0720	0.772E 05	11.200	0.707E 05	10.257	8.872	0.395	220.0
	5	S					0.797E 05	11.566	8.872	0.419	0.0
142- 4	1	FI	0.7370	2.4780	0.768E 05	11.140	0.710E 05	10.302	10.999	0.396	209.0
	5	S					0.810E 05	11.742	10.999	0.422	0.0
143- 4	1	FSS	0.7840	2.2400	0.784E 05	11.370	0.732E 05	10.621	12.167	0.402	209.0
	5	S					0.825E 05	11.969	12.167	0.426	0.0
143- *5	1	FSS	0.7930	2.2610	0.806E 05	11.690	0.753E 05	10.920	12.054	0.407	210.0
	5	S					0.848E 05	12.306	12.054	0.432	0.0
144- 4	1	LD	0.8730	1.6590	0.727E 05	10.550	0.679E 05	9.855	16.428	0.387	180.0
	5	FD					0.758E 05	10.999	16.428	0.409	144.0
144- 5	1	FSS	0.8930	1.6870	0.768E 05	11.140	0.717E 05	10.406	16.156	0.398	130.0
	5	FD					0.801E 05	11.614	16.156	0.420	140.0
145- 3	1	LD	0.8350	1.7990	0.732E 05	10.620	0.690E 05	10.013	15.150	0.390	200.0
	6	FSS					0.771E 05	11.180	15.150	0.412	145.0
145- 4	1	LD	0.8410	1.8420	0.757E 05	10.980	0.714E 05	10.353	14.796	0.397	200.0
	6	FD					0.797E 05	11.558	14.796	0.419	148.0
146- *5	1	FI	0.9700	1.5290	0.786E 05	11.400	0.741E 05	10.749	17.825	0.404	180.0
	7	FI					0.795E 05	11.537	17.825	0.419	134.0
147- 3	1	S	0.9040	1.5010	0.701E 05	10.160	0.648E 05	9.396	18.158	0.378	0.0
	7	FSS					0.733E 05	10.632	18.158	0.402	131.0
148- 6	1	FI	1.0400	1.4950	0.874E 05	12.670	0.824E 05	11.946	18.231	0.426	210.0
	7	S					0.930E 05	13.483	18.231	0.463	0.0
150- 4	1	FSS	1.0980	1.3790	0.894E 05	12.960	0.843E 05	12.220	19.764	0.431	220.0
	7	S					0.951E 05	13.792	19.764	0.458	0.0
150- 6	1	FD	1.0670	1.7850	0.105E 06	15.240	0.991E 05	14.369	15.269	0.467	222.0
	7	S					0.112E 06	16.218	15.269	0.496	0.0
151- 4	1	FSS	1.1280	1.2860	0.871E 05	12.640	0.838E 05	12.153	21.194	0.430	210.0
	7	S					0.927E 05	13.451	21.194	0.452	0.0
151- *7	1	FSS	1.1450	1.9070	0.124E 06	17.950	0.119E 06	17.258	14.292	0.512	210.0
	7	S					0.132E 06	19.102	14.292	0.539	0.0
174- 5	9	FSS	0.7290	2.2630	0.696E 05	10.090	0.676E 05	9.800	12.044	0.386	220.0
	6	S					0.675E 05	9.795	12.044	0.386	0.0
174- *6	9	FSS	0.7290	2.3290	0.712E 05	10.320	0.691E 05	10.024	11.702	0.390	212.0
	6	S					0.691E 05	10.018	11.702	0.390	0.0
175- 3	9	FSS	0.7960	2.0750	0.747E 05	10.830	0.747E 05	10.833	13.135	0.406	210.0
	6	LD					0.711E 05	10.309	13.135	0.396	148.0
175- 4	9	FSS	0.7960	2.0850	0.751E 05	10.890	0.751E 05	10.893	13.072	0.407	210.0
	6	FSS					0.715E 05	10.366	13.072	0.397	156.0
176- 2	5	FSS	1.0360	1.1310	0.663E 05	9.620	0.602E 05	8.726	24.098	0.364	204.0
	7	S					0.685E 05	9.934	24.098	0.389	0.0
176- *4	5	FSS	1.1100	1.2490	0.809E 05	11.730	0.734E 05	10.639	21.821	0.402	206.0
	7	S					0.835E 05	12.113	21.821	0.429	0.0
177- 3	5	LD	0.8740	1.5850	0.712E 05	10.330	0.678E 05	9.833	17.195	0.387	196.0
	7	FD					0.691E 05	10.028	17.195	0.390	143.0
177- *4	5	LD	0.8690	1.6130	0.716E 05	10.380	0.681E 05	9.881	16.897	0.387	196.0
	7	FD					0.695E 05	10.076	16.897	0.391	143.0
178- 4	5	FD	1.0050	1.6770	0.927E 05	13.450	0.909E 05	13.189	16.252	0.448	216.0
	7	S					0.900E 05	13.056	16.252	0.445	0.0
178- 5	5	FD	0.9880	1.6860	0.905E 05	13.130	0.838E 05	12.875	16.165	0.442	0.0
	7	FSS					0.879E 05	12.746	16.165	0.440	148.0
179- 5	8	S	0.8320	1.7000	0.685E 05	9.930	0.660E 05	9.569	16.032	0.381	0.0
	6	FD					0.658E 05	9.547	16.032	0.381	145.0

TABLE VI - Continued

(h) MID LOW POSITION 070/032 - 100

RUN NO.	MODELS	MODEL BEHAVIOR	M(TEST)	SIGMA	Q(TEST) (N/M2)	Q(TEST) (PSI)	QADJ (N/M2)	QADJ (PSI)	MU	F.S.F.	FLUT FREQ (HZ)
131- 4	8	FD	0.6570	2.4830	0.718E 05	10.420	0.728E 05	10.564	10.977	0.401	200.0
	5	FD					0.796E 05	11.550	10.977	0.419	142.0
132- 4	1	FI	0.7220	1.9020	0.667E 05	9.680	0.624E 05	9.052	14.330	0.371	200.0
	6	S					0.705E 05	10.222	14.330	0.394	0.0
133- 3	1	FSS	0.7850	1.7810	0.725E 05	10.520	0.691E 05	10.020	15.303	0.390	200.0
	6	S					0.766E 05	11.109	15.303	0.411	0.0
133- *4	1	FSS	0.7820	1.8060	0.729E 05	10.570	0.694E 05	10.067	15.091	0.391	200.0
	6	S					0.770E 05	11.162	15.091	0.412	0.0
134- 4	1	S	0.8850	1.6760	0.832E 05	12.070	0.802E 05	11.631	16.262	0.420	0.0
	6	FSS					0.869E 05	12.603	16.262	0.438	143.0
134- *5	1	S	0.8940	1.7200	0.869E 05	12.600	0.837E 05	12.142	15.846	0.430	0.0
	6	FD					0.907E 05	13.156	15.846	0.447	143.0
135- 5	1	S	0.9990	1.6820	0.999E 05	14.490	0.943E 05	13.674	16.204	0.456	0.0
	7	FSS					0.942E 05	13.658	16.204	0.456	142.0
135- *6	1	S	1.0100	1.6970	0.103E 06	14.880	0.968E 05	14.042	16.061	0.462	0.0
	7	FSS					0.967E 05	14.026	16.061	0.462	142.0
136- *7	1	LO	0.9450	2.4270	0.125E 06	18.180	0.118E 06	17.155	11.230	0.511	214.0
	7	FD					0.119E 06	17.305	11.230	0.513	152.0
137- 4	8	FD	0.8130	1.6360	0.646E 05	9.370	0.655E 05	9.500	16.659	0.380	190.0
	4	FD					0.680E 05	9.857	16.659	0.387	146.0
139- 3	1	FSS	1.0370	1.4880	0.866E 05	12.560	0.796E 05	11.540	18.316	0.419	210.0
	5	S					0.894E 05	12.970	18.316	0.444	0.0
139- *4	1	FSS	1.0490	1.6290	0.955E 05	13.850	0.877E 05	12.726	16.731	0.440	215.0
	5	S					0.986E 05	14.303	16.731	0.466	0.0
140- 4	1	FSS	0.6920	2.3460	0.669E 05	9.700	0.632E 05	9.166	11.618	0.373	208.0
	5	S					0.691E 05	10.017	11.618	0.390	0.0
140- *5	1	FSS	0.6920	2.3920	0.680E 05	9.860	0.642E 05	9.318	11.394	0.376	205.0
	5	S					0.702E 05	10.182	11.394	0.393	0.0

TABLE VI - Continued

(i) FORWARD MID POSITION 070/040 - 100

RUN NO.	MODELS	MODEL BEHAVIOR	M(TEST)	SIGMA	Q(TEST) (N/M2)	Q(TEST) (PSI)	QADJ (N/M2)	QADJ (PSI)	MU	F.S.I.	FLUT FREQ (HZ)
56- 3	4	S	0.6450	3.0650	0.779E 05	11.300	0.701E 05	10.170	8.892	0.393	0.0
	3	FD					0.812E 05	11.781	8.892	0.423	160.0
56- *4	4	S	0.6480	3.1050	0.792E 05	11.480	0.712E 05	10.332	8.778	0.396	0.0
	3	FD					0.825E 05	11.968	8.778	0.426	0.0
60- 4	4	S	0.7160	2.2790	0.676E 05	9.810	0.632E 05	9.164	11.959	0.373	0.0
	2	FI					0.704E 05	10.218	11.959	0.394	164.0
61- 3	4	S	0.7580	1.8000	0.609E 05	8.840	0.553E 05	8.020	15.142	0.349	0.0
	2	FI					0.635E 05	9.207	15.142	0.374	160.0
61- *4	4	S	0.7600	1.8200	0.618E 05	8.960	0.560E 05	8.129	14.975	0.351	0.0
	2	S					0.643E 05	9.332	14.975	0.377	0.0
62- 2	4	S	0.8320	1.4470	0.588E 05	8.530	0.534E 05	7.739	18.835	0.343	0.0
	2	FSS					0.632E 05	9.161	18.835	0.373	149.0
62- *3	4	FD	0.8280	1.4810	0.596E 05	8.640	0.540E 05	7.839	18.403	0.345	150.0
	2	FD					0.640E 05	9.279	18.403	0.375	148.0
64- 2	6	S	0.8690	1.2320	0.551E 05	7.990	0.529E 05	7.680	22.122	0.342	0.0
	3	FD					0.594E 05	8.670	22.122	0.363	0.0
64- 4	6	FSS	0.8770	1.2690	0.576E 05	8.350	0.553E 05	8.026	21.477	0.349	130.0
	3	FSS					0.625E 05	9.060	21.477	0.371	130.0
67- 2	6	LD	0.8880	1.1680	0.543E 05	7.880	0.560E 05	8.122	23.335	0.351	178.0
	2	FD					0.585E 05	8.479	23.335	0.359	130.0
67- 3	6	FSS	0.9140	1.1690	0.572E 05	8.290	0.589E 05	8.545	23.315	0.360	129.0
	2	FD					0.615E 05	8.920	23.315	0.368	129.0
68- 2	6	LD	0.9340	1.0820	0.547E 05	7.940	0.547E 05	7.940	25.189	0.347	180.0
	3	FI					0.576E 05	8.358	25.189	0.366	125.0
68- 3	6	S	0.9340	1.0930	0.552E 05	8.000	0.552E 05	8.000	24.936	0.349	0.0
	3	S					0.581E 05	8.421	24.936	0.368	0.0
68- *8	6	S	1.1530	1.7470	0.115E 06	16.620	0.115E 06	16.620	15.601	0.503	0.0
	3	S					0.121E 06	17.496	15.601	0.516	0.0
69- 3	6	S	0.9000	1.1100	0.523E 05	7.590	0.523E 05	7.590	24.554	0.340	0.0
	3	FI					0.556E 05	8.069	24.554	0.360	126.0
69- 5	6	LD	0.9590	1.1420	0.598E 05	8.680	0.598E 05	8.680	23.866	0.363	180.0
	3	LD					0.636E 05	9.228	23.866	0.374	122.0
69- *7	6	LD	1.1030	1.4760	0.944E 05	13.690	0.944E 05	13.690	18.465	0.456	0.0
	3	LD					0.100E 06	14.555	18.465	0.470	0.0
172- 6	6	LD	0.9690	1.6790	0.863E 05	12.510	0.891E 05	12.919	16.233	0.443	200.0
	7	FD					0.968E 05	14.038	16.233	0.462	134.0
172- 7	6	FD	0.9640	1.6970	0.863E 05	12.520	0.891E 05	12.929	16.061	0.443	143.0
	7	FD					0.969E 05	14.049	16.061	0.462	130.0
187- 3	9	FI	1.1380	1.8330	0.119E 06	17.320	0.124E 06	17.919	14.869	0.522	220.0
	6	S					0.118E 06	17.149	14.869	0.510	0.0
187- 4	9	FSS	1.0560	2.0490	0.115E 06	16.700	0.119E 06	17.278	13.302	0.512	225.0
	6	S					0.114E 06	16.535	13.302	0.501	0.0
187- 5	9	FSS	0.9690	2.0960	0.101E 06	14.720	0.105E 06	15.229	13.003	0.481	190.0
	6	FD					0.100E 06	14.575	13.003	0.471	150.0

TABLE VI - Continued

(j) FORWARD LOW POSITION 070/040 - 100

RUN NO.	MODELS	MODEL BEHAVIOR	M(TEST)	SIGMA	Q(TEST) (N/M2)	Q(TEST) (PSI)	QADJ (N/M2)	QADJ (PSI)	MU	F.S.T.	FLUT FREQ (HZ)
70- *5	6	FSS	0.6510	3.5790	0.853E 05	12.370	0.862E 05	12.496	7.615	0.436	220.0
	3	LD					0.898E 05	13.022	7.615	0.445	216.0
71- 3	6	FSS	0.7180	2.4890	0.743E 05	10.780	0.736E 05	10.674	10.950	0.403	204.0
	3	S					0.806E 05	11.697	10.950	0.422	0.0
72- 3	6	FSS	0.7790	2.0770	0.728E 05	10.560	0.728E 05	10.560	13.122	0.401	195.0
	3	S					0.774E 05	11.227	13.122	0.413	0.0
72- *5	6	FD	0.7830	2.1490	0.756E 05	10.970	0.756E 05	10.970	12.683	0.408	200.0
	3	FD					0.804E 05	11.663	12.683	0.421	200.0
73- 3	6	FI	0.8460	1.6230	0.669E 05	9.710	0.690E 05	10.009	16.793	0.390	180.0
	3	FSS					0.704E 05	10.215	16.793	0.394	145.0
73- *5	6	FSS	0.8630	1.6770	0.714E 05	10.360	0.736E 05	10.679	16.252	0.403	184.0
	3	FD					0.751E 05	10.899	16.252	0.407	0.0
74- 3	6	FSS	0.8980	1.2740	0.603E 05	8.750	0.622E 05	9.019	21.393	0.370	129.0
	5	FD					0.655E 05	9.494	21.393	0.380	129.0
75- 6	6	S	1.1600	2.5040	0.154E 06	22.380	0.156E 06	22.607	10.885	0.586	0.0
	3	S					0.171E 06	24.831	10.885	0.614	0.0
128- 4	6	FI	0.8330	1.7820	0.800E 05	11.610	0.801E 05	11.624	15.295	0.420	196.0
	5	FD					0.898E 05	12.881	15.295	0.442	148.0
128- *5	6	FI	0.8400	1.8480	0.841E 05	12.200	0.842E 05	12.215	14.748	0.431	196.0
	5	FD					0.933E 05	13.536	14.748	0.454	148.0
130- 5	6	S	0.9790	1.4790	0.865E 05	12.550	0.885E 05	12.840	18.428	0.442	0.0
	4	FSS					0.929E 05	13.478	18.428	0.453	145.0
130- *6	6	FD	0.9660	1.4830	0.847E 05	12.280	0.866E 05	12.564	18.378	0.437	140.0
	4	FD					0.909E 05	13.188	18.378	0.448	140.0
170- 5	6	FI	0.9670	1.4720	0.743E 05	10.770	0.759E 05	11.002	18.516	0.409	192.0
	7	S					0.817E 05	11.857	18.516	0.424	0.0
170- 6	6	S	0.9360	1.5080	0.716E 05	10.380	0.731E 05	10.604	18.074	0.401	0.0
	7	FSS					0.788E 05	11.427	18.074	0.417	125.0
171- 5	6	S	0.9680	2.3070	0.109E 06	15.880	0.113E 06	16.399	11.814	0.499	0.0
	7	FSS					0.122E 06	17.689	11.814	0.518	149.0

TABLE VI - Continued

(k) MID UPPER POSITION 070/040 - 100

RUN NO.	MODELS	MODEL BEHAVIOR	M(TEST)	SIGMA	Q(TEST) (N/M2)	Q(TEST) (PSI)	QADJ (N/M2)	QADJ (PSI)	MU	F.S.I.	FLUT FREQ (HZ)
110- 5	8	FSS	0.6590	3.4310	0.936E 05	13.570	0.900E 05	13.058	7.944	0.445	500.0
	5	S					0.100E 06	14.573	7.944	0.471	160.0
111- 4	8	S	0.7930	2.0870	0.834E 05	12.090	0.826E 05	11.978	13.059	0.427	0.0
	5	FSS					0.877E 05	12.727	13.059	0.440	148.0
111- *5	8	S	0.7950	2.1230	0.850E 05	12.330	0.842E 05	12.216	12.838	0.431	0.0
	5	FSS					0.895E 05	12.980	12.838	0.444	145.0
112- 4	8	S	0.8680	1.5370	0.731E 05	10.600	0.732E 05	10.613	17.732	0.402	0.0
	5	FSS					0.769E 05	11.158	17.732	0.412	140.0
112- *5	8	S	0.8740	1.5660	0.752E 05	10.900	0.752E 05	10.913	17.404	0.407	0.0
	5	FSS					0.791E 05	11.474	17.404	0.418	140.0
113- 3	8	S	0.9270	1.2020	0.652E 05	9.450	0.652E 05	9.461	22.675	0.379	0.0
	5	FI					0.693E 05	10.047	22.675	0.391	130.0
113- *5	8	S	0.9980	1.5460	0.927E 05	13.450	0.928E 05	13.466	17.629	0.462	0.0
	5	LD					0.986E 05	14.299	17.629	0.466	0.0
114- 4	8	S	0.8940	1.3180	0.667E 05	9.680	0.661E 05	9.590	20.679	0.382	0.0
	5	FSS					0.710E 05	10.301	20.679	0.396	132.0
114- *5	8	S	0.9110	1.3760	0.716E 05	10.380	0.709E 05	10.284	19.807	0.395	0.0
	5	FSS					0.762E 05	11.046	19.807	0.410	135.0
115- *6	8	S	1.0390	1.4370	0.917E 05	13.300	0.909E 05	13.177	18.966	0.447	0.0
	5	S					0.985E 05	14.293	18.966	0.466	0.0
116- *5	8	S	0.7320	2.7680	0.911E 05	13.210	0.912E 05	13.226	9.846	0.448	0.0
	5	LD					0.989E 05	14.338	9.846	0.467	168.0
117- 4	8	S	0.8330	1.8330	0.796E 05	11.550	0.806E 05	11.688	14.869	0.421	0.0
	4	FSS					0.922E 05	11.927	14.869	0.426	156.0
117- *5	8	S	0.8430	1.8590	0.821E 05	11.910	0.831E 05	12.053	14.661	0.428	0.0
	4	FSS					0.848E 05	12.299	14.661	0.432	152.0
118- .1	8	S	0.9900	1.0290	0.640E 05	9.280	0.660E 05	9.571	26.487	0.381	150.0
	4	FSS					0.661E 05	9.583	26.487	0.382	126.0
118- .2	8	S	1.0100	1.0670	0.686E 05	9.950	0.709E 05	10.282	25.543	0.395	0.0
	4	LD					0.708E 05	10.275	25.543	0.395	130.0
118- *7	8	S	1.1160	2.2290	0.148E 06	21.490	0.153E 06	22.165	12.227	0.580	0.0
	4	LD					0.153E 06	22.192	12.227	0.581	140.0
119- 4	8	LD	0.6950	3.2450	0.941E 05	13.650	0.981E 05	14.231	8.399	0.465	484.0
	4	LD					0.961E 05	13.944	8.399	0.460	166.0
126- 2	6	S	0.9870	1.2790	0.777E 05	11.270	0.778E 05	11.284	21.310	0.414	0.0
	4	FI					0.745E 05	11.391	21.310	0.416	138.0
126- 3	6	S	1.0050	1.4430	0.898E 05	13.030	0.899E 05	13.046	18.888	0.445	0.0
	4	LD					0.908E 05	13.170	18.888	0.447	140.0
126- 6	6	LD	0.9390	1.7660	0.953E 05	13.820	0.954E 05	13.837	15.433	0.459	250.0
	4	FD					0.963E 05	13.969	15.433	0.461	150.0
127- 4	6	FSS	1.0640	1.5870	0.110E 06	15.930	0.111E 06	16.121	17.174	0.495	240.0
	6	LD					0.114E 06	16.522	17.174	0.501	170.0
127- *5	6	FSS	1.0640	1.6440	0.113E 06	16.390	0.114E 06	16.587	16.578	0.502	240.0
	6	FD					0.117E 06	16.999	16.578	0.508	152.0

TABLE VI - Continued

(1) MID MID POSITION 070/040 - 100

RUN NO.	MODELS	MODEL BEHAVIOR	M(TEST)	SIGMA	Q(TEST) (N/M2)	Q(TEST) (PSI)	QADJ (N/M2)	QADJ (PSI)	MU	F.S.I.	FLUT FREQ (HZ)
102- 3	6	S	0.7330	2.2650	0.799E 05	11.590	0.824E 05	11.954	12.033	0.426	0.0
	4	FSS					0.793E 05	11.496	12.033	0.418	155.0
103- *5	6	S	0.7850	1.8180	0.734E 05	10.640	0.749E 05	10.859	14.992	0.406	0.0
	4	FI					0.736E 05	10.669	14.992	0.403	152.0
104- 4	6	S	0.8690	1.4500	0.704E 05	10.210	0.718E 05	10.420	18.796	0.398	0.0
	4	FSS					0.705E 05	10.222	18.796	0.394	146.0
104- *5	6	S	0.8650	1.4780	0.712E 05	10.320	0.726E 05	10.531	18.440	0.400	0.0
	4	FSS					0.712E 05	10.332	18.440	0.396	142.0
105- 4	6	S	0.9730	1.3440	0.791E 05	11.470	0.807E 05	11.706	20.279	0.422	0.0
	4	FSS					0.809E 05	11.735	20.279	0.422	130.0
105- *5	6	S	0.9760	1.3790	0.814E 05	11.810	0.831E 05	12.053	19.764	0.428	0.0
	4	FSS					0.833E 05	12.083	19.764	0.428	136.0
106- 4	6	S	0.9840	1.2210	0.722E 05	10.470	0.737E 05	10.686	22.322	0.403	0.0
	4	FSS					0.731E 05	10.596	22.322	0.401	132.0
106- *5	6	S	0.9950	1.2190	0.733E 05	10.630	0.748E 05	10.849	22.358	0.406	0.0
	4	FSS					0.742E 05	10.757	22.358	0.404	132.0
107- 6	6	S	0.6600	3.1590	0.874E 05	12.670	0.892E 05	12.931	8.628	0.443	0.0
	4	FSS					0.875E 05	12.685	8.628	0.439	170.0
108- 4	6	S	1.1470	1.4720	0.109E 06	15.760	0.111E 06	16.085	18.516	0.494	0.0
	4	FI					0.108E 06	15.633	18.516	0.487	170.0
124- 3	6	S	0.8990	1.2840	0.668E 05	9.690	0.657E 05	9.524	21.227	0.380	0.0
	4	FSS					0.668E 05	9.693	21.227	0.384	140.0
125- 2	6	S	1.1090	1.4270	0.104E 06	15.070	0.104E 06	15.111	19.099	0.479	0.0
	4	S					0.103E 06	14.930	19.099	0.476	0.0
125- 3	6	LD	1.0940	1.5530	0.109E 06	15.760	0.109E 06	15.803	17.550	0.490	230.0
	4	LD					0.108E 06	15.614	17.550	0.487	142.0
125- 4	6	FSS	1.0590	1.6290	0.107E 06	15.540	0.107E 06	15.582	16.731	0.487	205.0
	4	S					0.106E 06	15.396	16.731	0.484	0.0
160- *5	1	LD	1.1800	1.6820	0.118E 06	17.090	0.109E 06	15.801	16.204	0.490	210.0
	6	S					0.125E 06	18.187	16.204	0.526	0.0
161- 1	1	S	0.9080	1.1090	0.532E 05	7.710	0.492E 05	7.130	24.576	0.329	0.0
	6	FI					0.585E 05	8.488	24.576	0.359	120.0
161- 3	1	LD	1.0980	1.3610	0.874E 05	12.680	0.809E 05	11.727	20.026	0.422	190.0
	6	LD					0.962E 05	13.959	20.026	0.461	132.0
161- 5	1	FSS	1.1220	1.7760	0.114E 06	16.490	0.105E 06	15.250	15.346	0.481	225.0
	6	LD					0.125E 06	18.154	15.346	0.525	146.0
161- 6	1	LD	1.0570	2.0480	0.117E 06	16.980	0.108E 06	15.703	13.308	0.488	218.0
	6	LD					0.129E 06	18.693	13.308	0.533	150.0
161- 7	1	S	1.0190	2.1660	0.115E 06	16.640	0.106E 06	15.389	12.583	0.484	0.0
	6	FSS					0.126E 06	18.319	12.583	0.528	159.0

TABLE VI - Continued

(m) MID LOW POSITION 070/040 - 100

RUN NO.	MODELS	MODEL BEHAVIOR	M(TEST)	SIGMA	Q(TEST) (N/M2)	Q(TEST) (PSI)	QADJ (N/M2)	QADJ (PSI)	MU	F.S.I.	FLUT FREQ (HZ)
94- *5	8	S	0.6550	3.7030	0.830E 05	12.040	0.799E 05	11.586	7.360	0.420	0.0
	4	S					0.807E 05	11.708	7.360	0.422	0.0
95- 3	6	FSS	0.7260	2.6650	0.827E 05	12.000	0.853E 05	12.369	10.227	0.434	205.0
	5	LD					0.844E 05	12.247	10.227	0.431	160.0
95- 4	6	FSS	0.7380	2.6820	0.854E 05	12.390	0.881E 05	12.771	10.162	0.441	205.0
	5	FI					0.872E 05	12.645	10.162	0.438	167.0
96- 4	6	S	0.7810	2.0740	0.748E 05	10.850	0.764E 05	11.074	13.141	0.410	0.0
	3	FSS					0.903E 05	11.652	13.141	0.421	150.0
97- 3	6	S	0.8610	1.4710	0.651E 05	9.440	0.671E 05	9.730	18.528	0.385	0.0
	3	FSS					0.706E 05	10.243	18.528	0.395	140.0
97- 5	6	FSS	0.8680	1.5250	0.683E 05	9.910	0.704E 05	10.215	17.872	0.394	138.0
	3	FD					0.741E 05	10.753	17.872	0.404	138.0
98- 6	6	S	0.9960	1.8460	0.976E 05	14.160	0.103E 06	14.906	14.764	0.476	0.0
	5	FSS					0.987E 05	14.312	14.764	0.466	150.0
98- *7	6	S	0.9990	1.8850	0.996E 05	14.440	0.105E 06	15.201	14.459	0.481	0.0
	5	FSS					0.101E 06	14.595	14.459	0.471	150.0
99- 5	6	S	1.1380	1.4040	0.938E 05	13.610	0.977E 05	14.176	19.412	0.464	0.0
	5	S					0.948E 05	13.756	19.412	0.457	142.0
100- 5	6	FSS	0.8440	2.1440	0.858E 05	12.450	0.876E 05	12.707	12.712	0.439	220.0
	5	FD					0.850E 05	12.327	12.712	0.433	152.0
120- 2	8	S	0.9880	1.1460	0.705E 05	10.220	0.698E 05	10.125	23.783	0.392	0.0
	7	FI					0.719E 05	10.431	23.783	0.398	124.0
120- 3	8	S	0.9970	1.2610	0.776E 05	11.250	0.768E 05	11.146	21.614	0.412	0.0
	7	FI					0.792E 05	11.482	21.614	0.418	120.0
120- 5	8	S	0.9090	1.3840	0.712E 05	10.330	0.706E 05	10.234	19.693	0.394	0.0
	7	LD					0.727E 05	10.543	19.693	0.400	130.0
120- 6	8	S	0.8780	1.4140	0.676E 05	9.800	0.669E 05	9.709	19.275	0.384	0.0
	7	FI					0.690E 05	10.002	19.275	0.390	126.0
121- 3	8	FSS	1.0410	1.3670	0.898E 05	13.020	0.899E 05	13.036	19.938	0.445	204.0
	7	FI					0.945E 05	13.706	19.938	0.456	142.0
121- 4	8	S	1.0480	1.5340	0.101E 06	14.660	0.101E 06	14.678	17.767	0.472	0.0
	7	S					0.106E 06	15.432	17.767	0.484	0.0
121- 5	8	FSS	1.0520	1.6840	0.111E 06	16.090	0.111E 06	16.109	16.185	0.495	220.0
	7	FSS					0.117E 06	16.938	16.185	0.507	145.0
122- 3	8	LD	0.9240	1.3690	0.732E 05	10.620	0.719E 05	10.423	19.909	0.398	188.0
	4	FSS					0.720E 05	10.438	19.909	0.398	139.0
122- *4	8	LD	0.9340	1.4050	0.765E 05	11.090	0.750E 05	10.884	19.398	0.407	164.0
	4	FSS					0.752E 05	10.900	19.398	0.407	136.0
123- 4	8	FD	0.7020	2.6490	0.864E 05	12.530	0.865E 05	12.545	10.289	0.437	213.0
	4	FI					0.865E 05	12.545	10.289	0.437	164.0
123- *5	8	FD	0.6940	2.7250	0.864E 05	12.530	0.965E 05	12.545	10.002	0.437	210.0
	4	FSS					0.965E 05	12.545	10.002	0.437	164.0
168- 4	6	FI	0.8160	2.0980	0.806E 05	11.690	0.839E 05	12.176	12.991	0.430	190.0
	6	FD					0.790E 05	11.460	12.991	0.417	153.0
169- 4	6	FSS	1.0230	1.4670	0.836E 05	12.130	0.845E 05	12.261	18.579	0.432	199.0
	7	S					0.967E 05	14.030	18.579	0.462	0.0
169- 5	6	LD	1.0190	1.5420	0.865E 05	12.550	0.875E 05	12.685	17.675	0.439	196.0
	7	LD					0.100E 06	14.515	17.675	0.470	130.0
169- 6	6	S	0.9900	1.6040	0.853E 05	12.370	0.862E 05	12.503	16.992	0.436	0.0
	7	FSS					0.986E 05	14.307	16.992	0.466	127.0

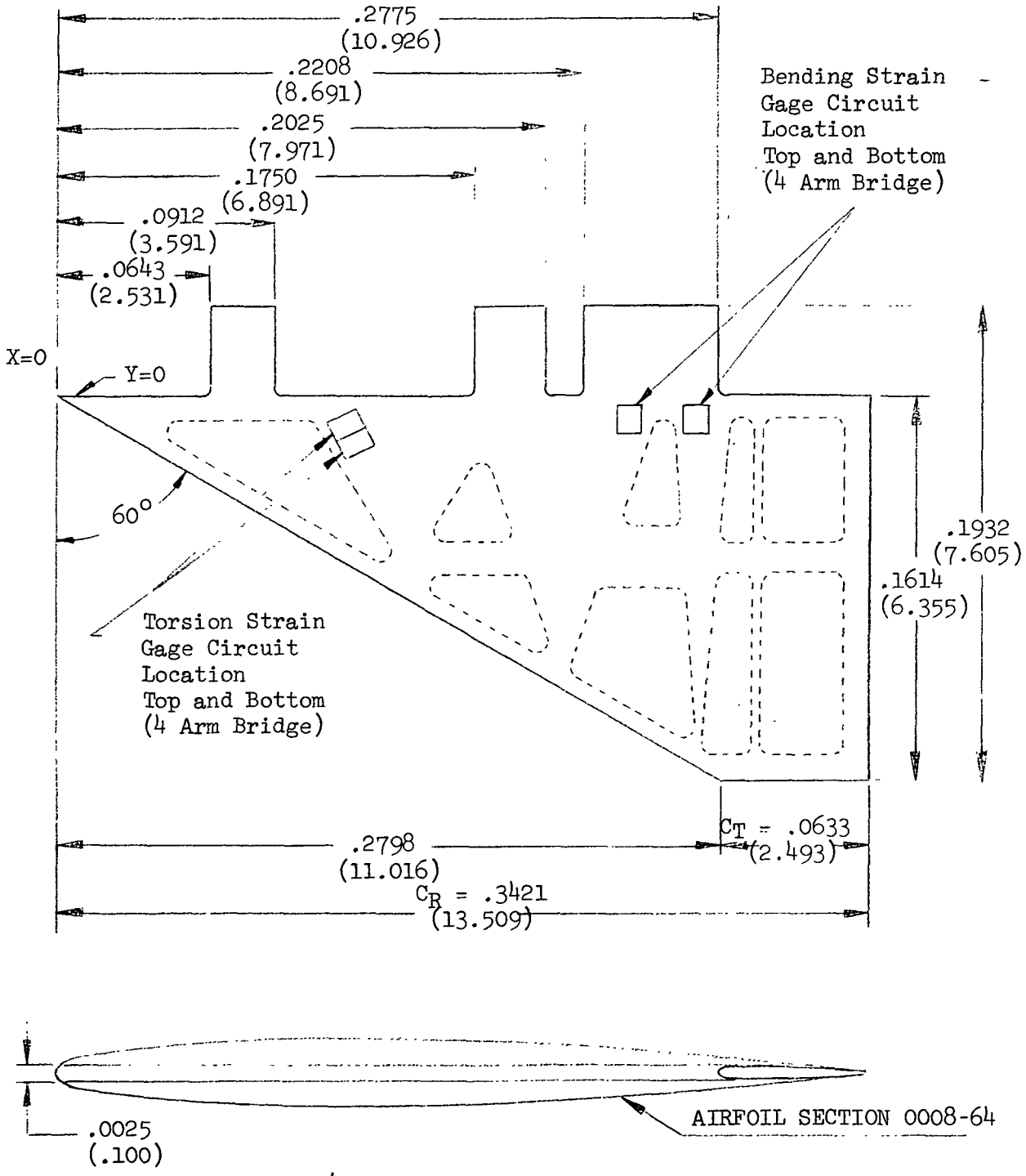

Figure 1 1/80 Scale 100 Booster Model

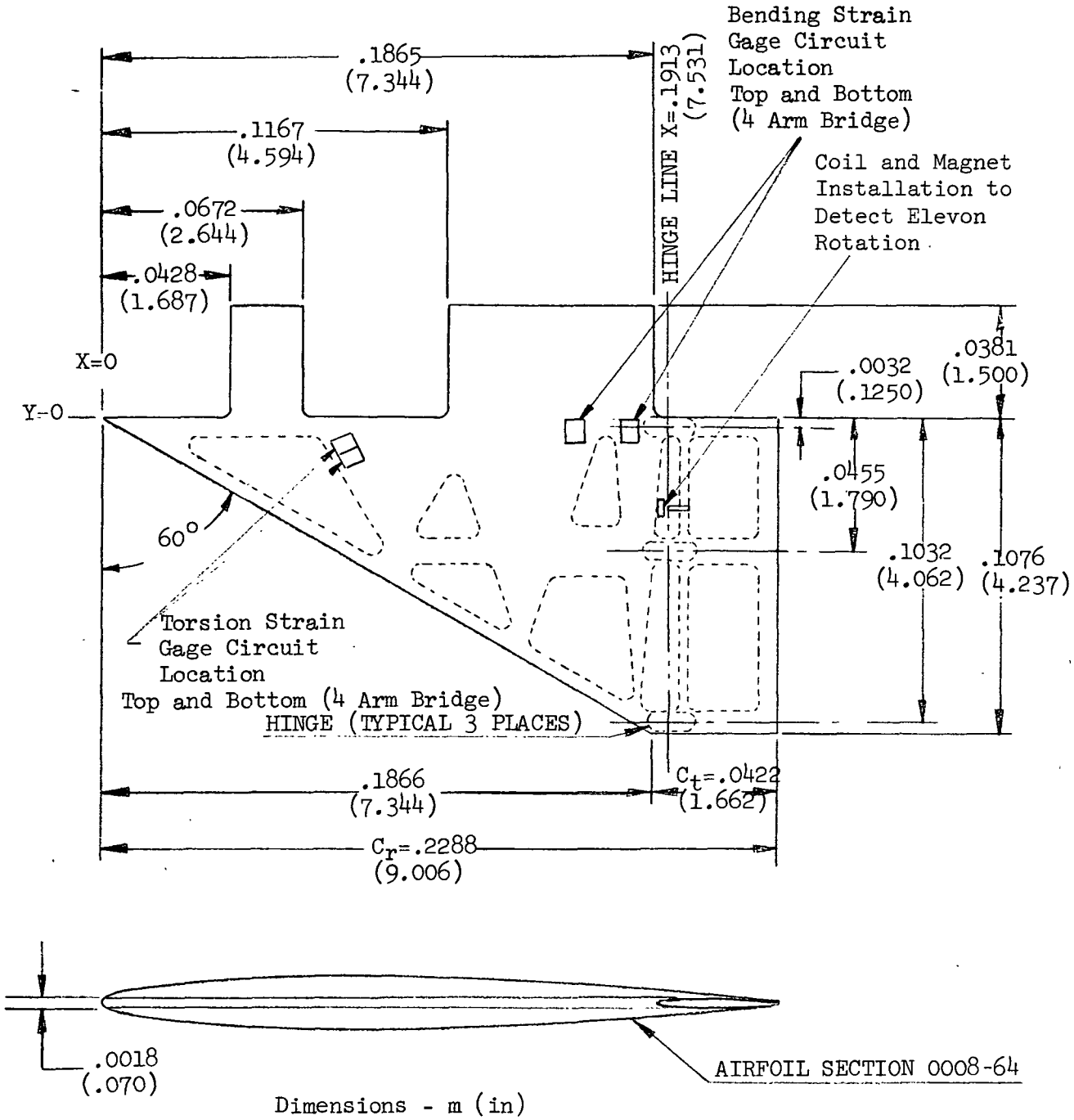

Figure 2 1/80 Scale 070 Orbiter Model

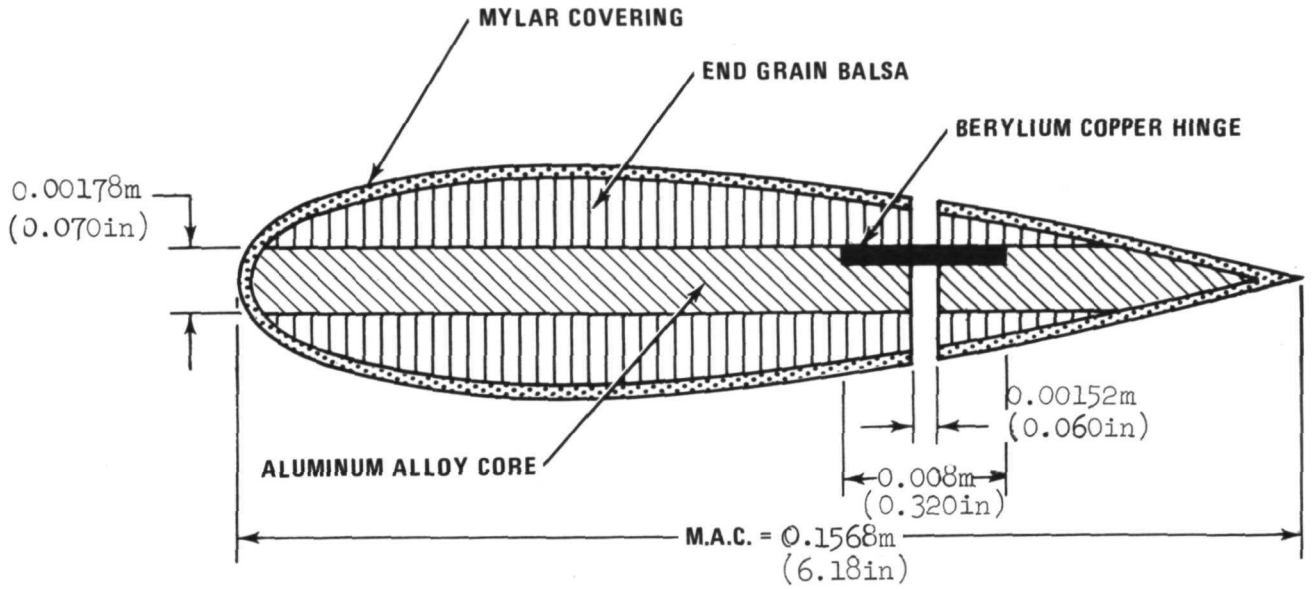

Figure 3. Section of Leading Wing Showing Control Surface Detail (Not to Scale)

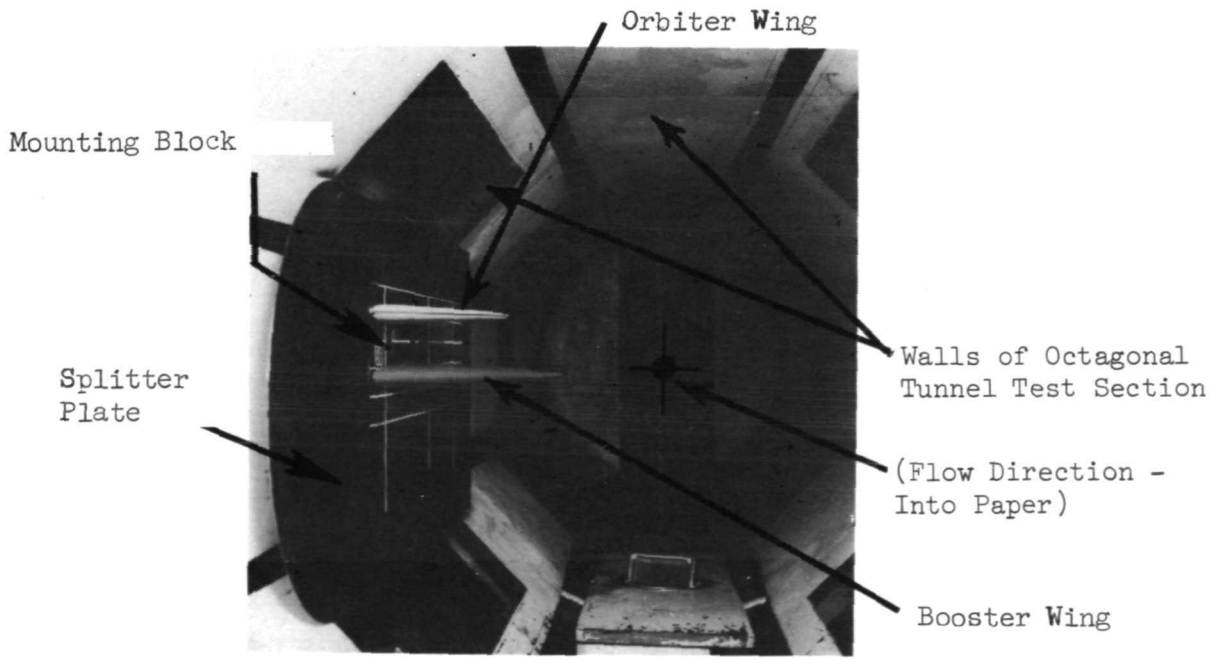

Figure 4. Test Wings in Tunnel

(a) Frequency = 129.5 Hz Damping Coefficient .016

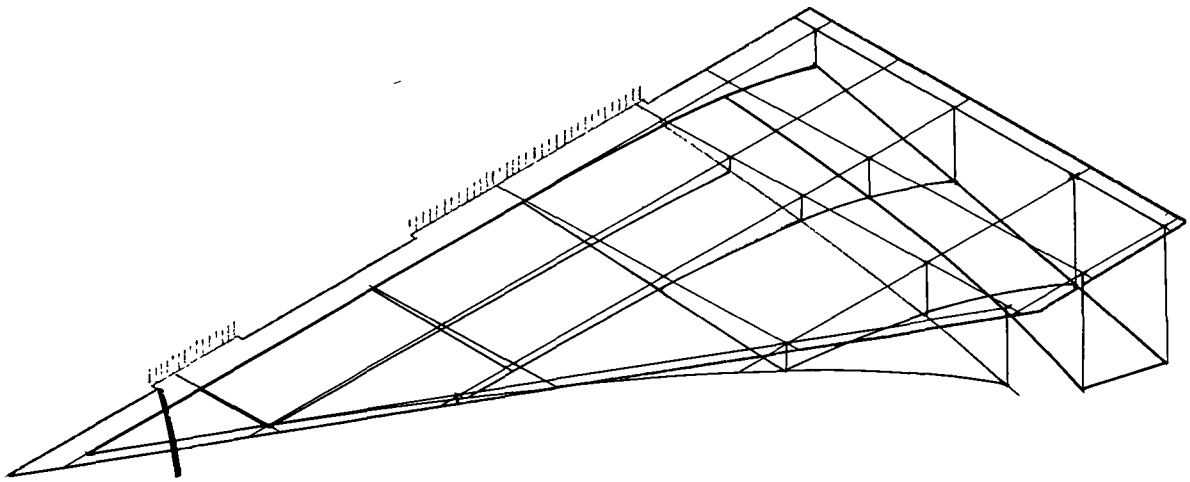

Point	Normalized Deflection	Point	Normalized Deflection	Point	Normalized Deflection
1	-.003	9	.030	17	.556
2	.002	10	.059	18	.211
3	.007	11	.098	19	.378
4	.011	12	.047	20	.800
5	.014	13	.060	21	.578
6	.111	14	.111	22	.856
7	.244	15	.178	23	1.00
8	.008	16	.300		

Figure 5. Mode Shape Data, 1/80th Scale 070/032 Orbiter

(b) Frequency = 261.4 Hz Damping Coefficient .018

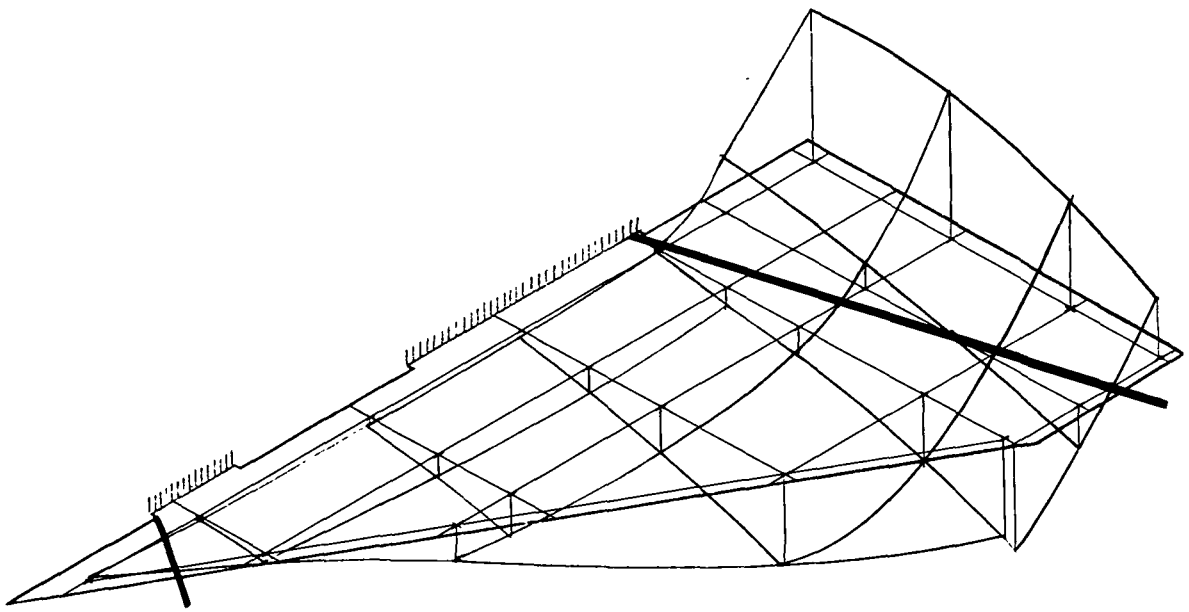

Point	Normalized Deflection	Point	Normalized Deflection	Point	Normalized Deflection
1	-.015	9	.150	17	-.980
2	.009	10	.150	18	.600
3	.050	11	.065	19	.470
4	.040	12	.240	20	-.690
5	-.003	13	.280	21	.650
6	-.370	14	.300	22	.280
7	-1.000	15	.170	23	-.400
8	.050	16	-.170		

Fig. 5 Continued

(c) Frequency = 385 Hz Damping Coefficient . 023

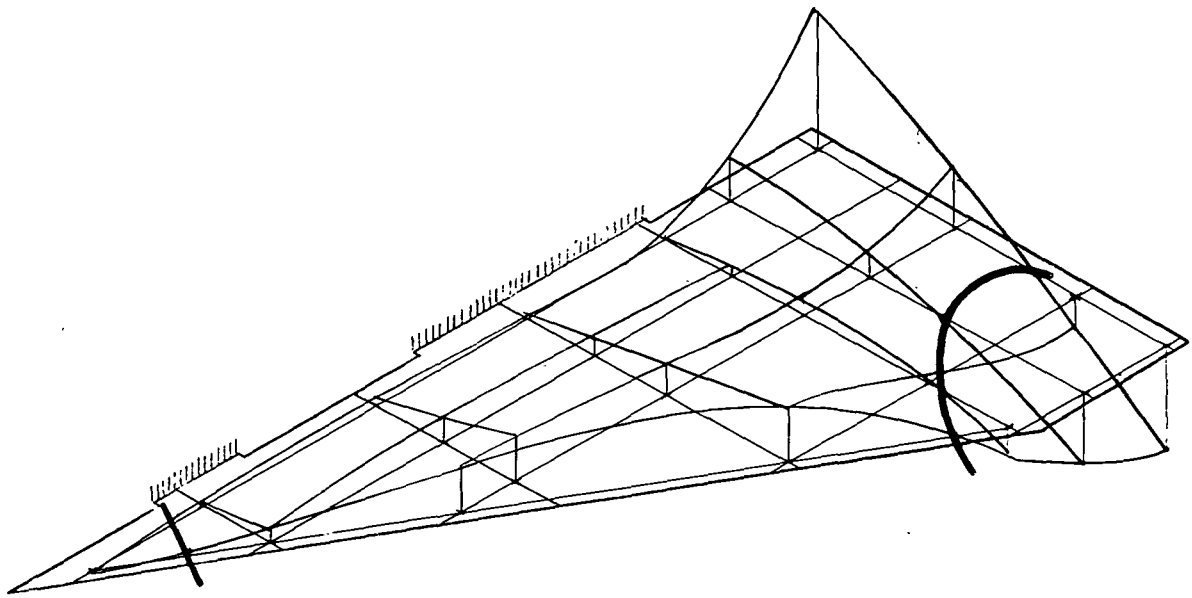

Point	Normalized Deflection	Point	Normalized Deflection	Point	Normalized Deflection
1	.022	9	-.182	17	-.455
2	-.011	10	-.127	18	-.400
3	-.069	11	-.073	19	-.045
4	-.036	12	-.327	20	.236
5	-.018	13	-.345	21	.182
6	-.309	14	-.236	22	.509
7	-1.00	15	-.127	23	.745
8	-.615	16	-.182		

Fig.5 Continued

(d) Frequency = 581.2 Hz Damping Coefficient .013

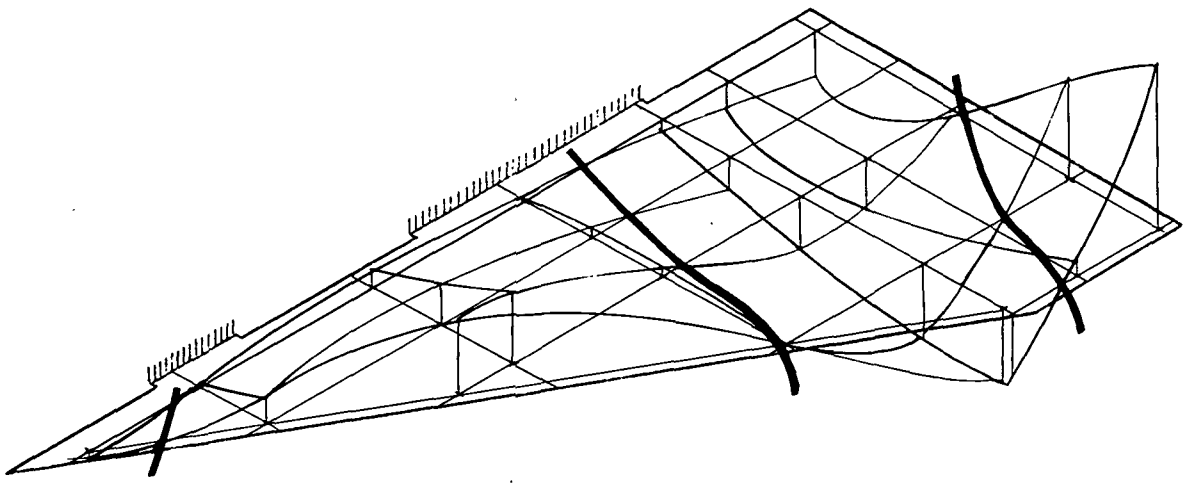

Point	Normalized Deflection	Point	Normalized Deflection	Point	Normalized Deflection
1	-.042	9	.242	17	-.048
2	.027	10	.045	18	.021
3	.106	11	-.197	19	-.455
4	.024	12	.455	20	.606
5	-.055	13	.424	21	-.455
6	-.167	14	.058	22	.085
7	-.273	15	-.303	23	1.000
8	.145	16	-.303		

Fig. 5 Continued

(e) Frequency = 656 Hz Damping Coefficient .015

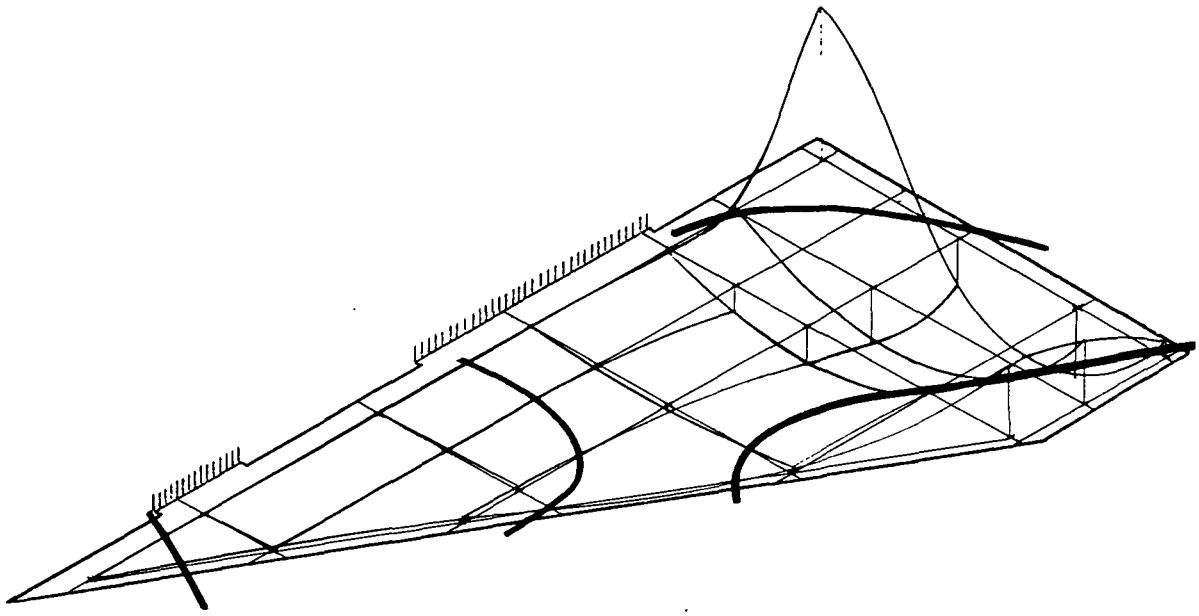

Point	Normalized Deflection	Point	Normalized Deflection	Point	Normalized Deflection
1	-.010	9	.019	17	-.308
2	0	10	-.035	18	.036
3	.012	11	-.169	19	0
4	-.013	12	.042	20	-.462
5	-.032	13	.035	21	.462
6	.033	14	-.046	22	.423
7	1.000	15	-.254	23	.112
8	.015	16	-.362		

Fig. 5 Concluded

(a) Frequency = 129.8 Hz Damping Coefficient .014

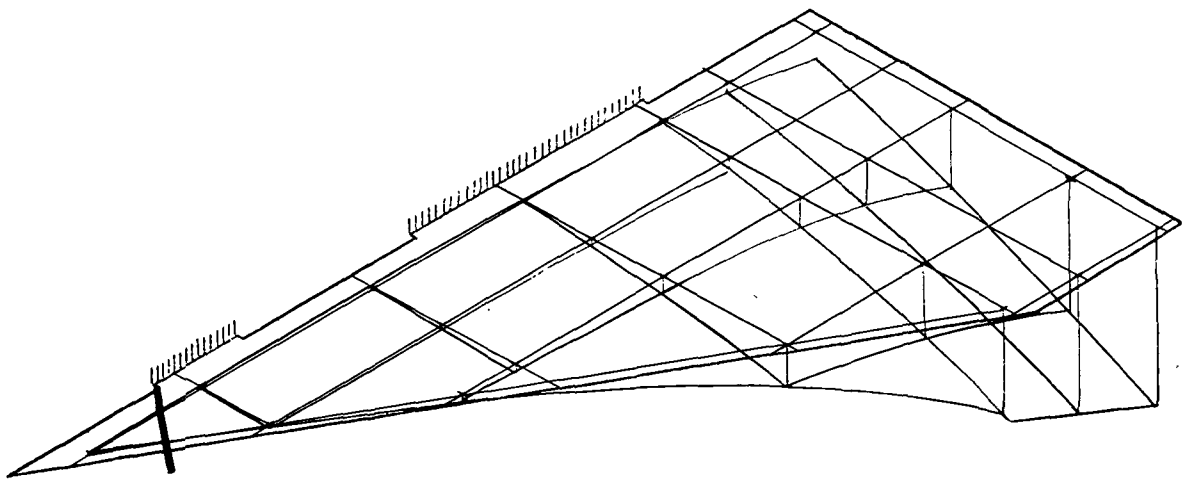

Point	Normalized Deflection	Point	Normalized Deflection	Point	Normalized Deflection
1	-.003	9	.021	17	.441
2	.002	10	.036	18	.227
3	.003	11	.061	19	.412
4	.005	12	.033	20	.739
5	.006	13	.042	21	.588
6	.047	14	.101	22	.756
7	.149	15	.160	23	1.000
8	.005	16	.261		

Figure 6. Mode Shape Data, 1/80th Scale, 070/040 Orbiter

(b) Frequency = 283.8 Hz Damping Coefficient .017

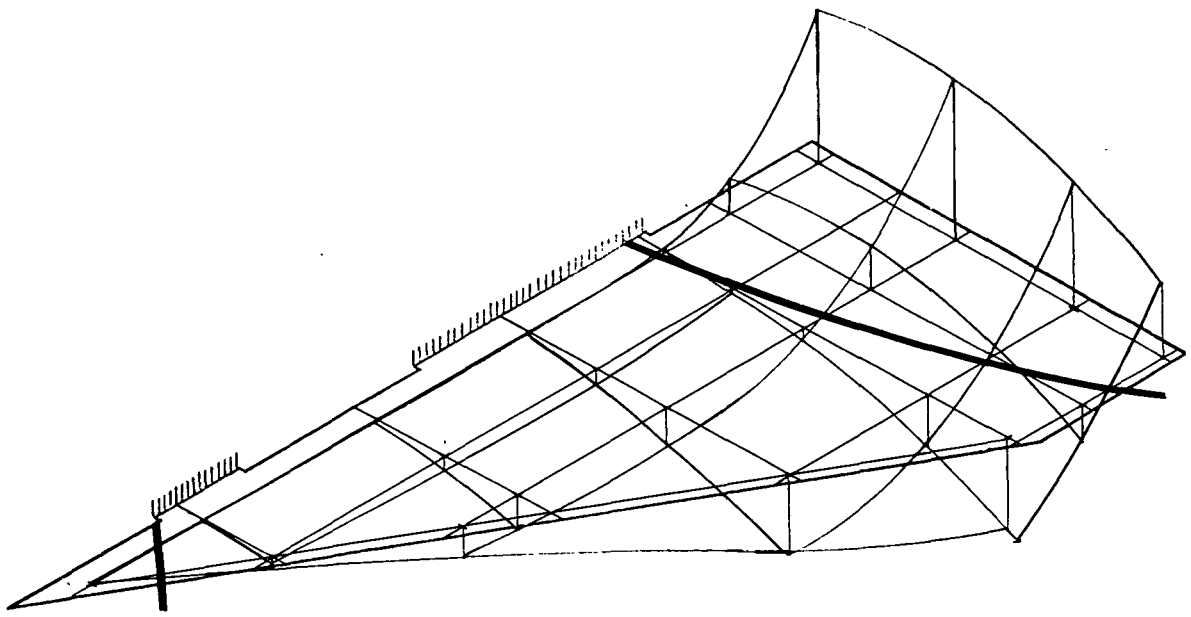

Point	Normalized Deflection	Point	Normalized Deflection	Point	Normalized Deflection
1	.011	9	-.088	17	1.000
2	-.009	10	-.091	18	-.488
3	-.029	11	-.029	19	-.319
4	-.017	12	-.194	20	.800
5	.003	13	-.213	21	-.569
6	.219	14	-.225	22	-.225
7	.950	15	-.084	23	.456
8	-.041	16	.275		

Fig. 6 Continued

(c) Frequency = 393.6 Hz Damping Coefficient .013

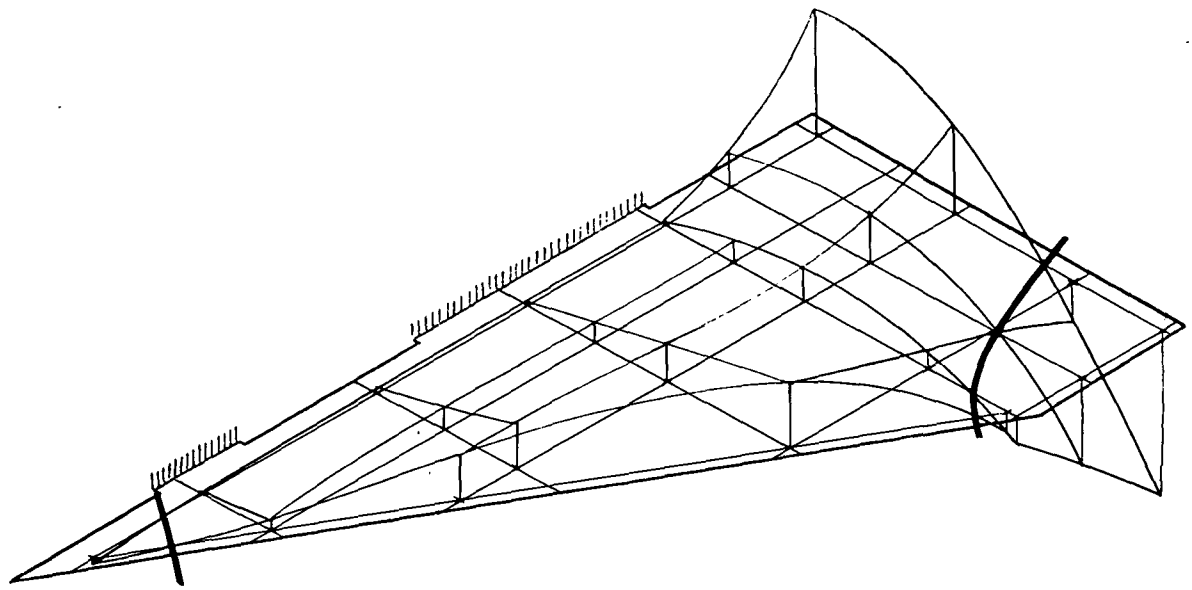

Point	Normalized Deflection	Point	Normalized Deflection	Point	Normalized Deflection
1	.028	9	-.137	17	-.554
2	-.009	10	-.117	18	-.400
3	-.038	11	-.123	19	-.109
4	-.018	12	-.274	20	.240
5	-.011	13	-.286	21	.132
6	-.209	14	-.248	22	.538
7	-.754	15	-.203	23	1.000
8	-.062	16	-.308		

Fig.6 Continued

(d) Frequency = 592.8 Hz Damping Coefficient .015

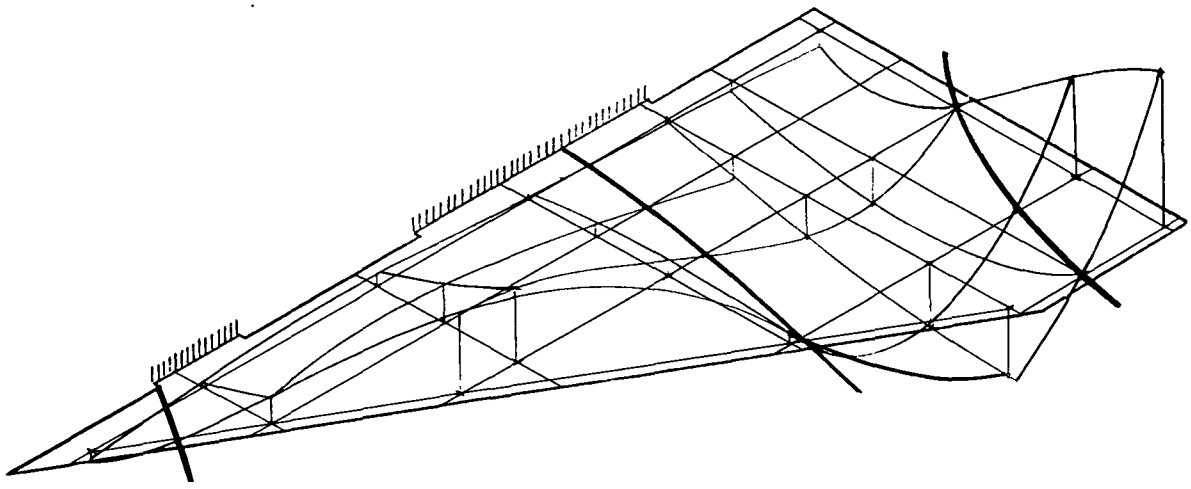

Point	Normalized Deflection	Point	Normalized Deflection	Point	Normalized Deflection
1	-.061	9	.245	17	.013
2	.032	10	.077	18	.071
3	.087	11	-.148	19	-.419
4	.019	12	.516	20	.645
5	-.019	13	.452	21	-.452
6	-.077	14	.097	22	0
7	-.090	15	-.271	23	1.000
8	.161	16	-.310		

Fig. 6 Continued

(e) Frequency = 726.9 Hz Damping Coefficient .015

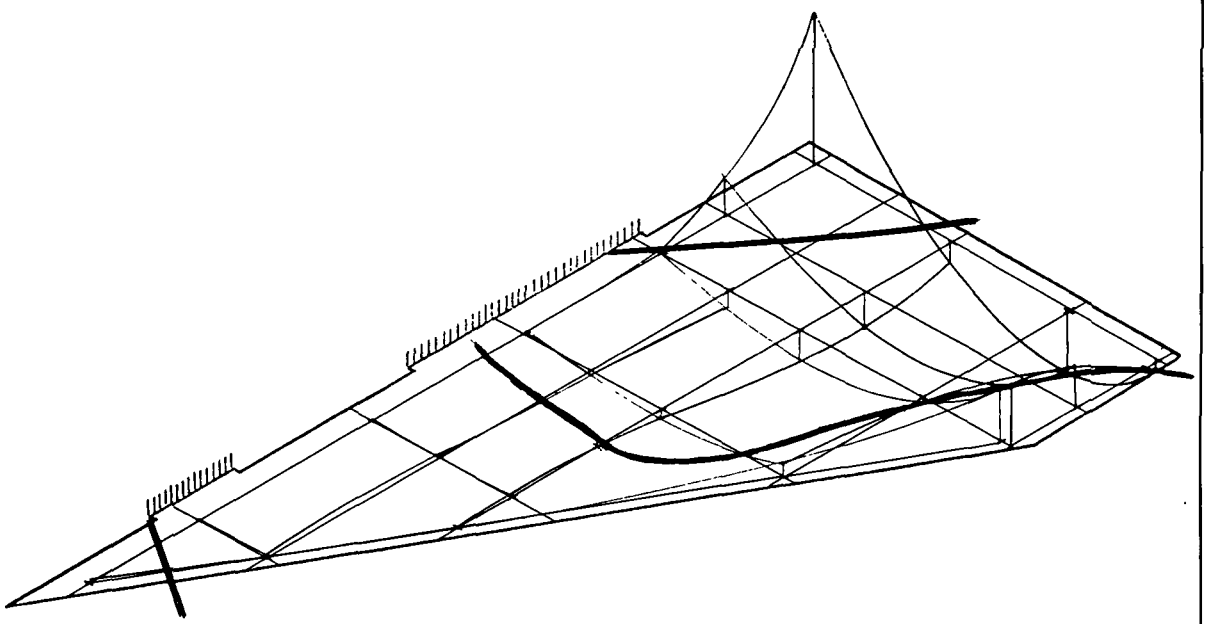

Point	Normalized Deflection	Point	Normalized Deflection	Point	Normalized Deflection
1	0	9	-.006	17	.104
2	.004	10	.024	18	-.086
3	.004	11	.116	19	.018
4	.008	12	-.010	20	.416
5	.010	13	-.008	21	-.360
6	-.240	14	.042	22	-.280
7	-1.00	15	.210	23	.068
8	-.006	16	.240		

Fig. 6 Concluded

(a) Frequency = 104.0 Hz Damping Coefficient .022

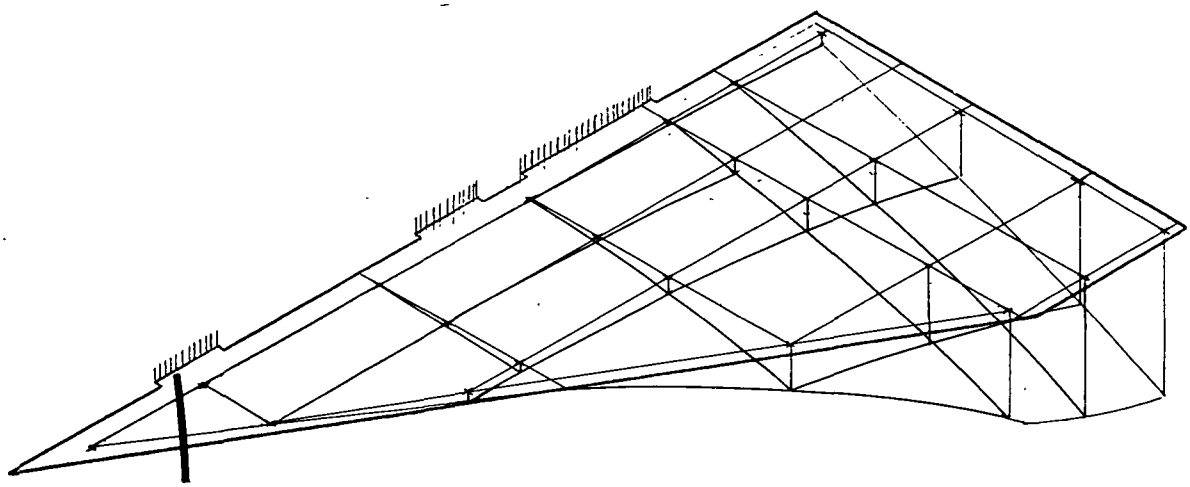

Point	Normalized Deflection	Point	Normalized Deflection	Point	Normalized Deflection
1	- .009	9	.021	17	.385
2	.006	10	.046	18	.266
3	.006	11	.076	19	.474
4	0	12	.043	20	.755
5	.006	13	.052	21	.651
6	.006	14	.113	22	.835
7	.058	15	.199	23	1.00
8	.003	16	.260		

Figure 7. Mode Shape Data, 1/80th Scale, 100 Booster

(b) Frequency = 223.0 Hz Damping Coefficient .026

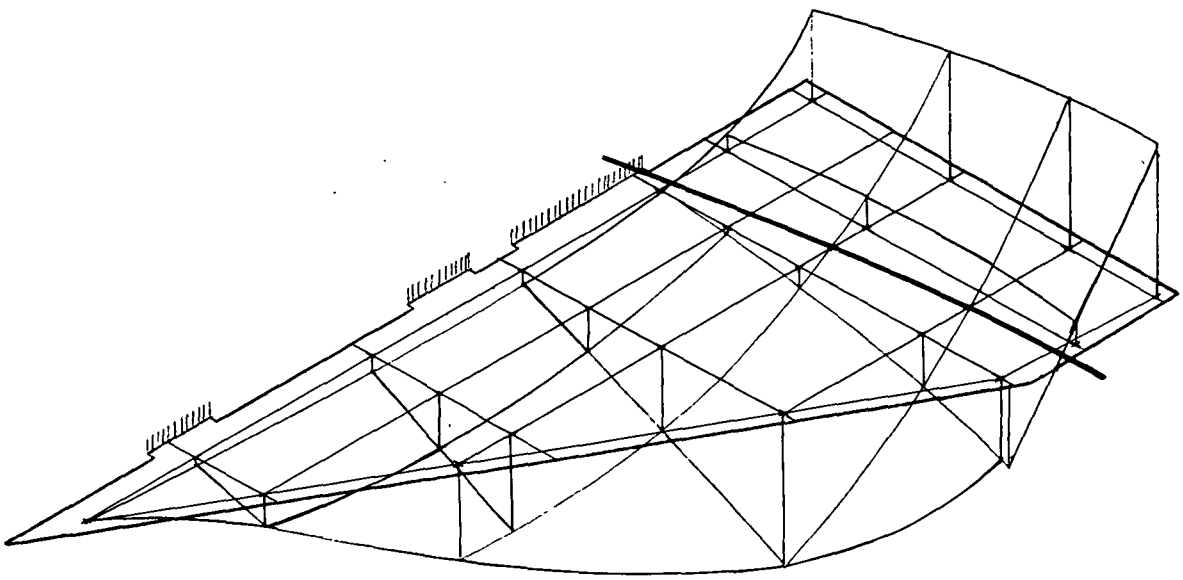

Point	Normalized Deflection	Point	Normalized Deflection	Point	Normalized Deflection
1	.015	9	.338	17	-.863
2	.050	10	.263	18	.999
3	.097	11	.034	19	.346
4	.061	12	.605	20	-1.00
5	.018	13	.639	21	.526
6	-.097	14	.528	22	-.148
7	-.588	15	.130	23	-1.00
8	.196	16	-.199		

Fig. 7 Continued

(c) Frequency = 328.0 Hz Damping Coefficient .025

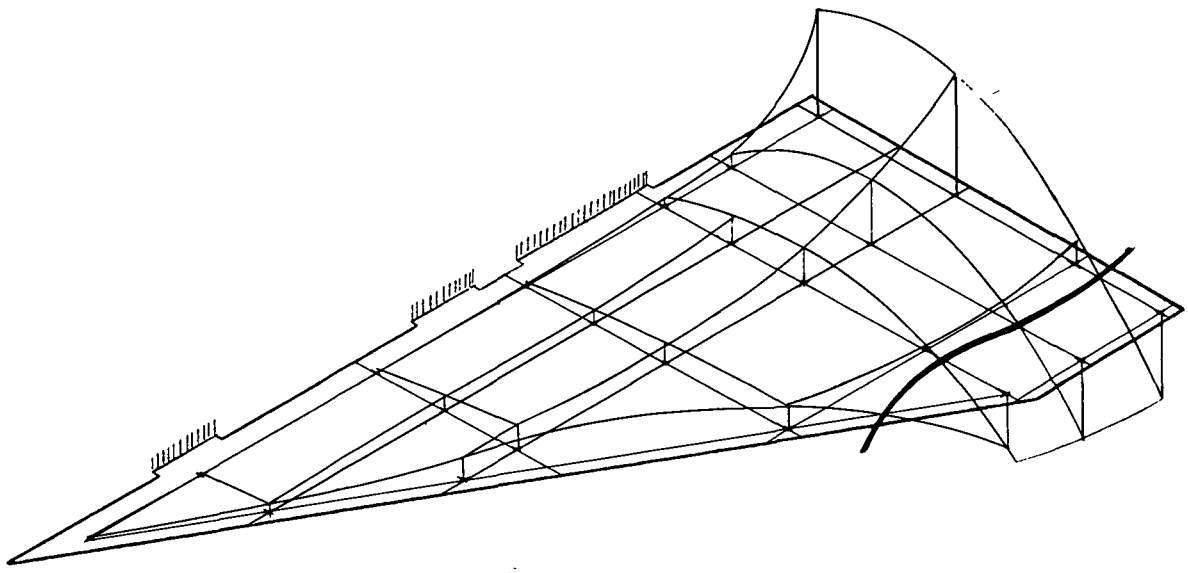

Point	Normalized Deflection	Point	Normalized Deflection	Point	Normalized Deflection
1	.018	9	.119	17	1.00
2	.031	10	.108	18	.192
3	.039	11	.200	19	.049
4	.035	12	.214	20	.204
5	.062	13	.219	21	-.463
6	.109	14	.164	22	-.623
7	.880	15	.292	23	-.683
8	.084	16	.517		

Fig. 7 Continued

(d) Frequency = 460 Hz Damping Coefficient .025

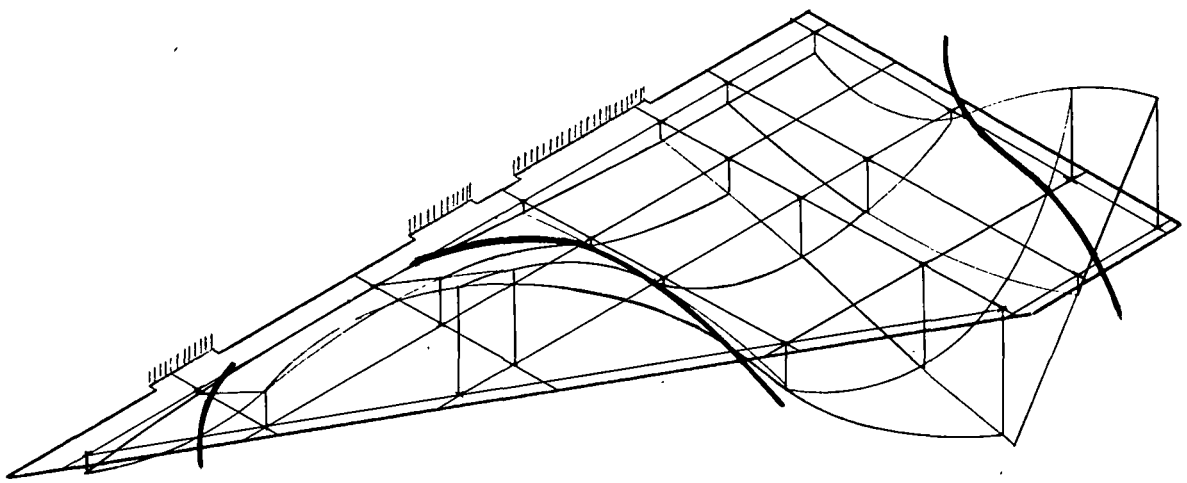

Point	Normalized Deflection	Point	Normalized Deflection	Point	Normalized Deflection
1	.126	9	-.349	17	.074
2	.034	10	.040	18	.343
3	-.040	11	.246	19	.794
4	.086	12	-.840	20	-.691
5	.126	13	-.737	21	.949
6	.166	14	.063	22	.160
7	.171	15	.440	23	-1.00
8	-.269	16	.405		

Fig.7 Continued

(e) Frequency = 613 Hz Damping Coefficient .024

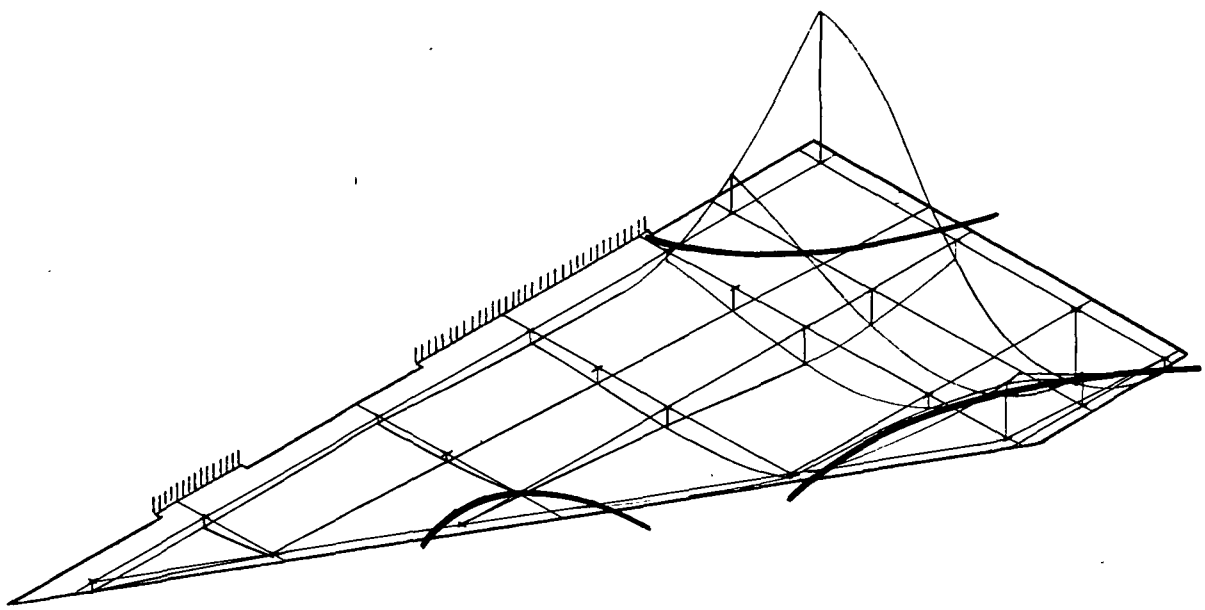

Point	Normalized Deflection	Point	Normalized Deflection	Point	Normalized Deflection
1	.073	9	.029	17	.136
2	.068	10	.112	18	.039
3	.058	11	.146	19	.092
4	.083	12	-.024	20	.500
5	.078	13	0	21	-.364
6	-.252	14	.136	22	-.209
7	-1.00	15	.248	23	.068
8	.024	16	.238		

Fig. 7 Concluded

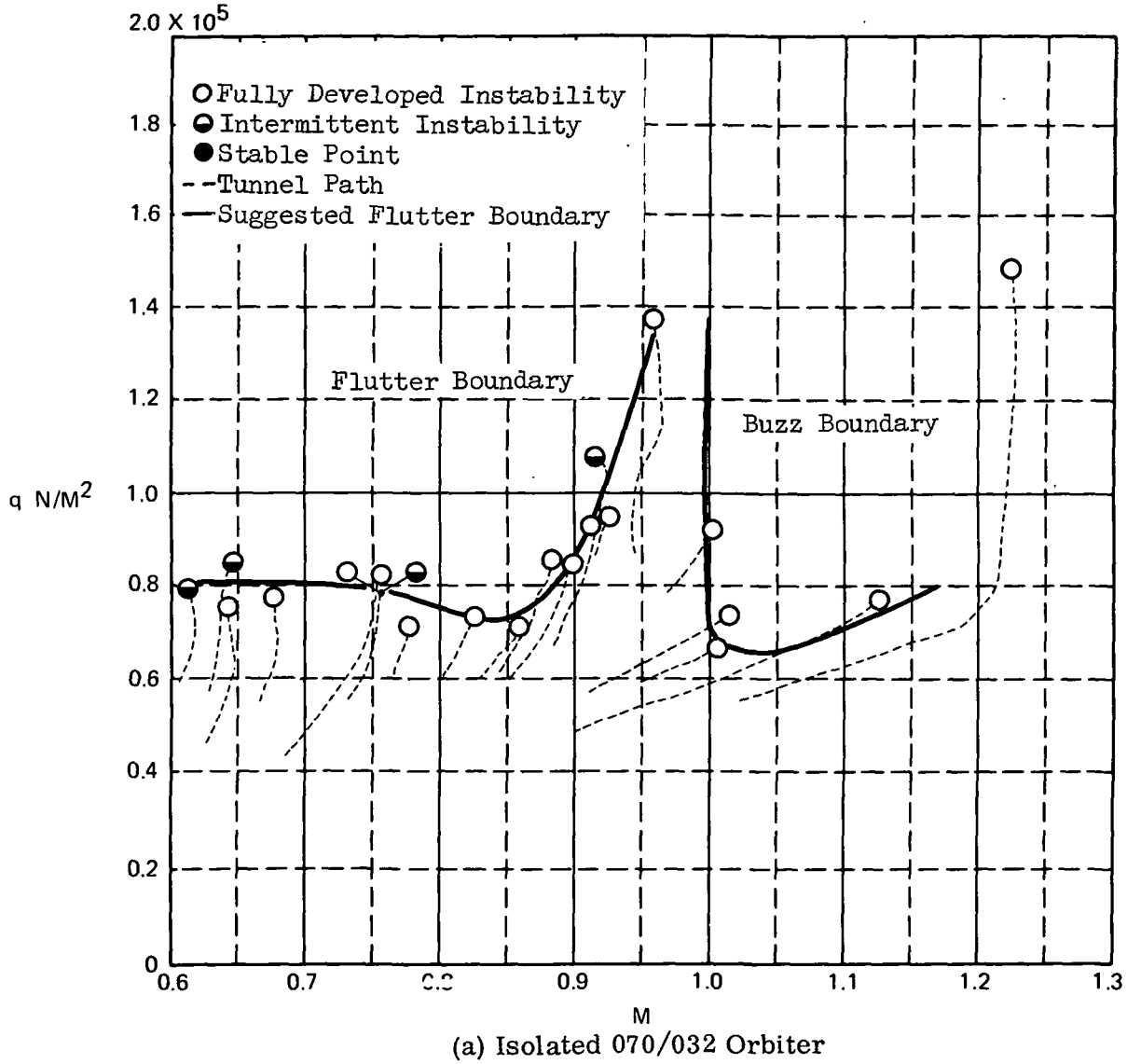

(a) Isolated 070/032 Orbiter

Figure 8 Variation of Dynamic Pressure with Mach Number

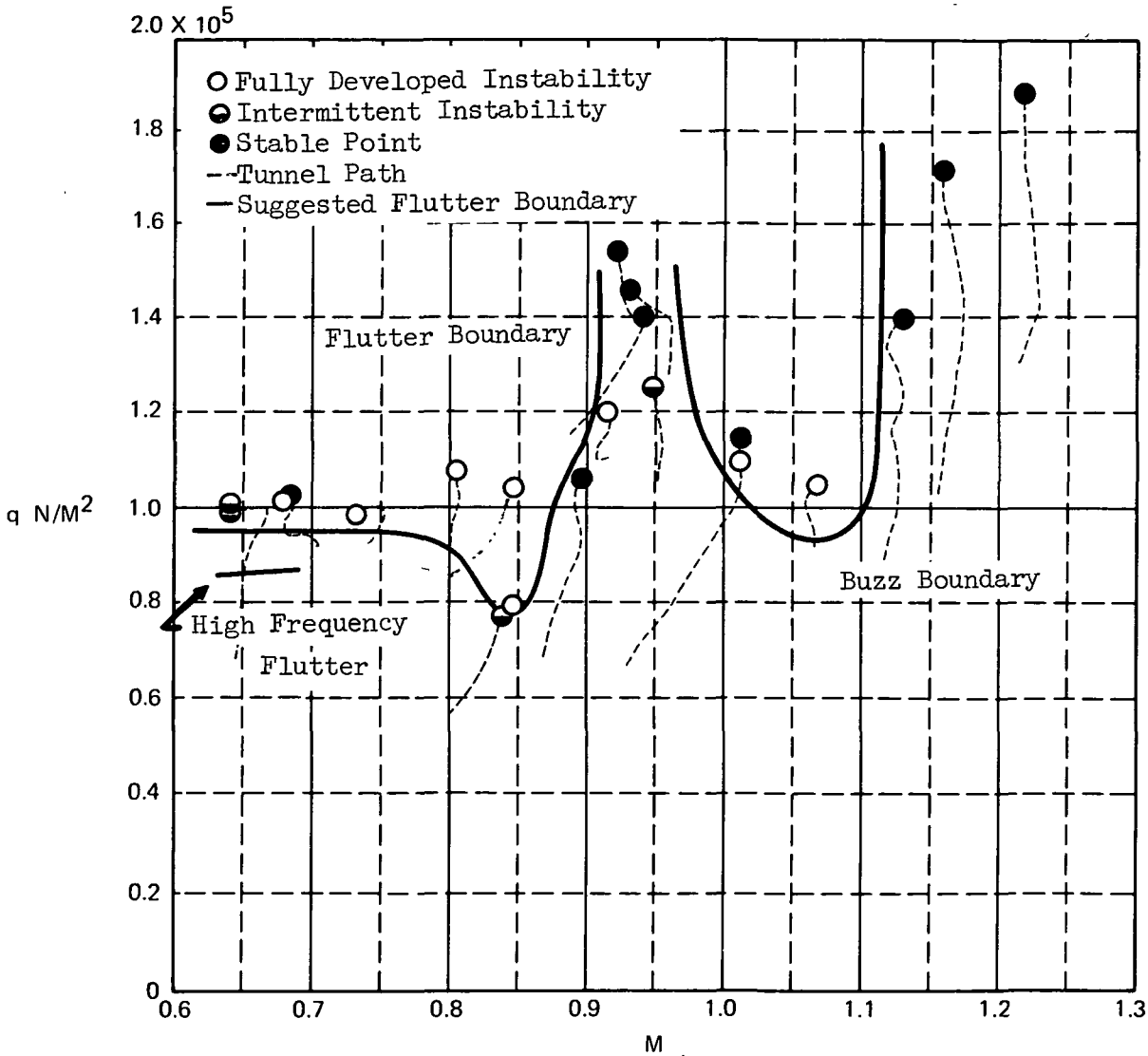

(b) Isolated 070/040 Orbiter

Fig. 8 Continued

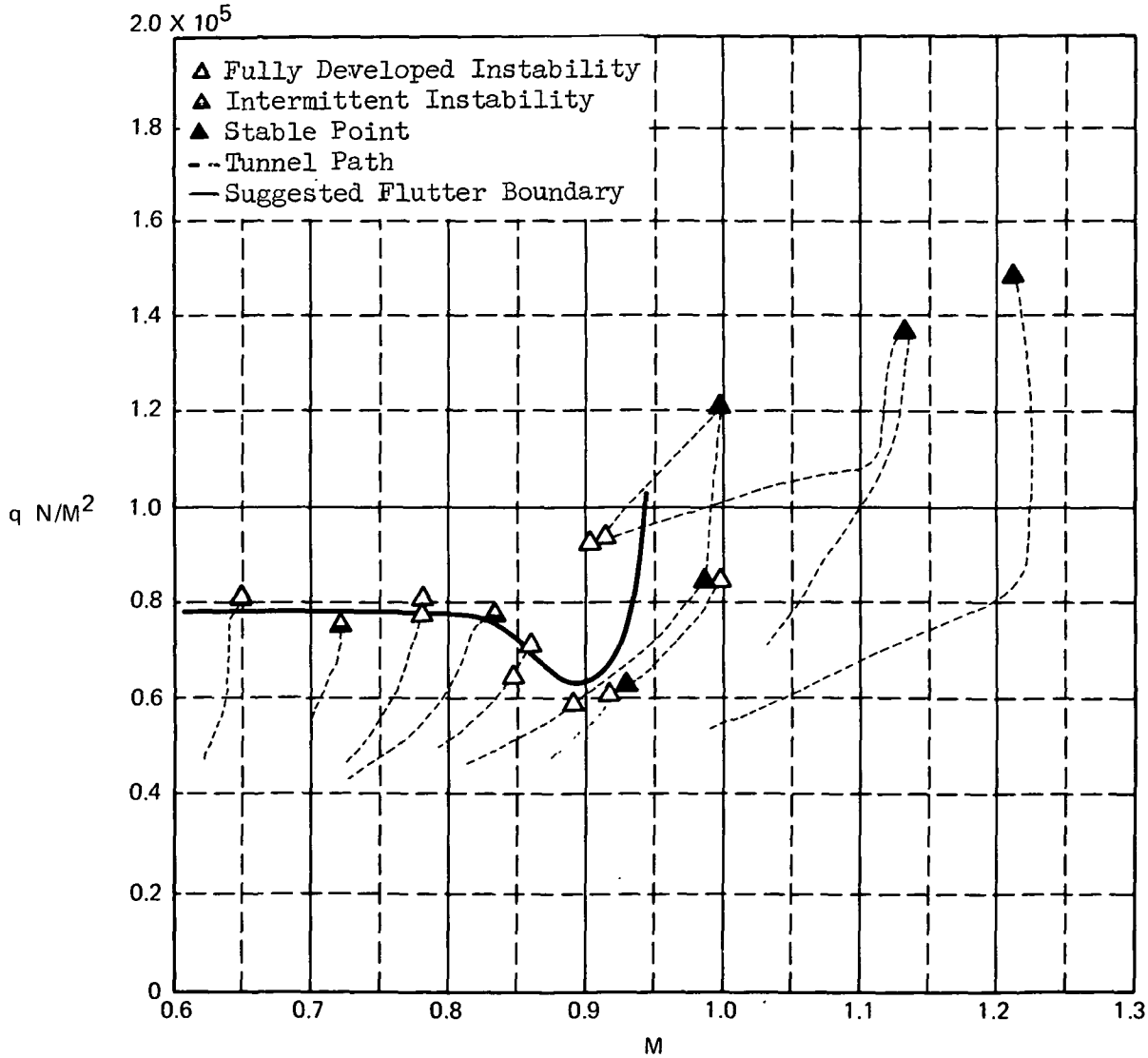

(c) Isolated 100 Booster

Fig. 8 Continued

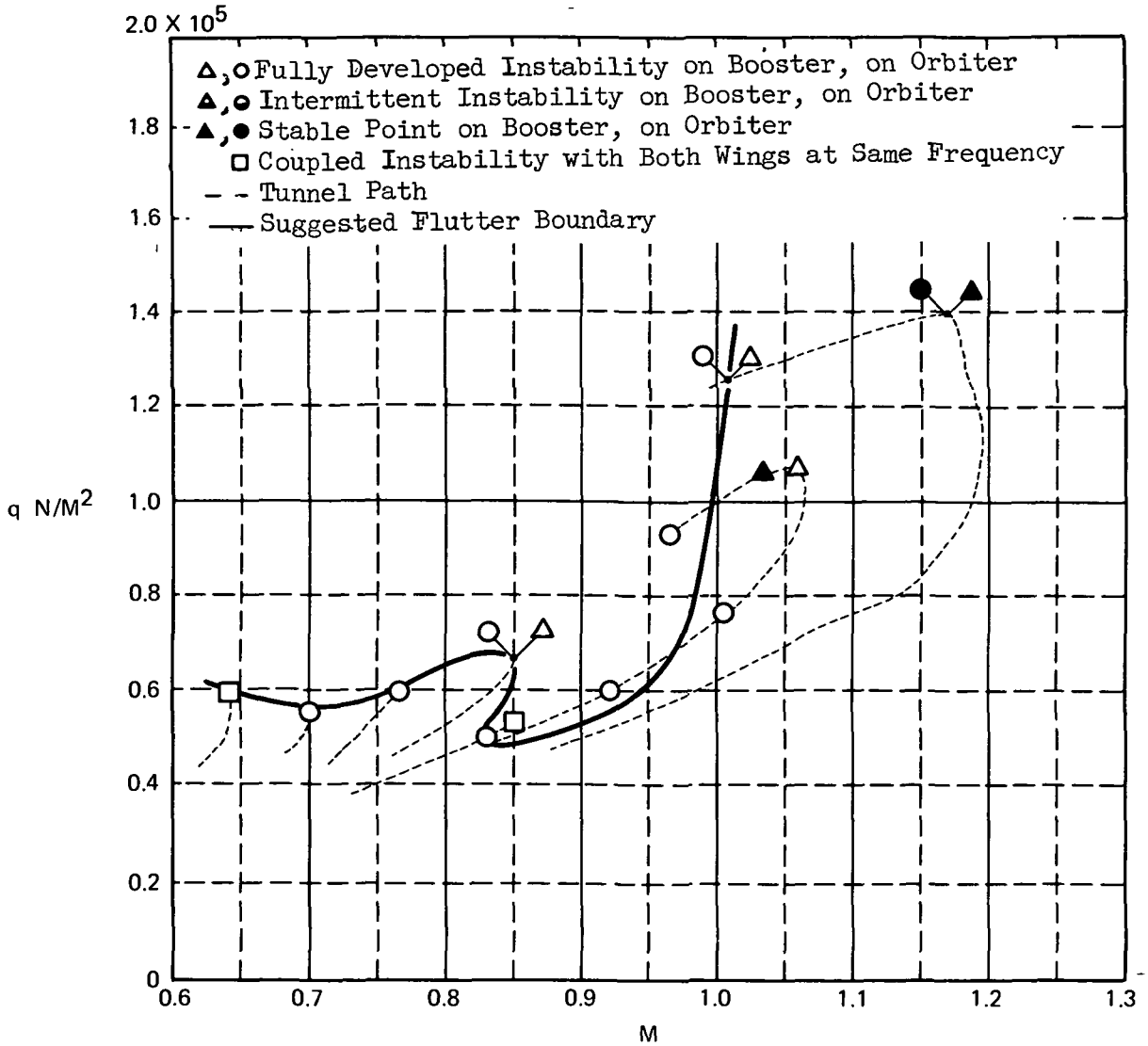

(d) 070/032-100 Forward Mid Position

Fig. 8 Continued

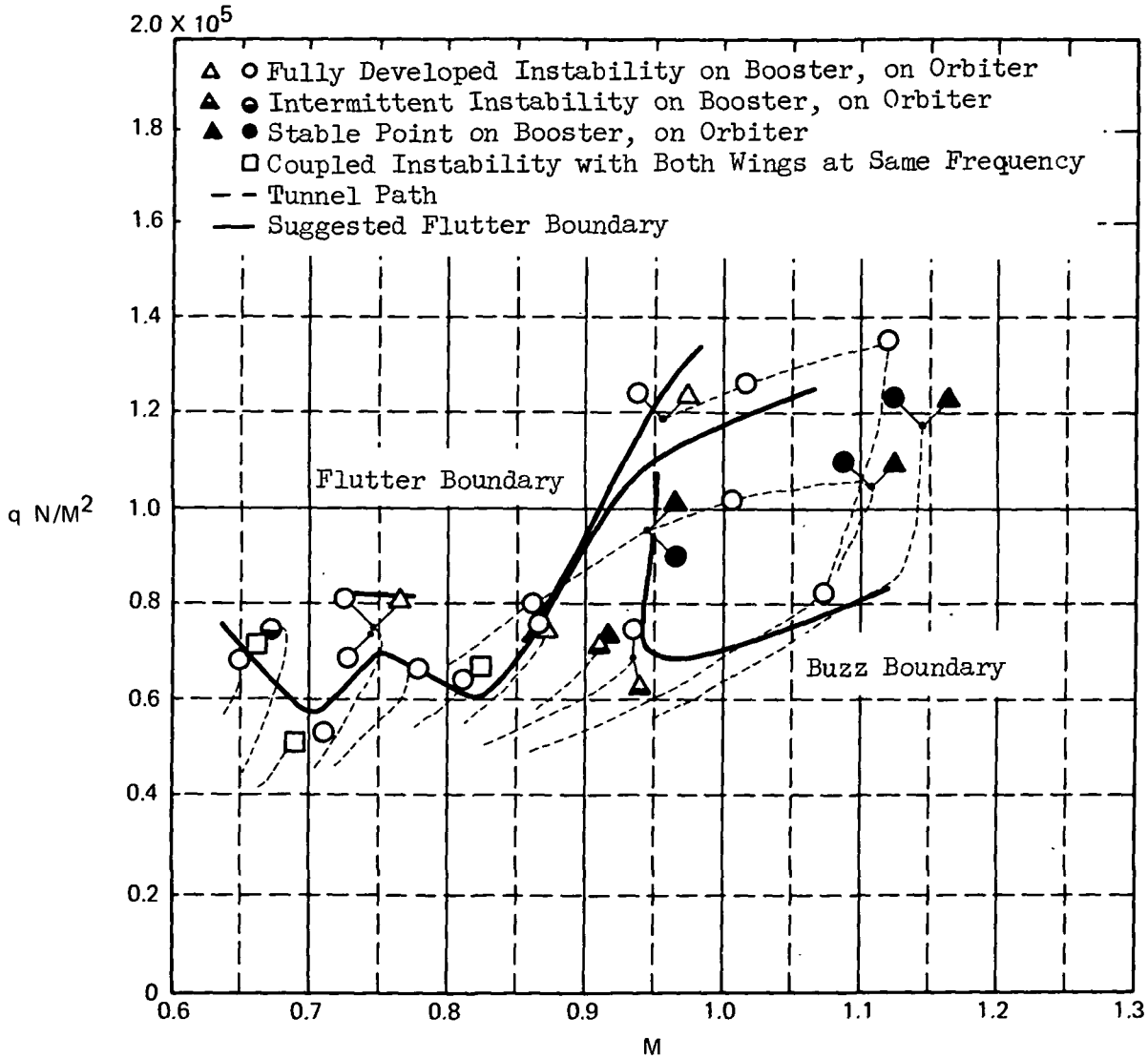

(e) 070/032-100 Forward Low Position

Fig. 8 Continued

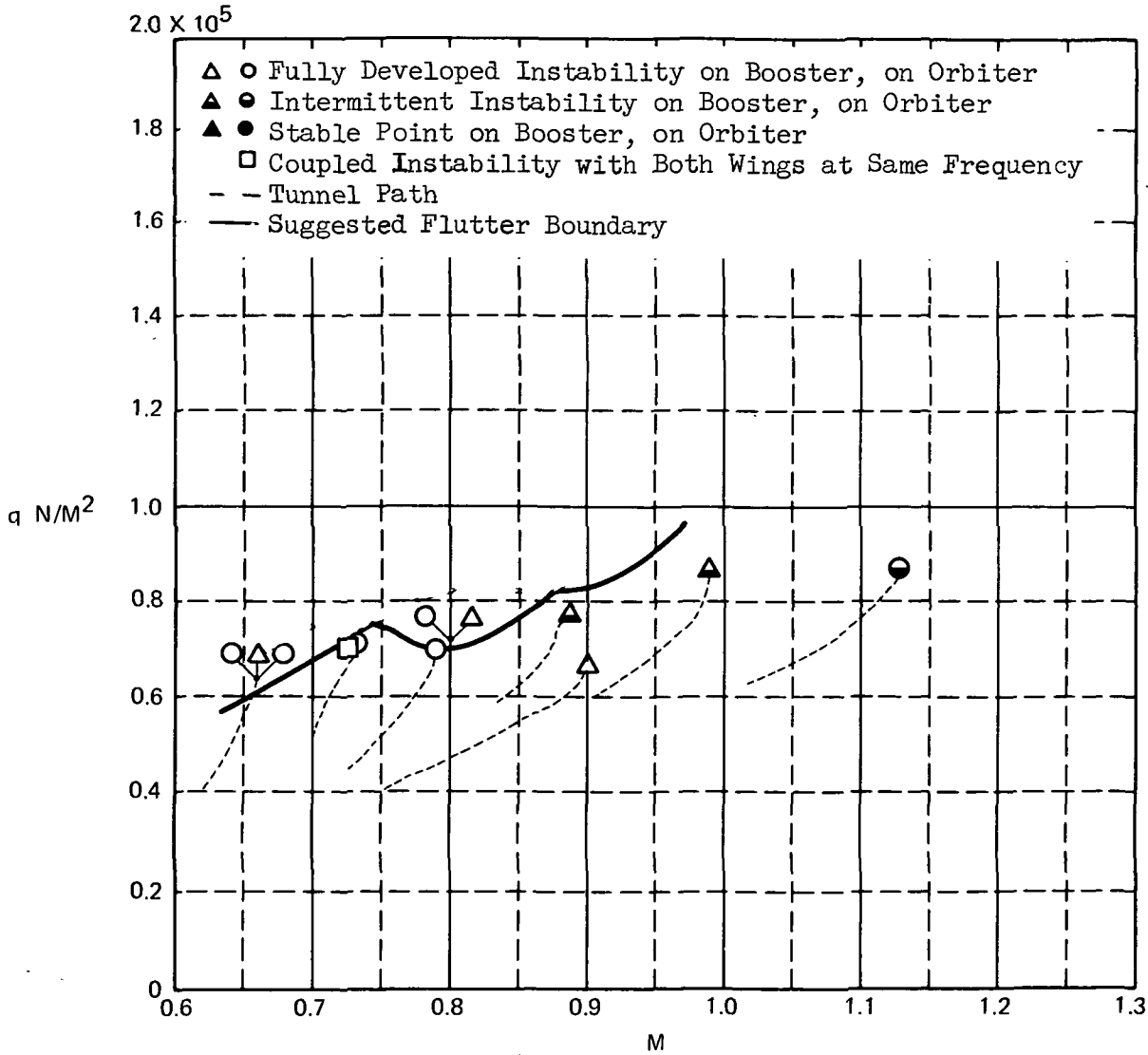

(f) 070/032-100 Mid Upper Position

Fig. 8 Continued

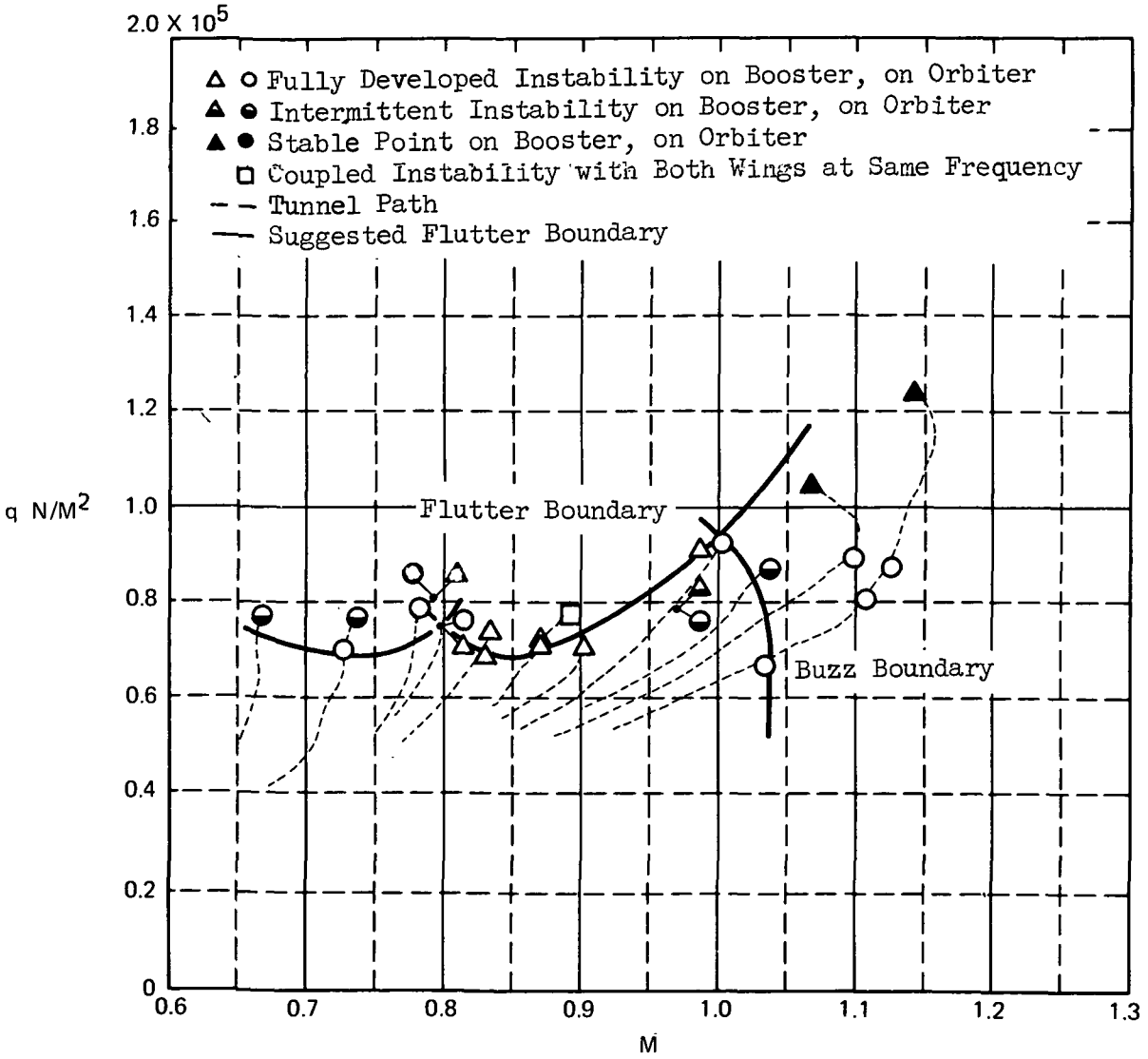

(g) 070/032-100 Mid Mid Position

Fig. 8 Continued

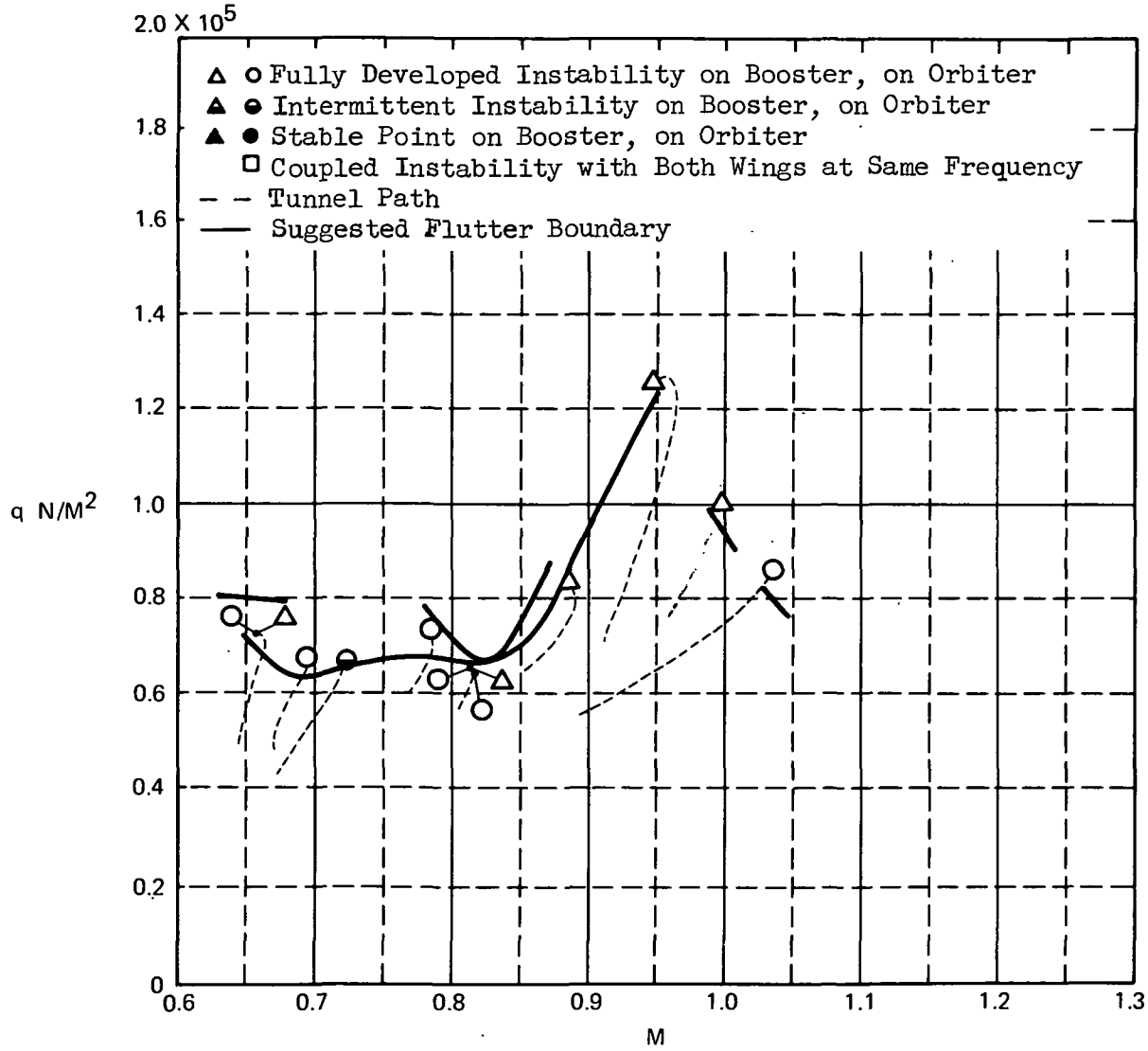

(h) 070/032-100 Mid Low Position

Fig. 8 Continued

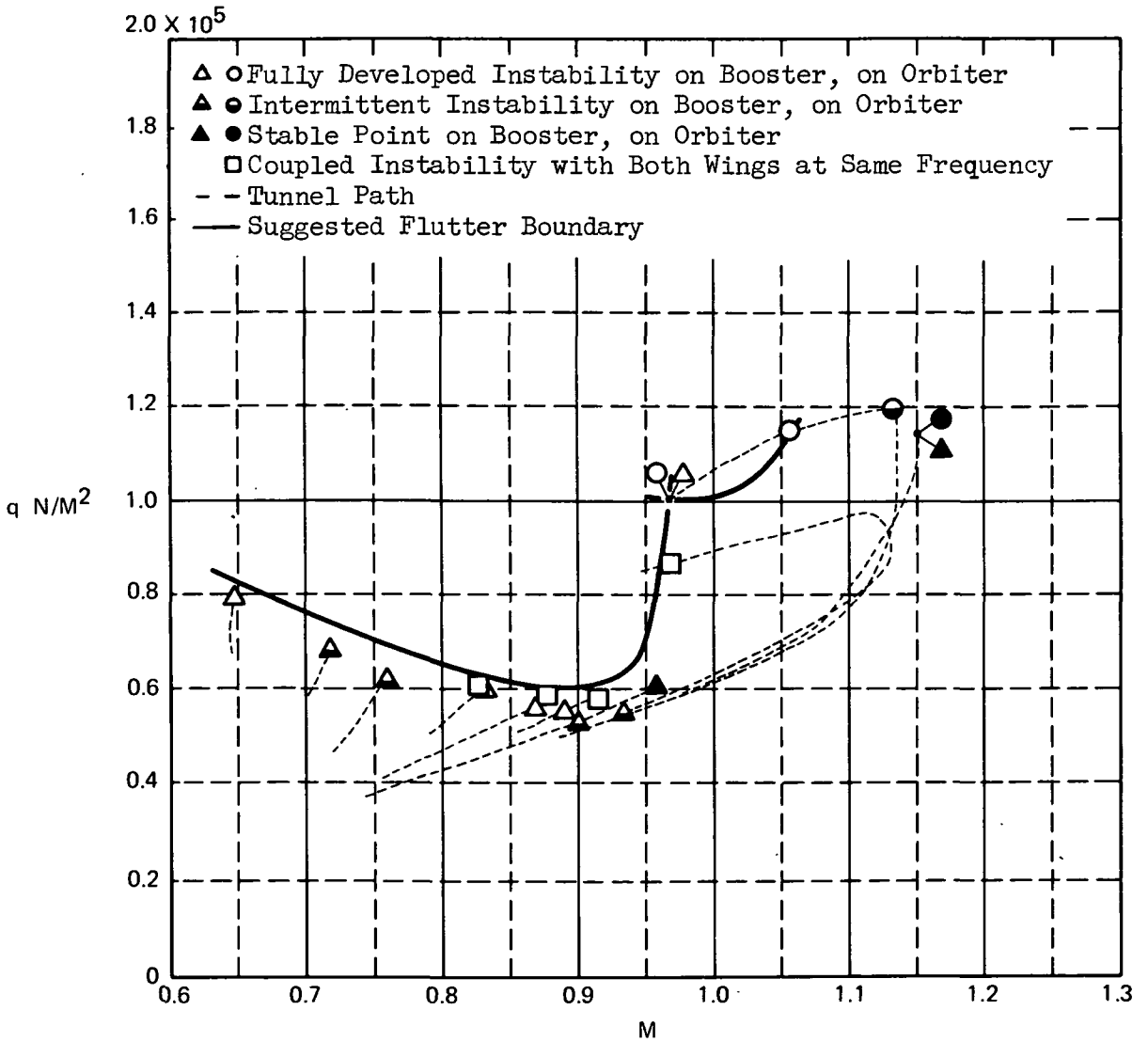

(i) 070/040-100 Forward Mid Position

Fig. 8 Continued

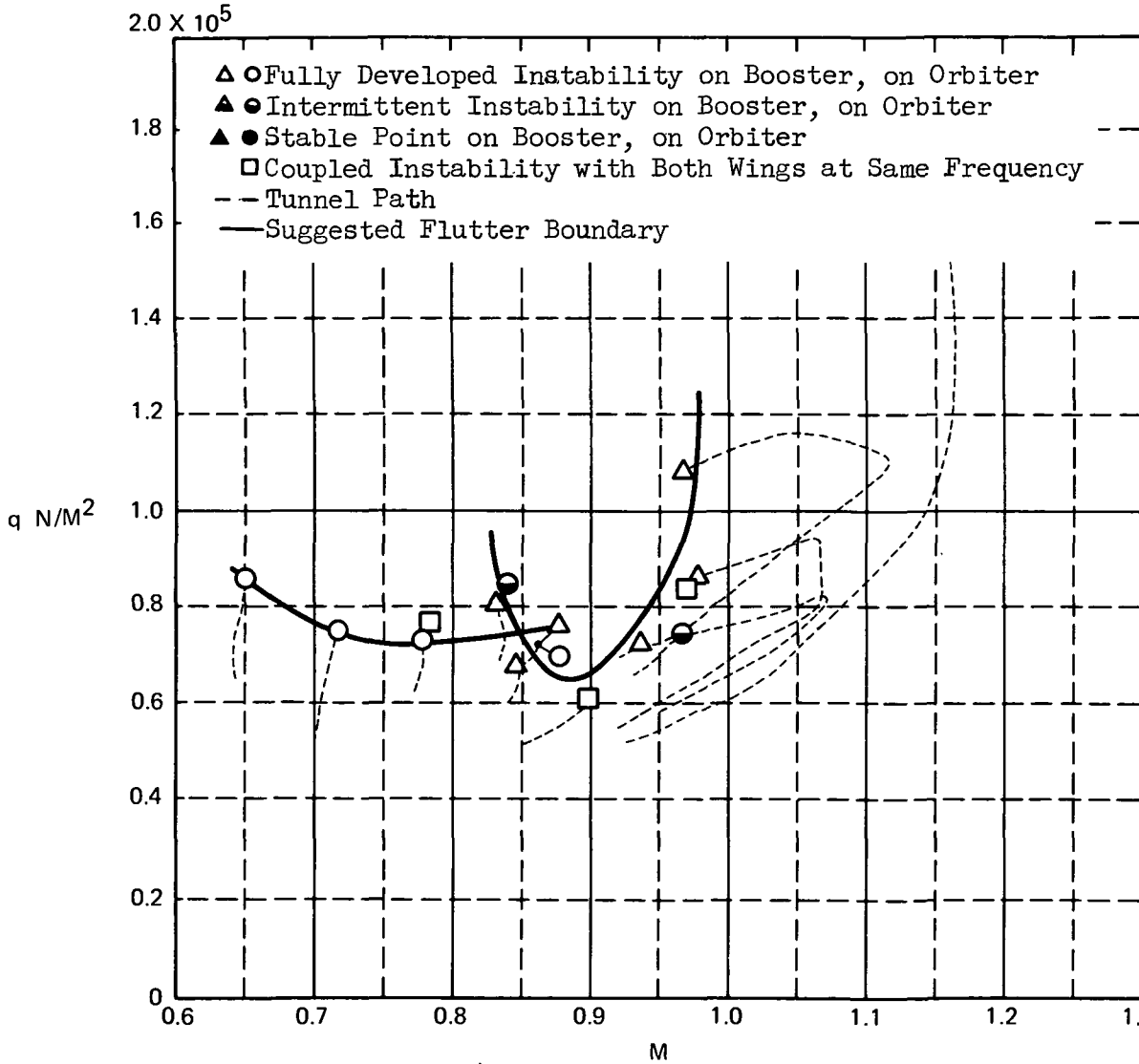

(j) 070/040-100 Forward Low Position

Fig. 8 Continued

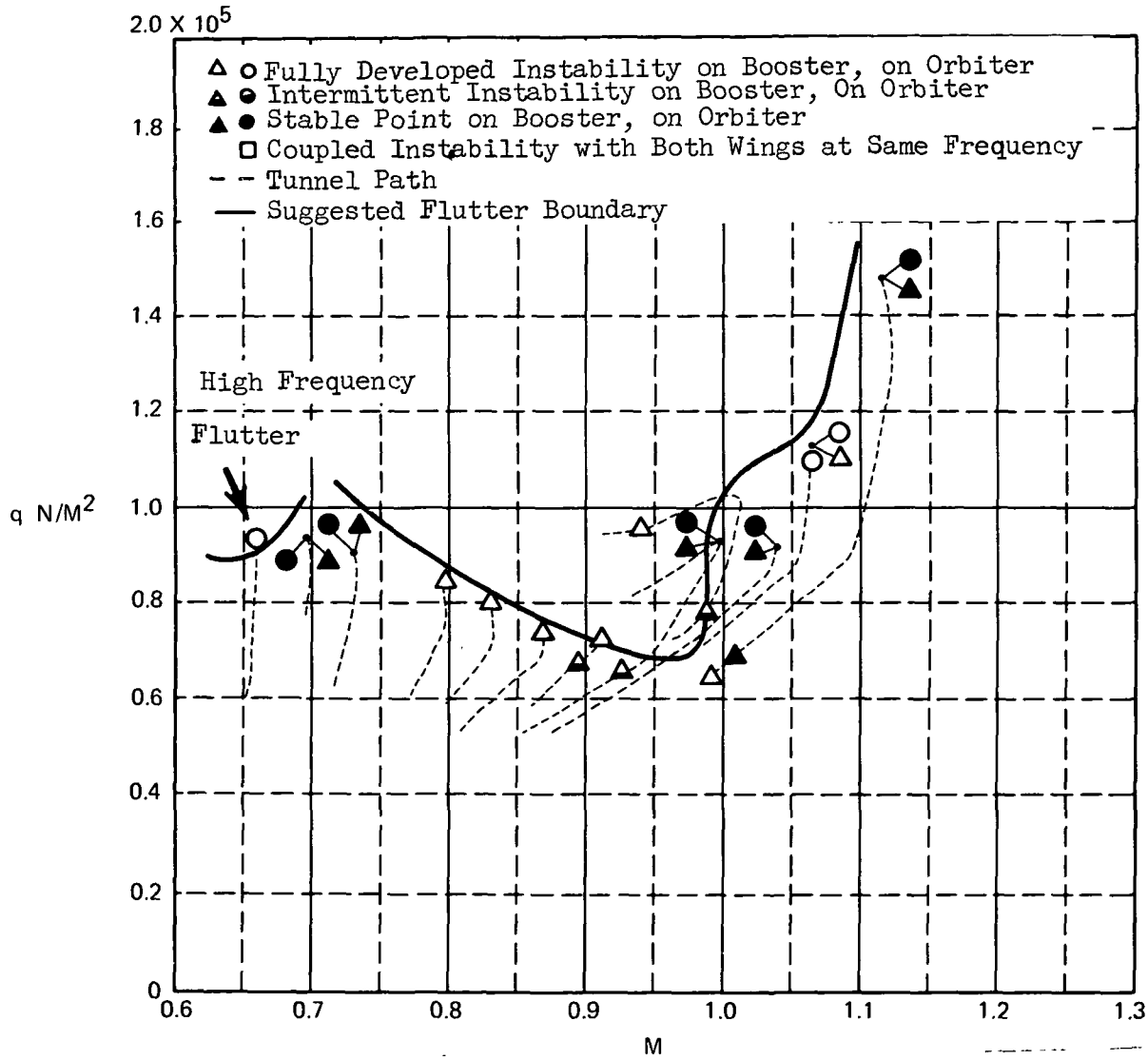

(k) 070/040-100 Mid Upper Position

Fig. 8 Continued

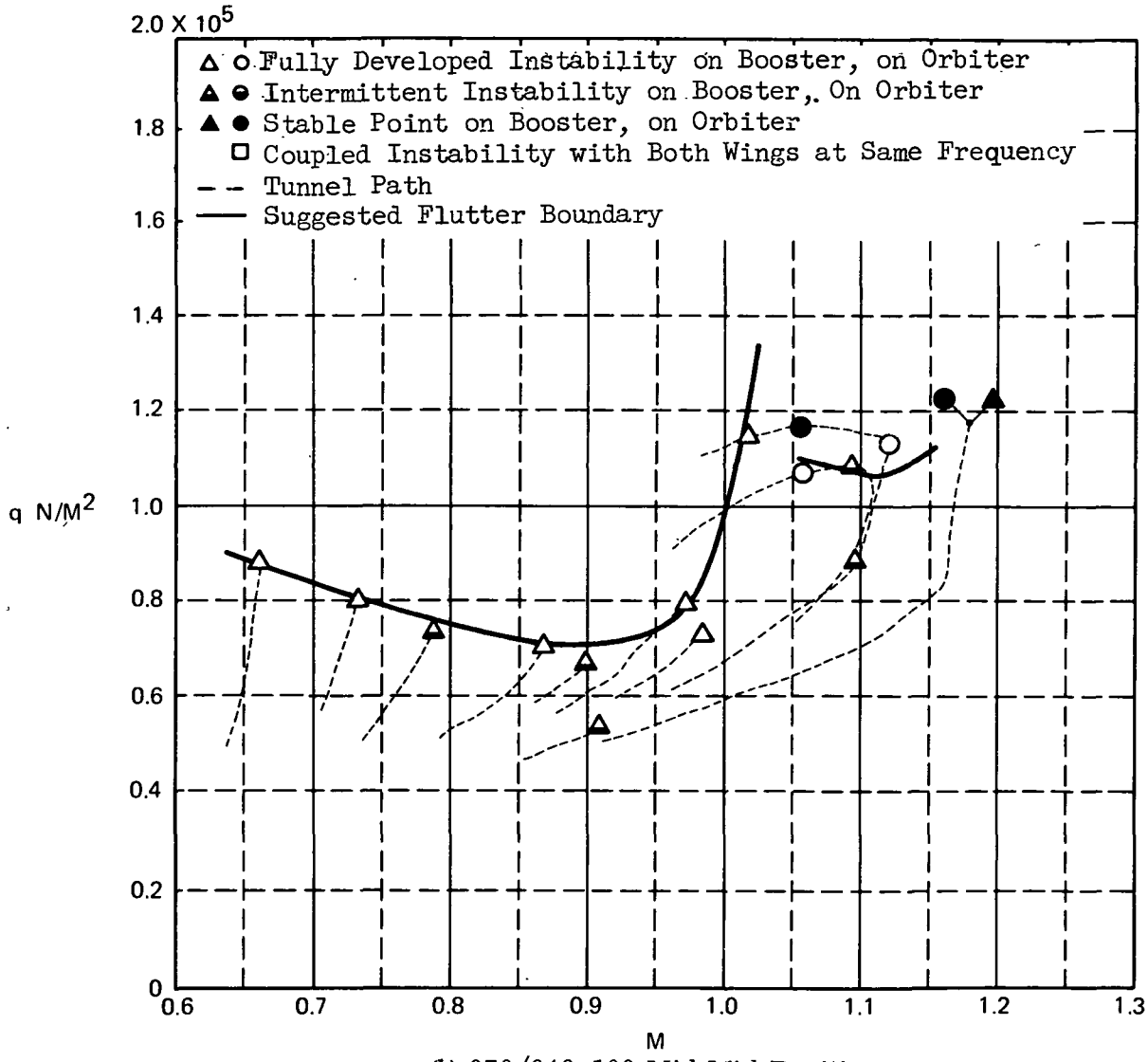

(1) 070/040-100 Mid Mid Position

Fig. 8 Continued

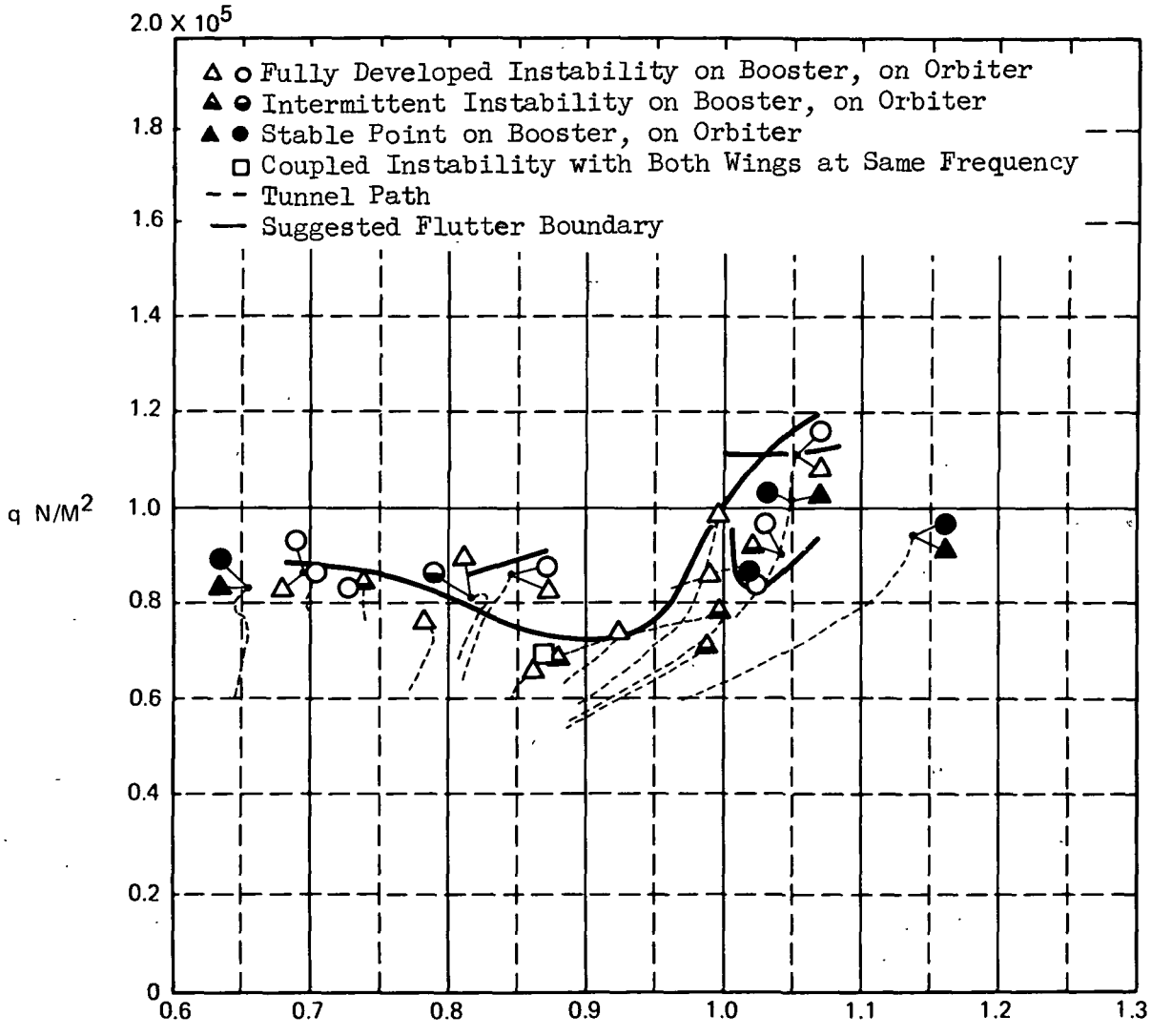

(m) 070/040-100 Mid Low Position

Fig.8 Concluded

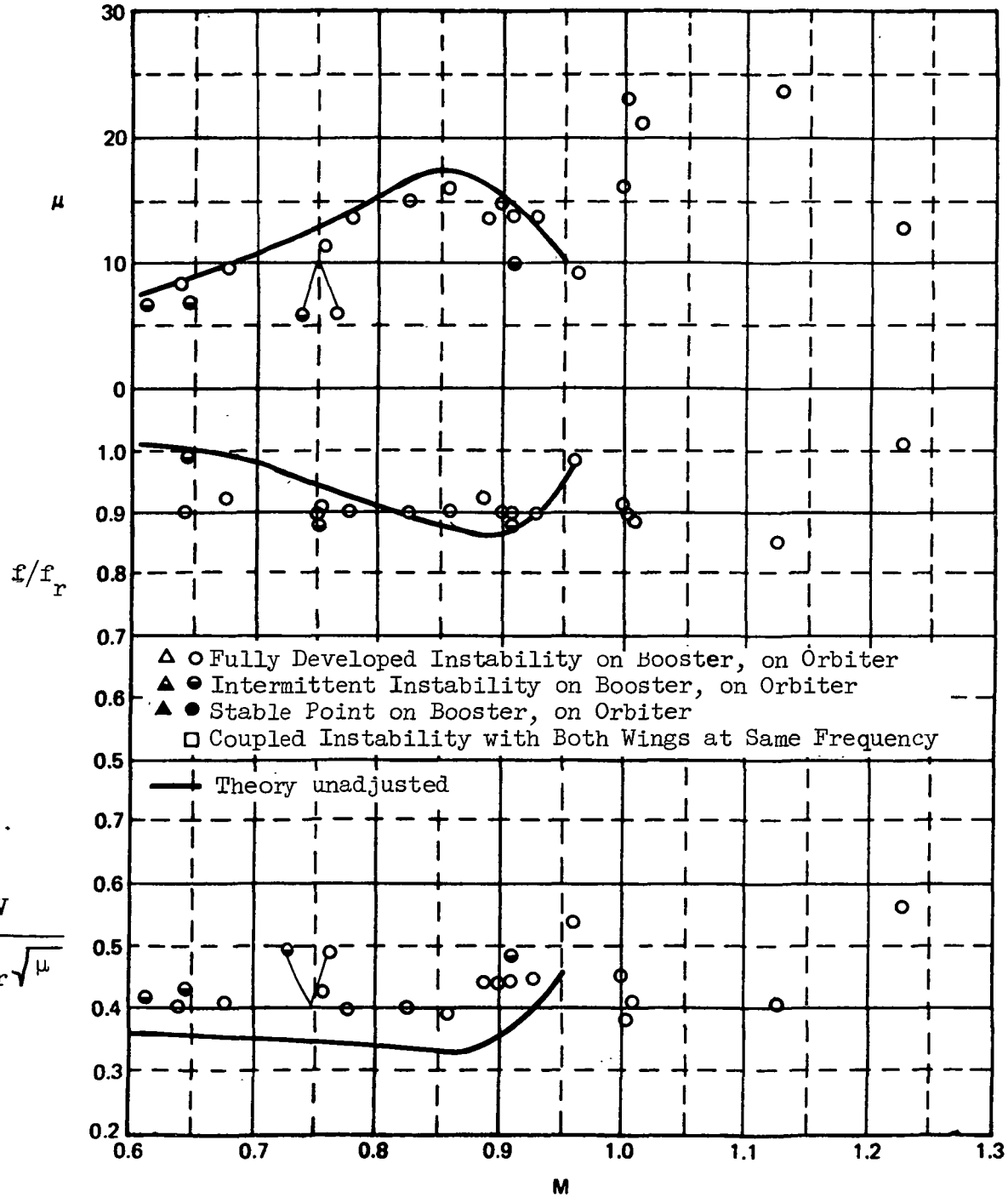

(a) Isolated 070/032 Orbiter

Figure 9. **Variation of Mass Density Ratio, Flutter Frequency Ratio, and Flutter Speed Index With Mach Number**

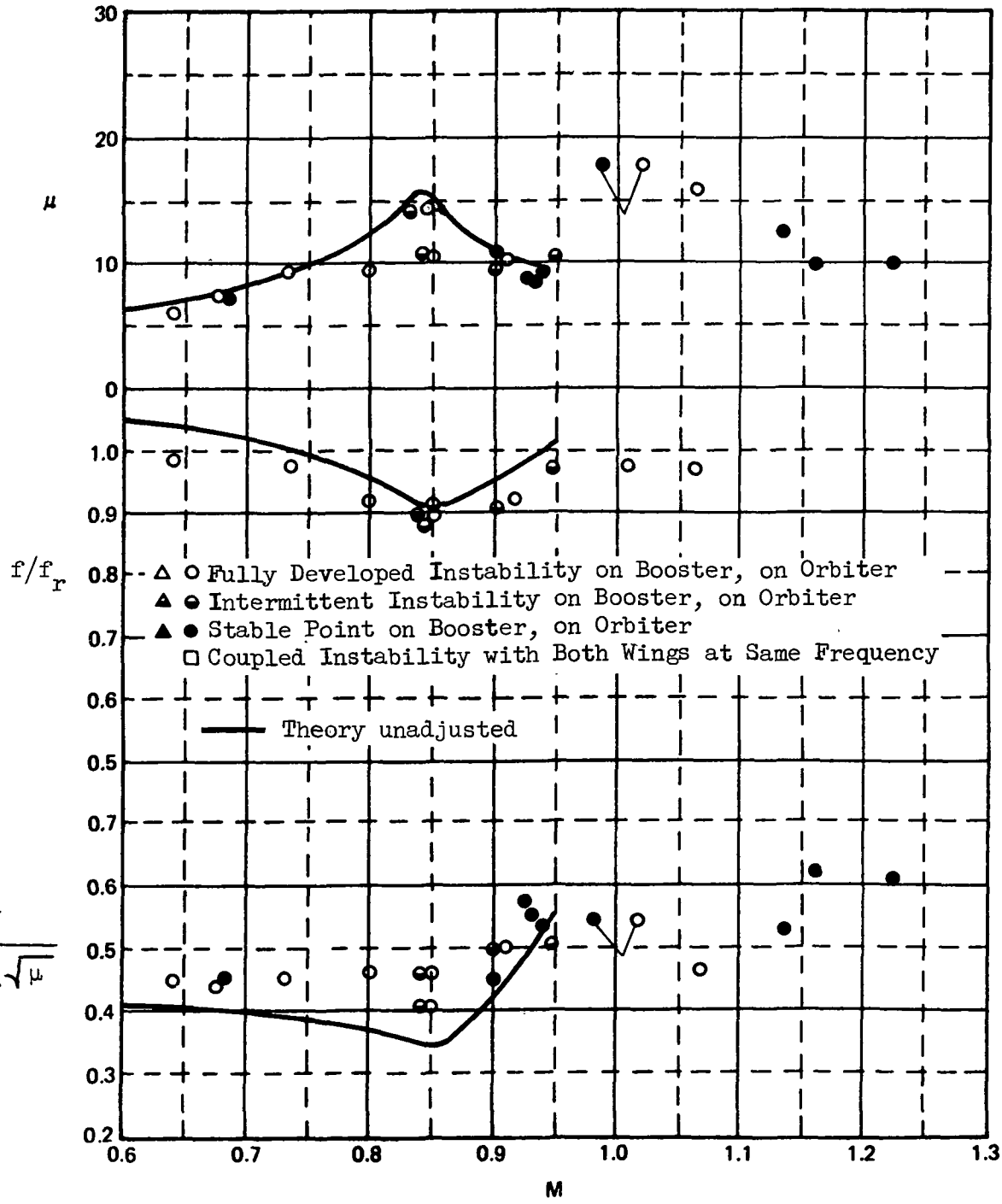

(b) Isolated 070/040 Orbiter
Fig. 9 Continued

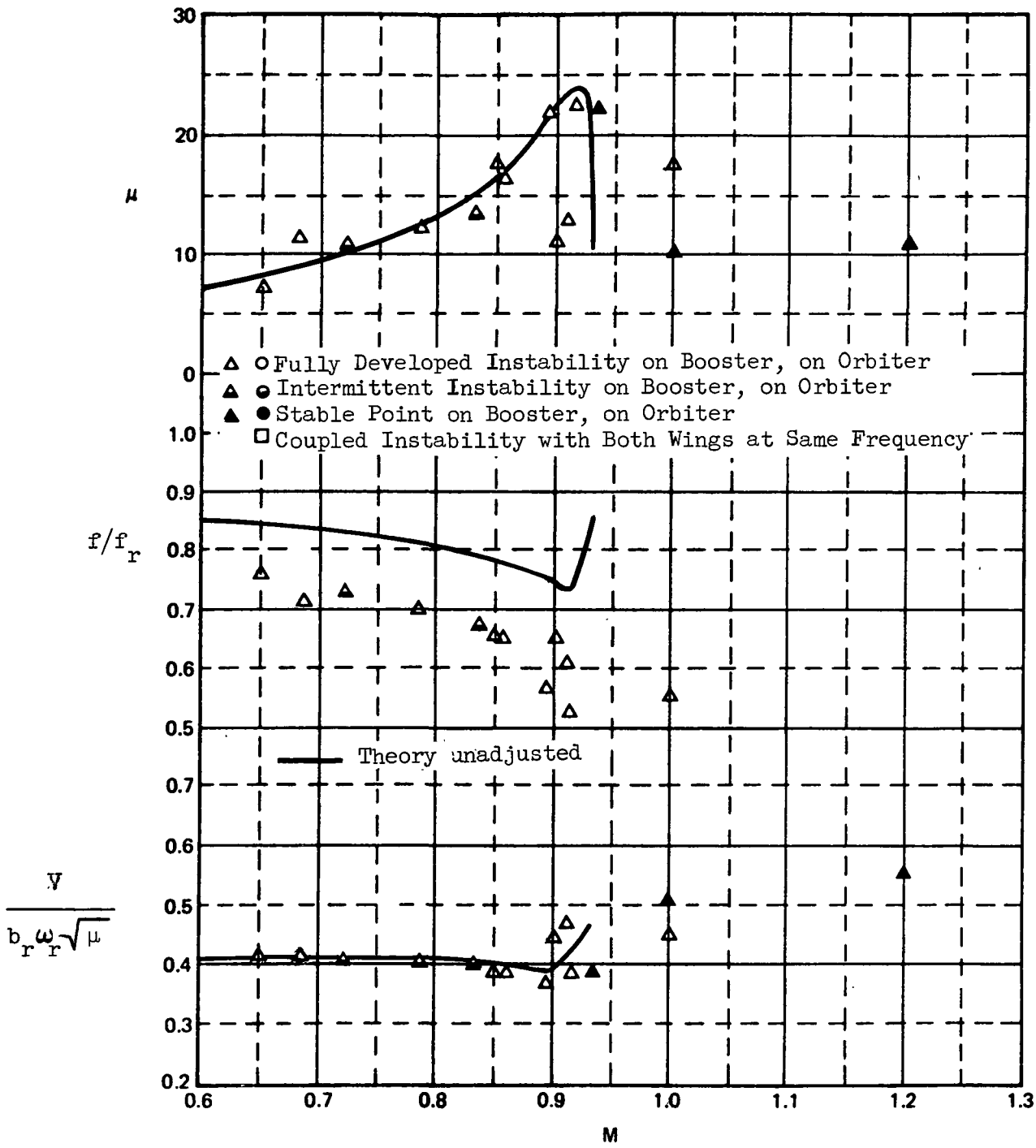

(c) Isolated 100 Booster
Fig. 9 Continued

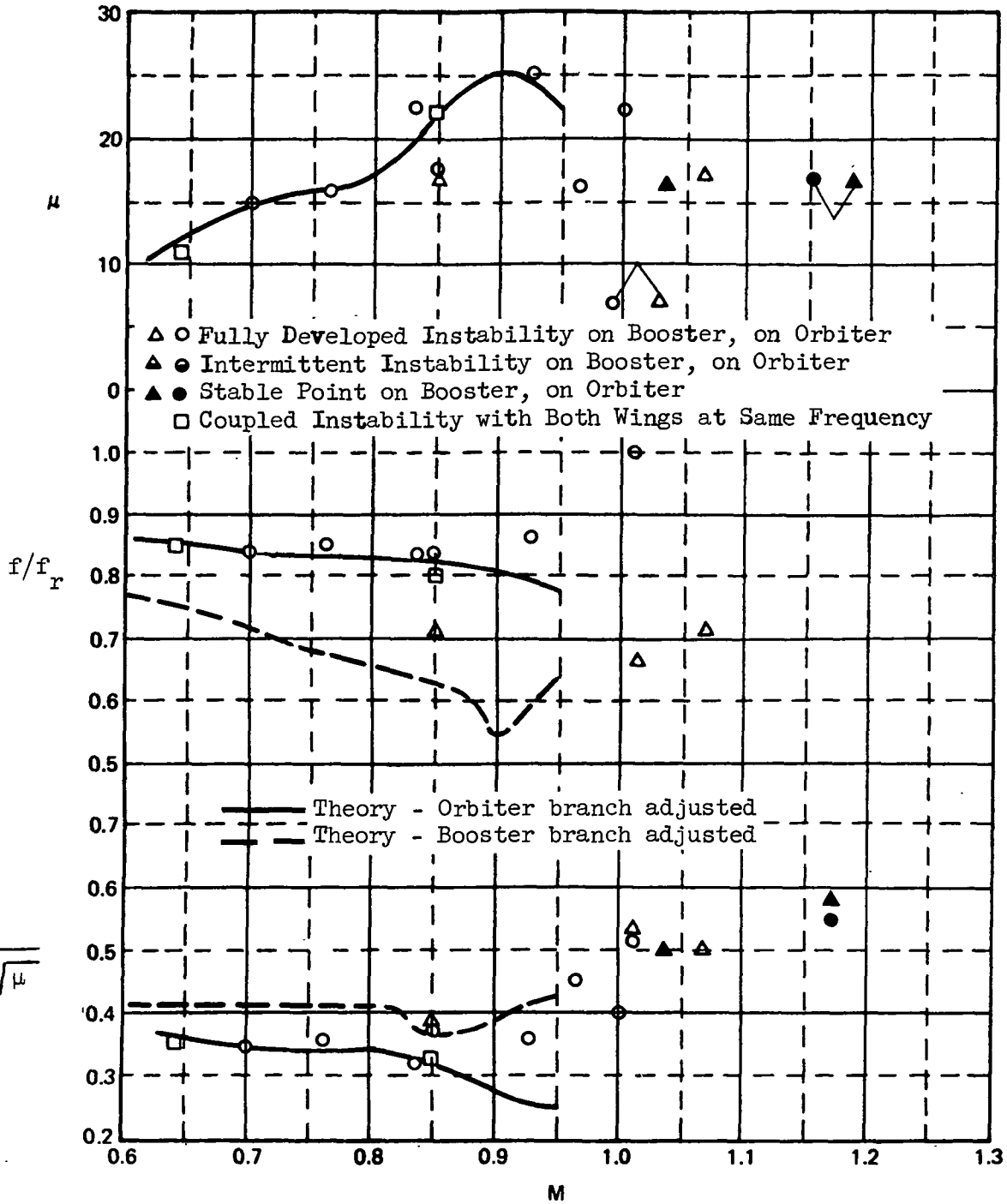

(d) 070/032-100 ℓ/c = 0.00 h/c = 0.4
Fig. 9 Continued

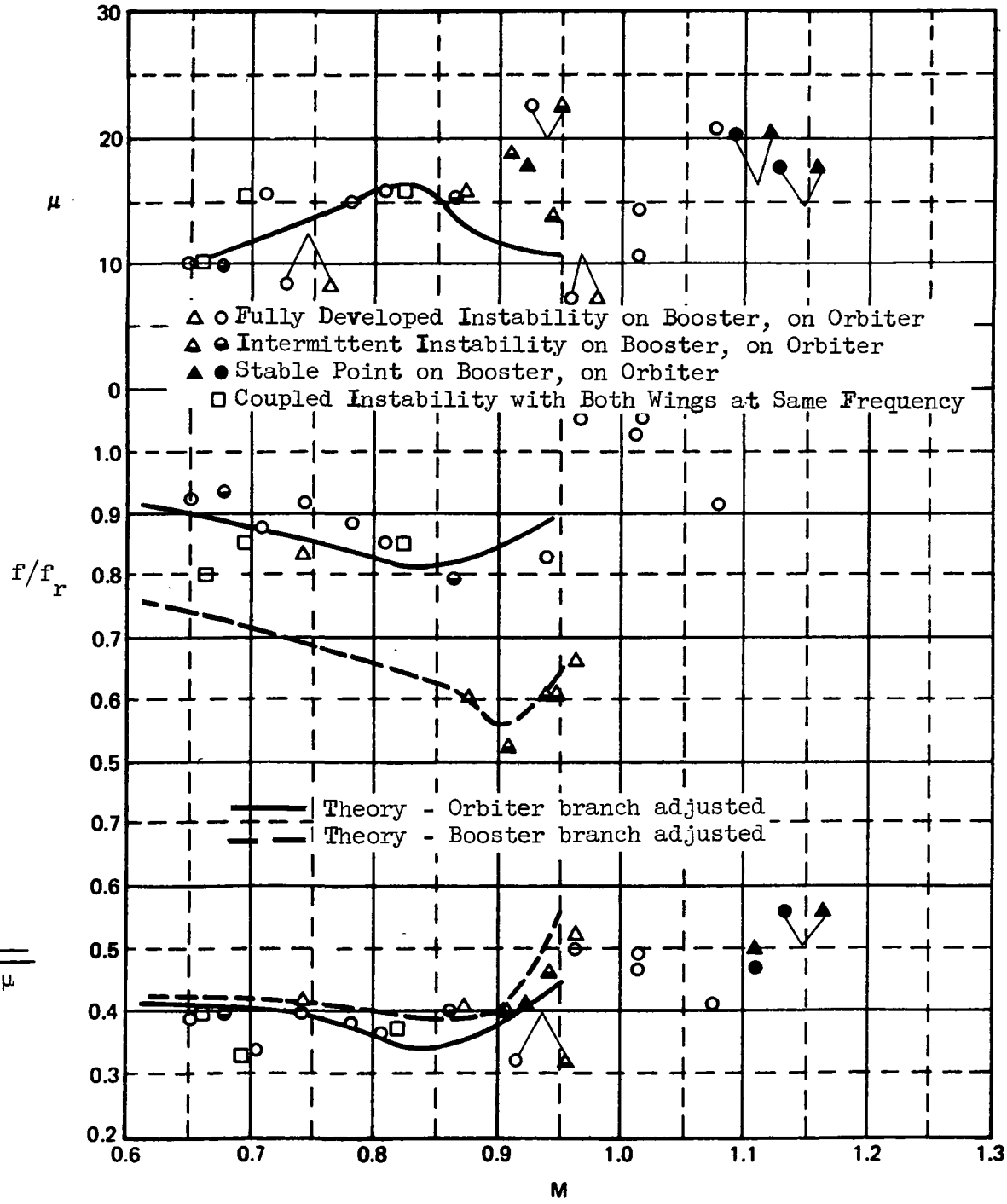

(e) 070/032-100 ℓ/c = 0.00 h/c = 0.6

Fig. 9 Continued

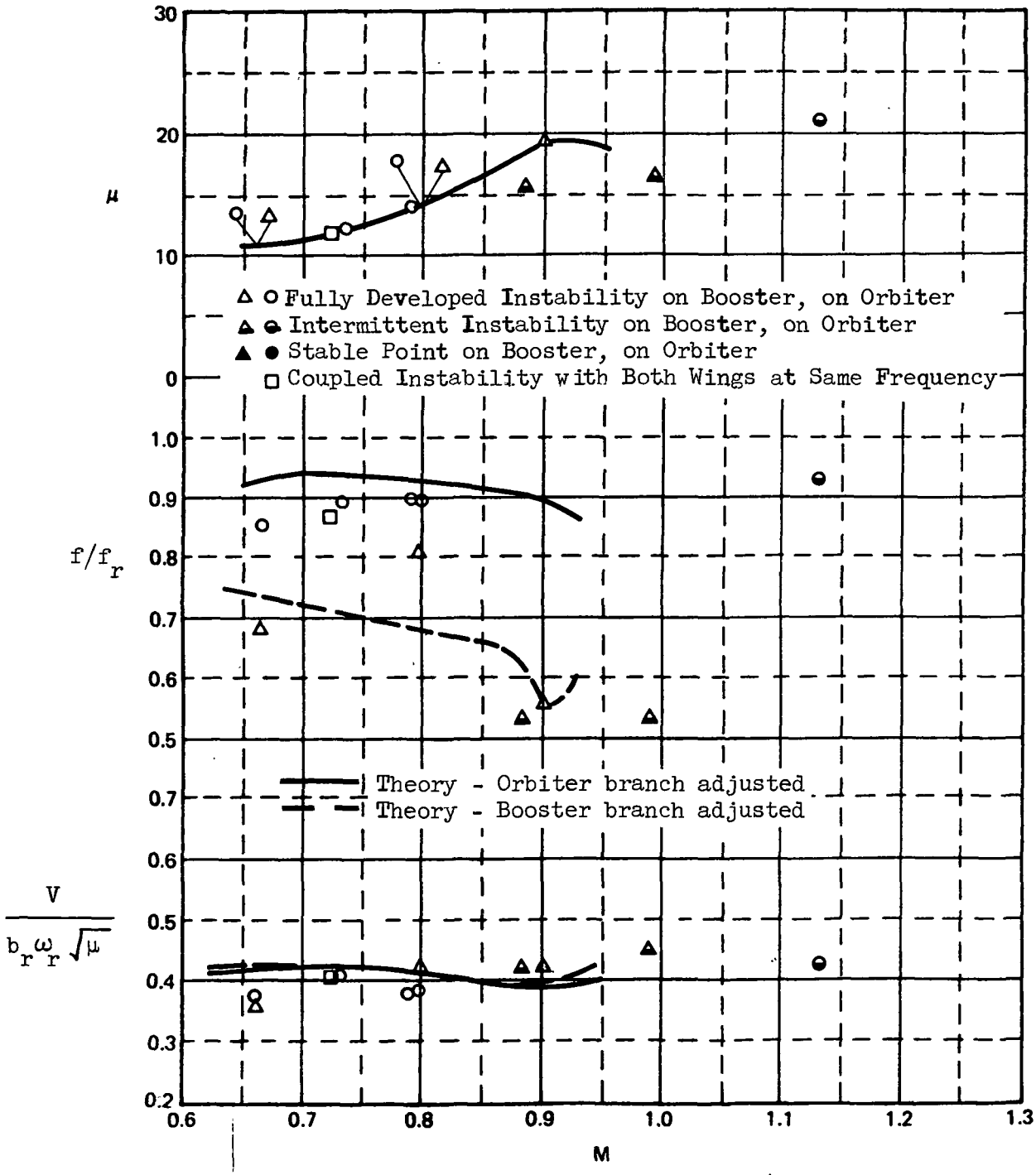

(f) 070/032-100 ℓ/c = 0.73 h/c = 0.2

Fig. 9 Continued

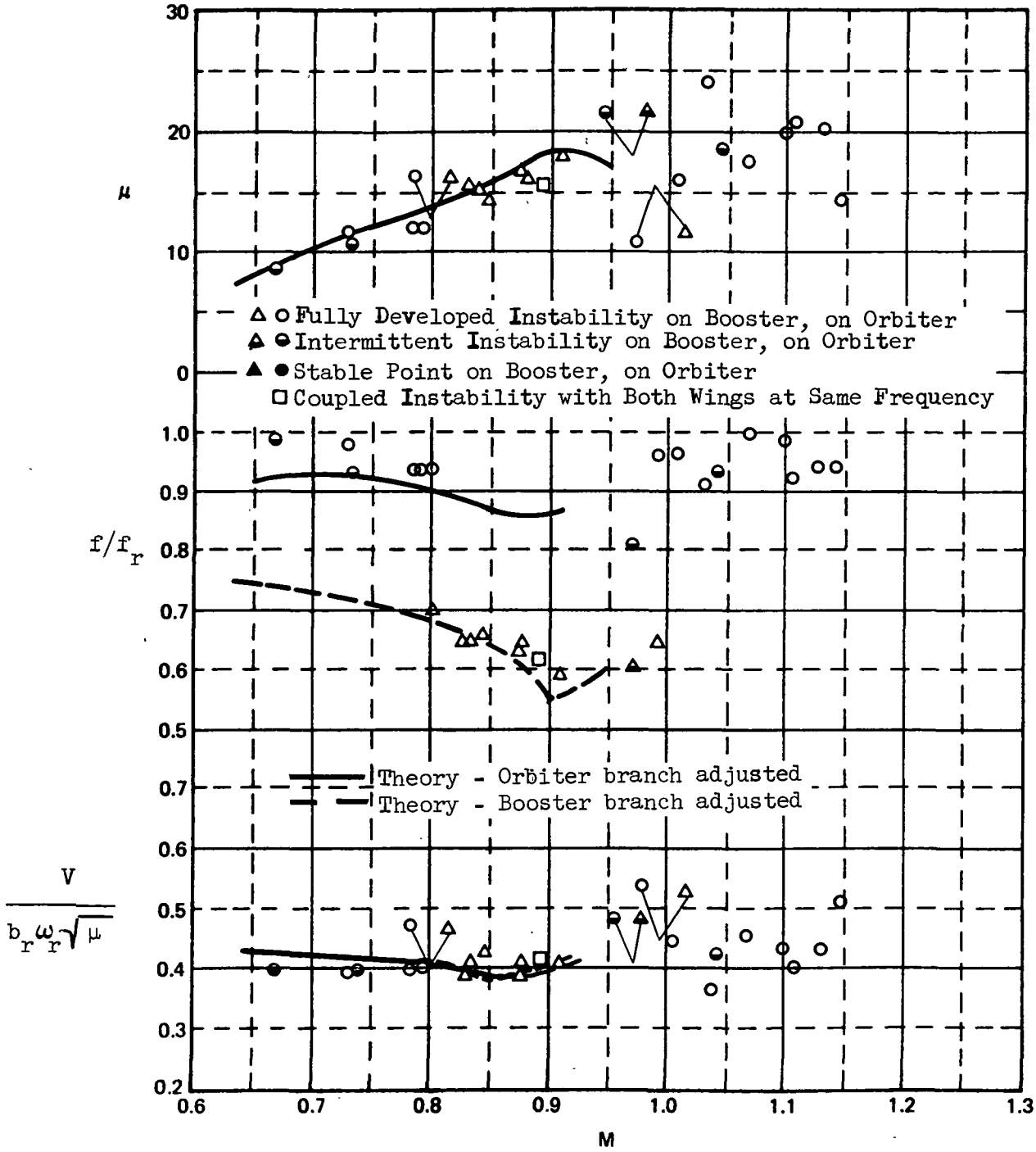

(g) 070/032-100 ℓ/c = 0.73 h/c = 0.4

Fig. 9 Continued

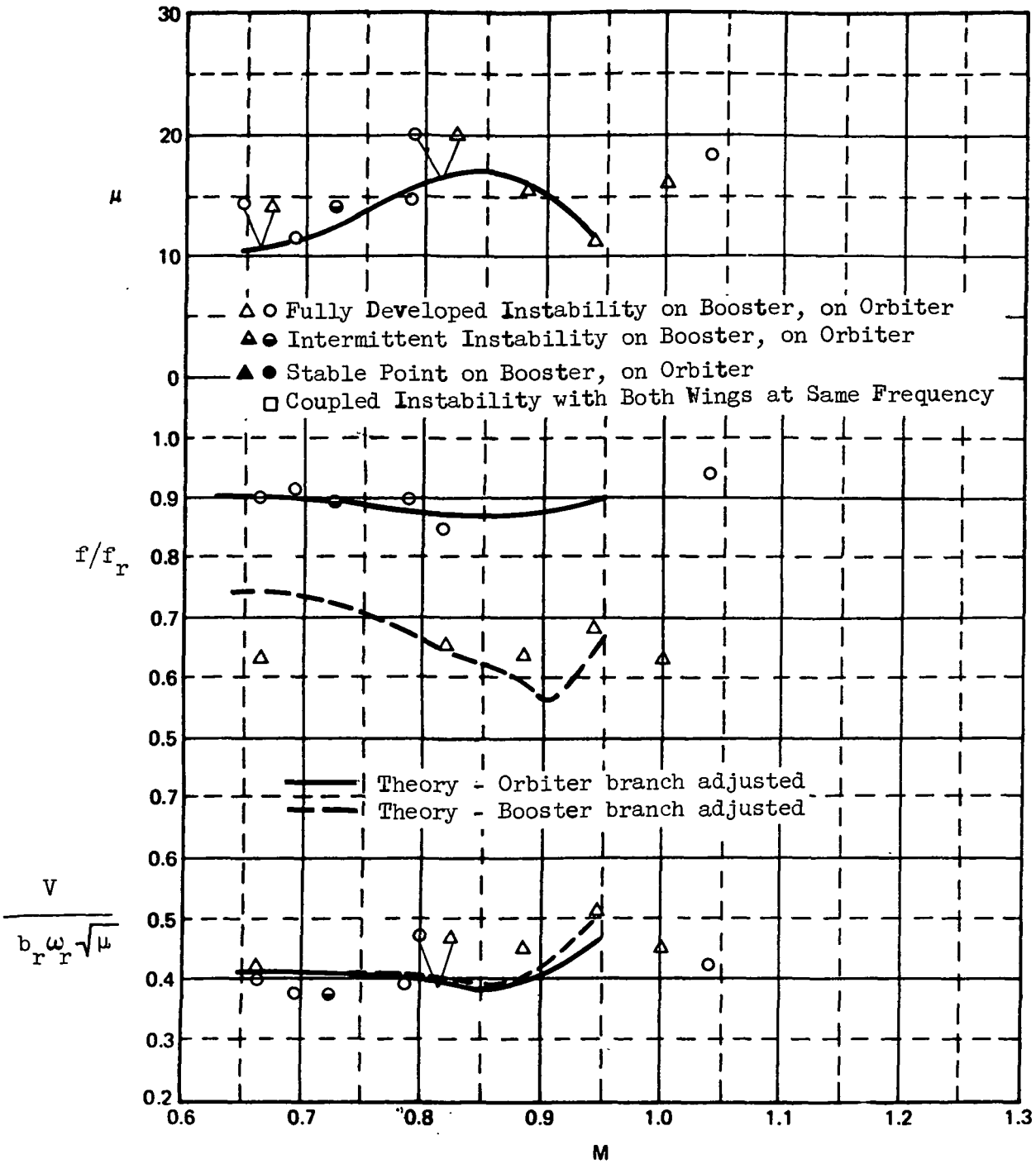

(h) 070/032-100 ℓ/c = 0.73 h/c = 0.6
Fig. 9 Continued

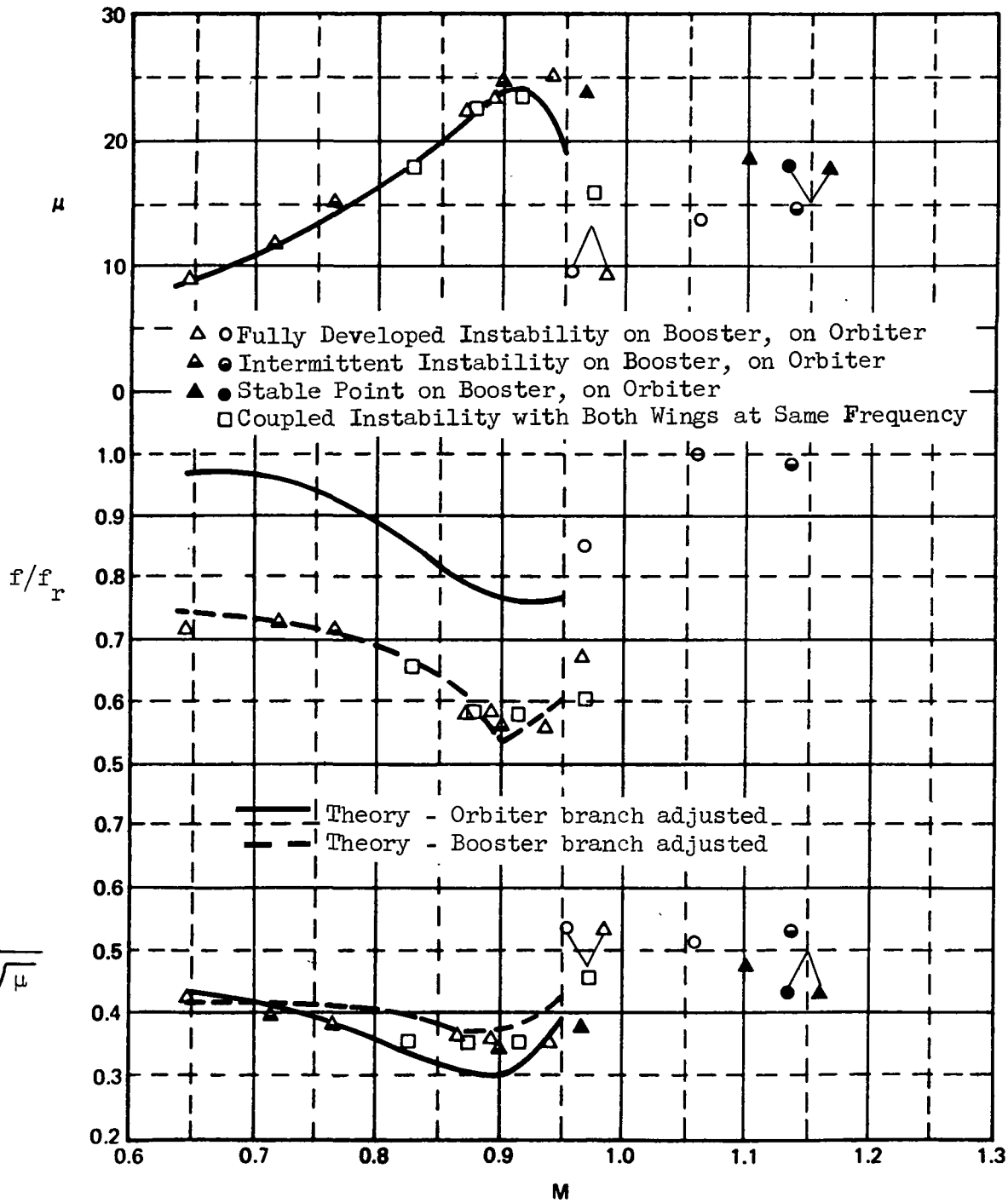

(i) 070/040-100 ℓ/c = 0.00 h/c = 0.4

Fig. 9 Continued

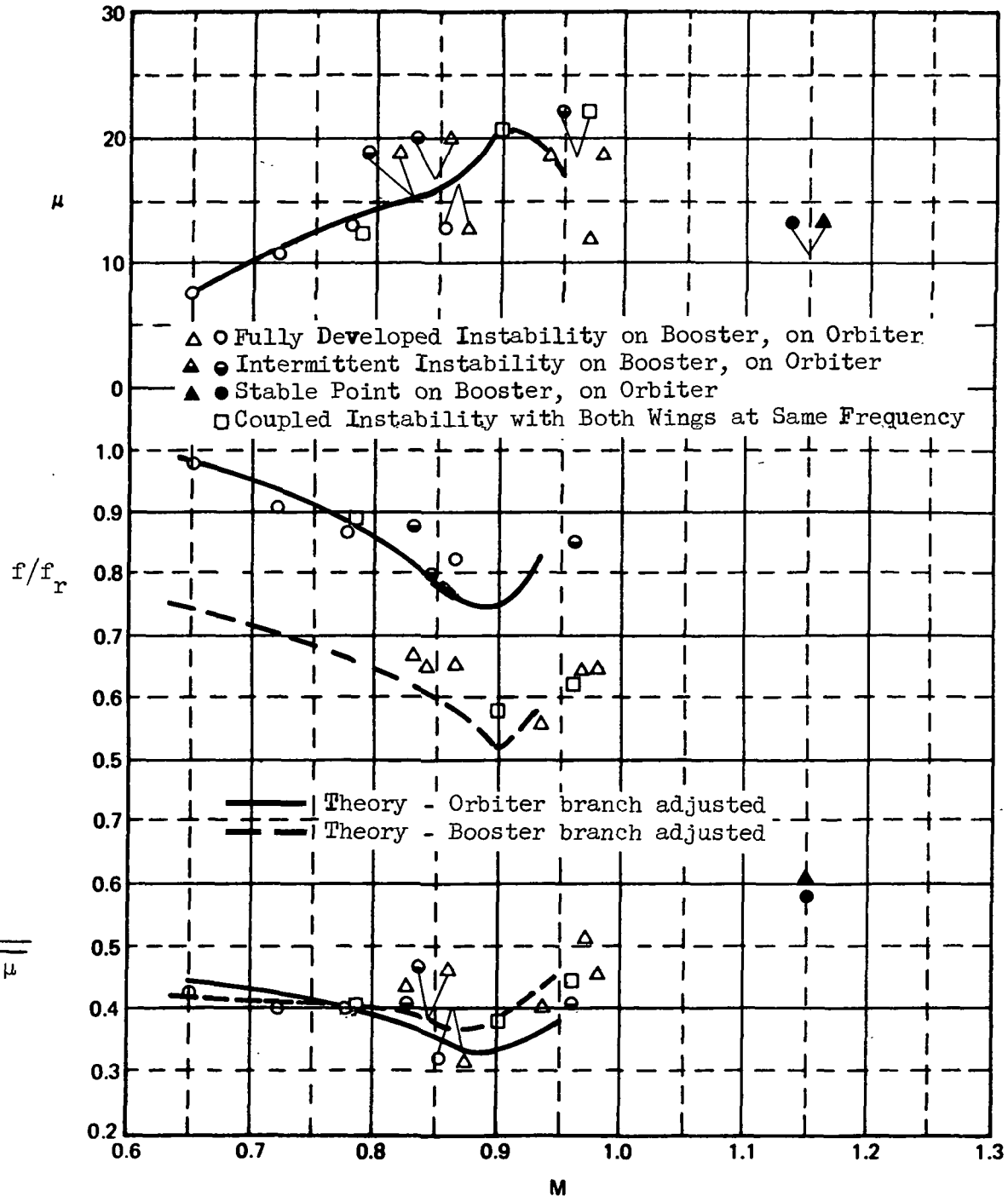

(j) 070/040-100 ℓ/c = 0.00 h/c = 0.6
Fig. 9 Continued

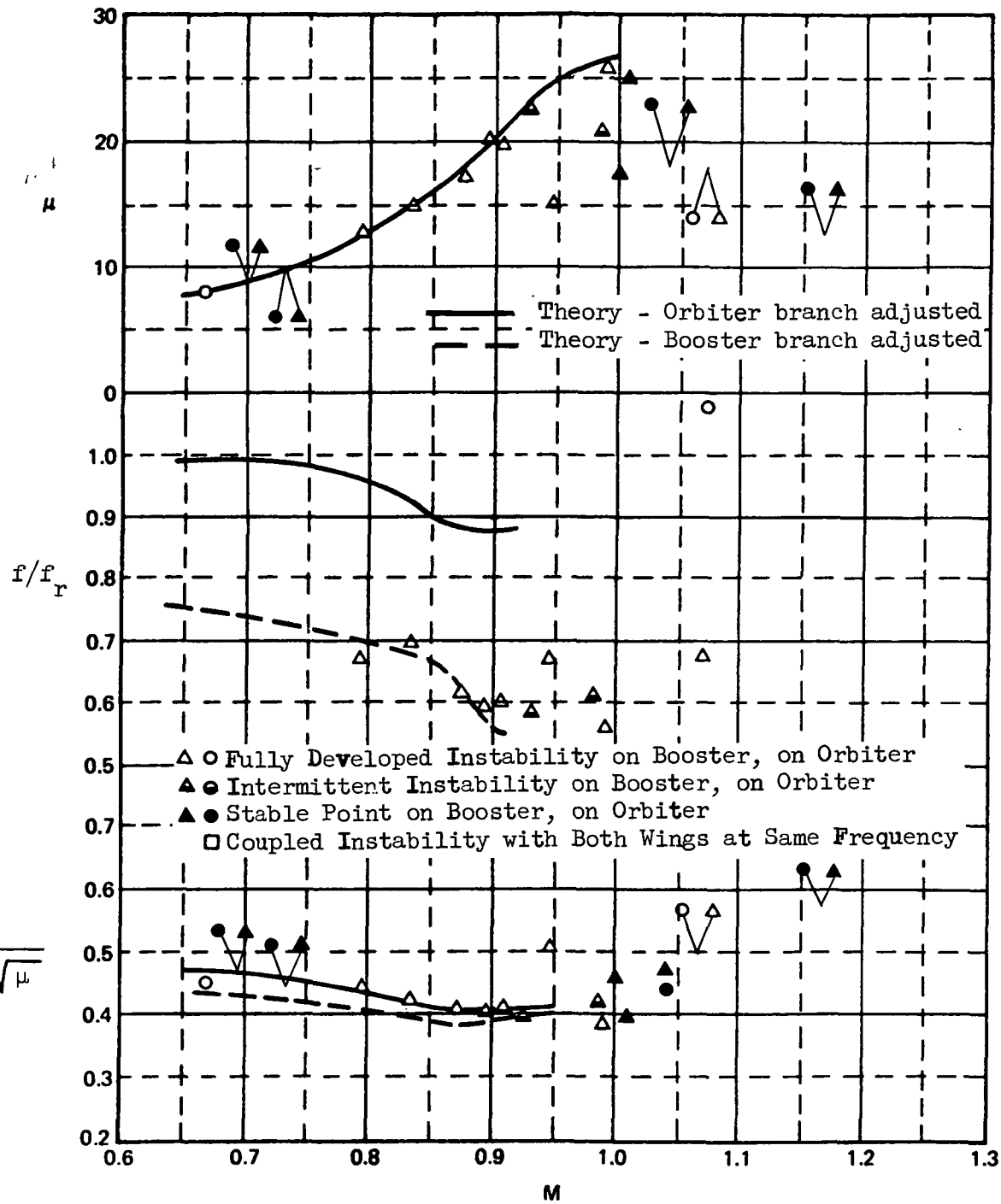

(k) 070/040-100 ℓ/c = 0.73 h/c = 0.2

Fig. 9 Continued

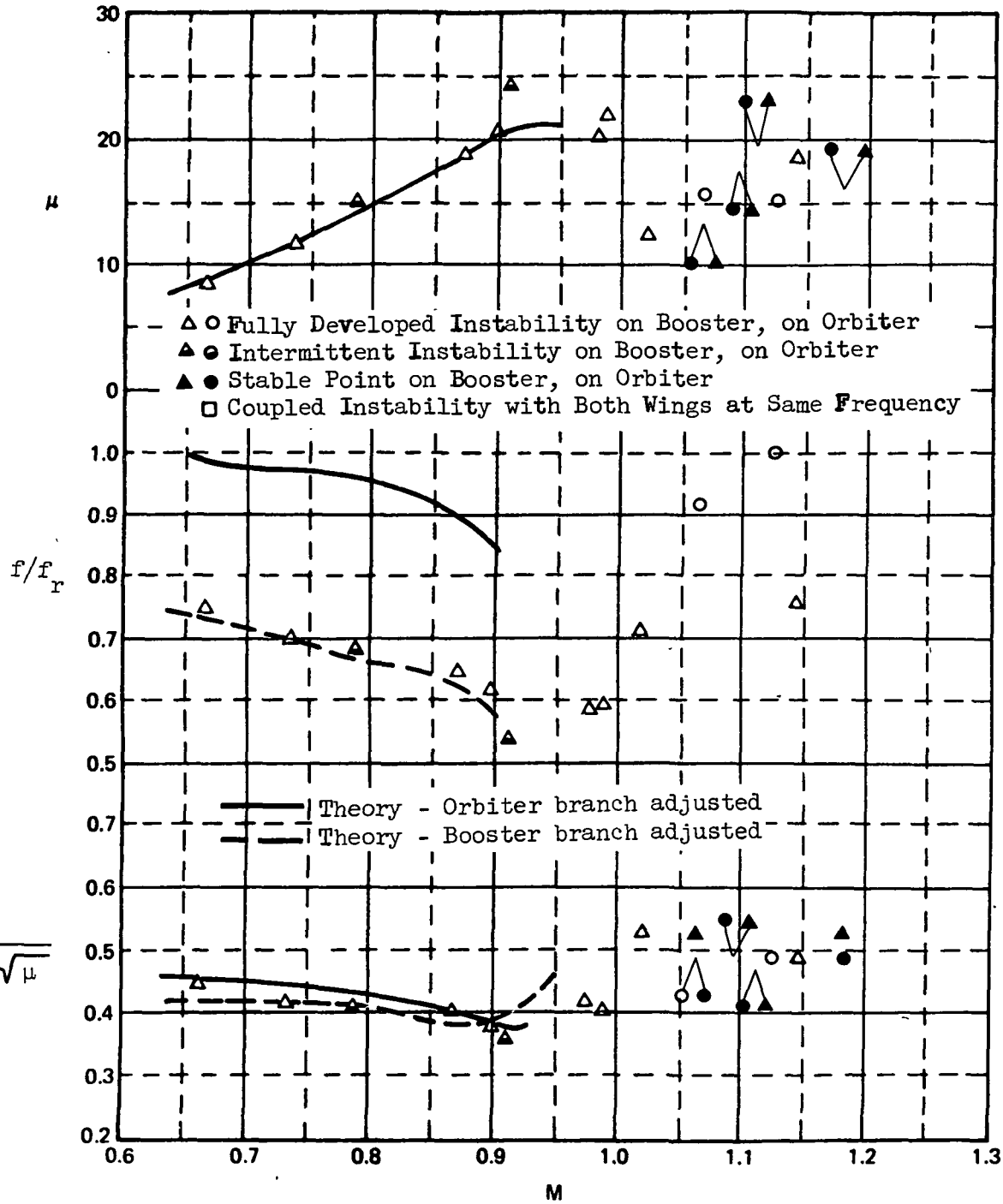

(ℓ) 070/040-100 ℓ/c = 0.73 h/c = 0.4

Fig. 9 Continued

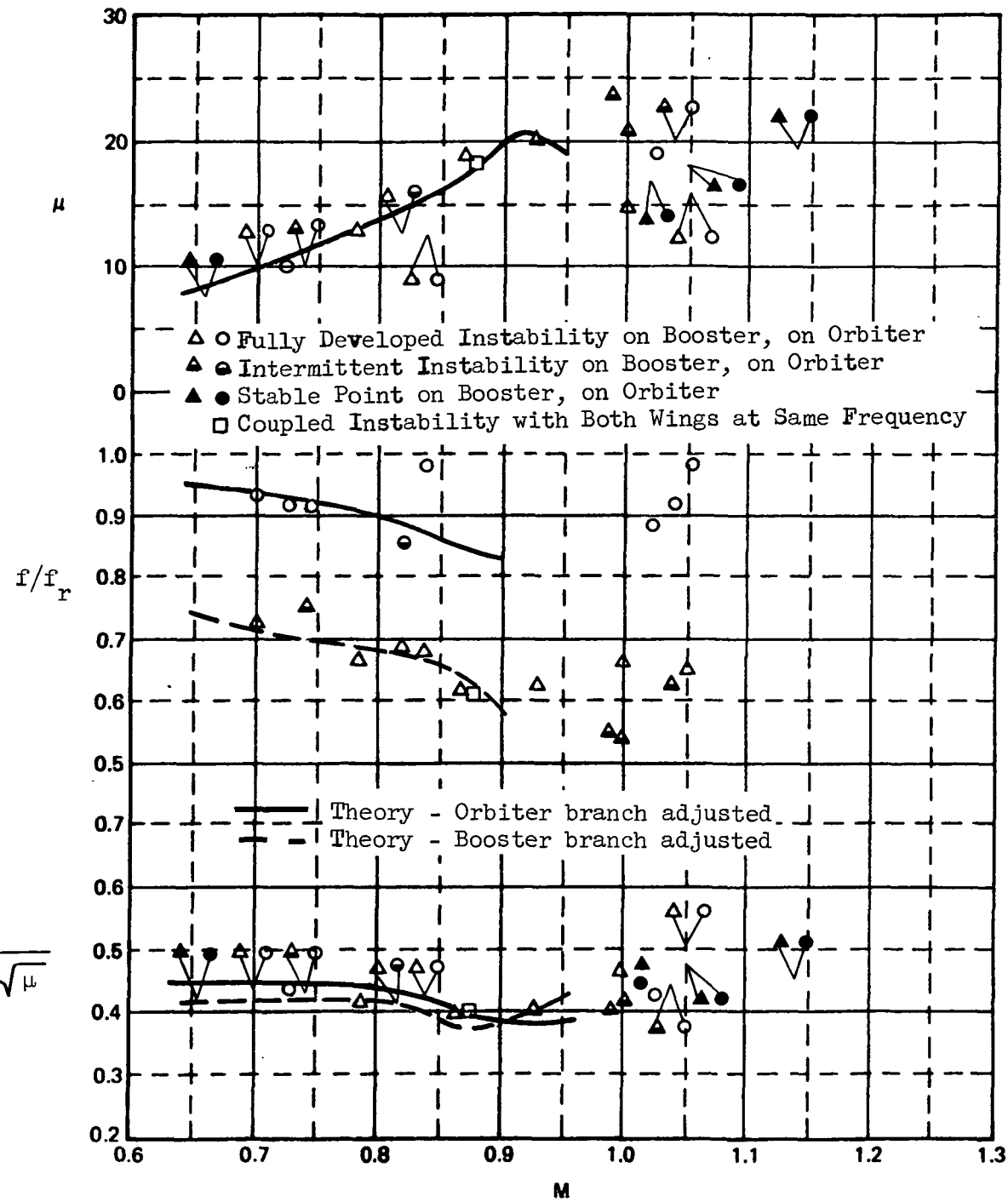

(m) 070/040-100 ℓ/c = 0.73 h/c = 0.6

Fig. 9 - Continued

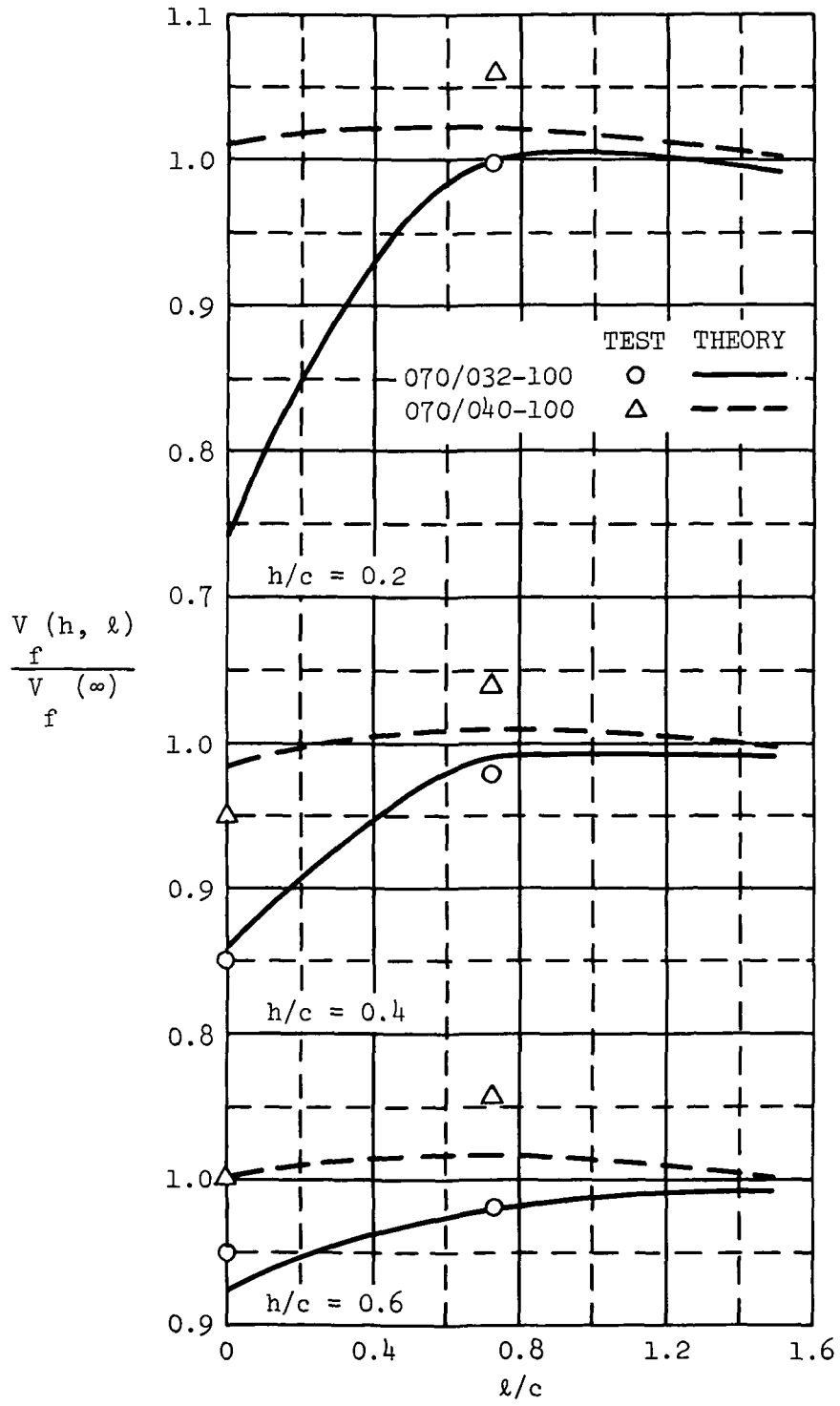

Figure 10. Minimum Subsonic Flutter Speed as a Function of Streamwise and Vertical Separations (for 070/032-100 and 070/040-100 Wing Pairings.) (Theoretical Curve Faired through Analytical Points at ℓ/c = 0.0, 0.73, 1.45.)

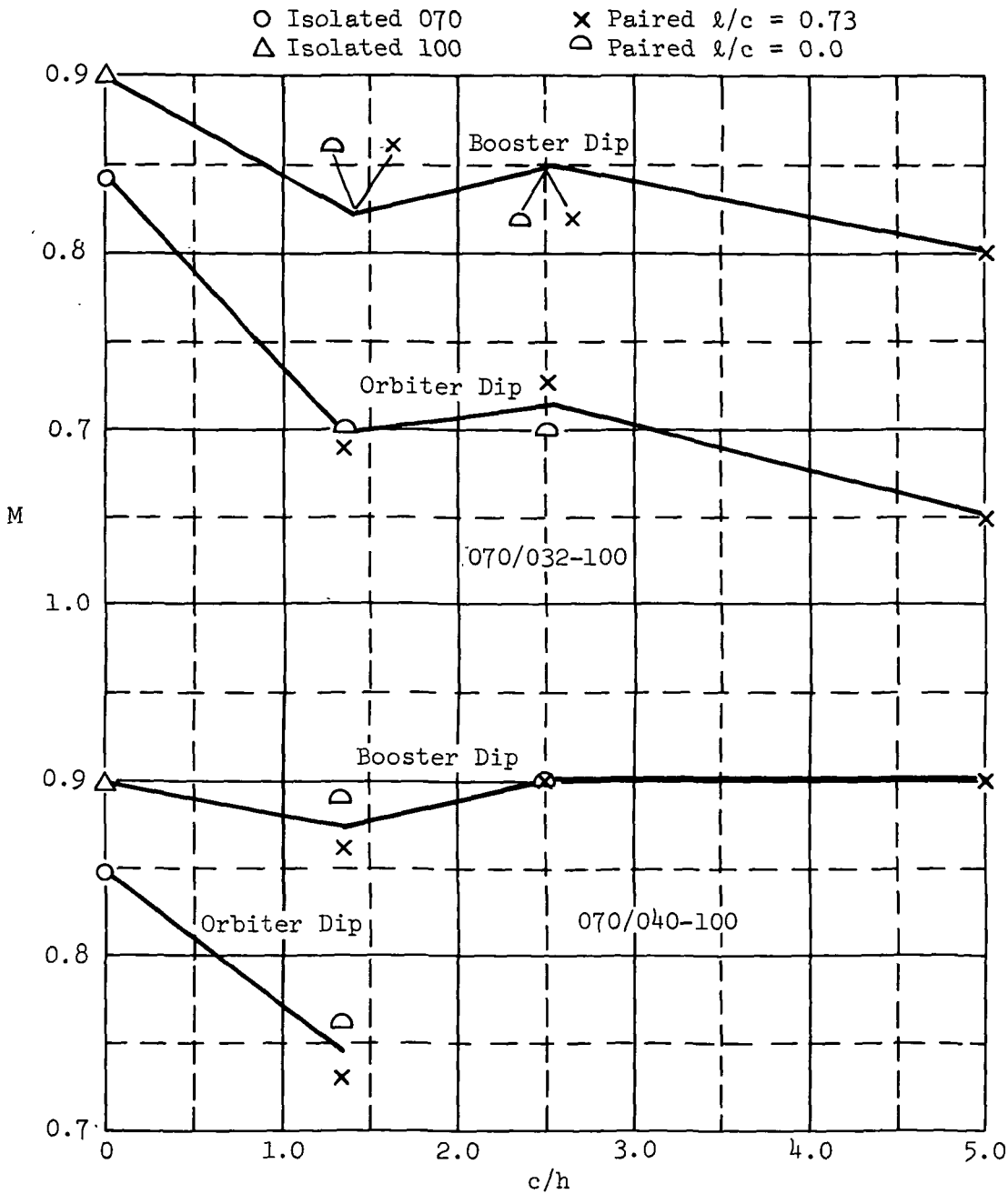

Figure 11. Experimental Variation of the Mach Number of the Minimum V_f with Vertical Separation (for 070/032-100 and 070/040-100).

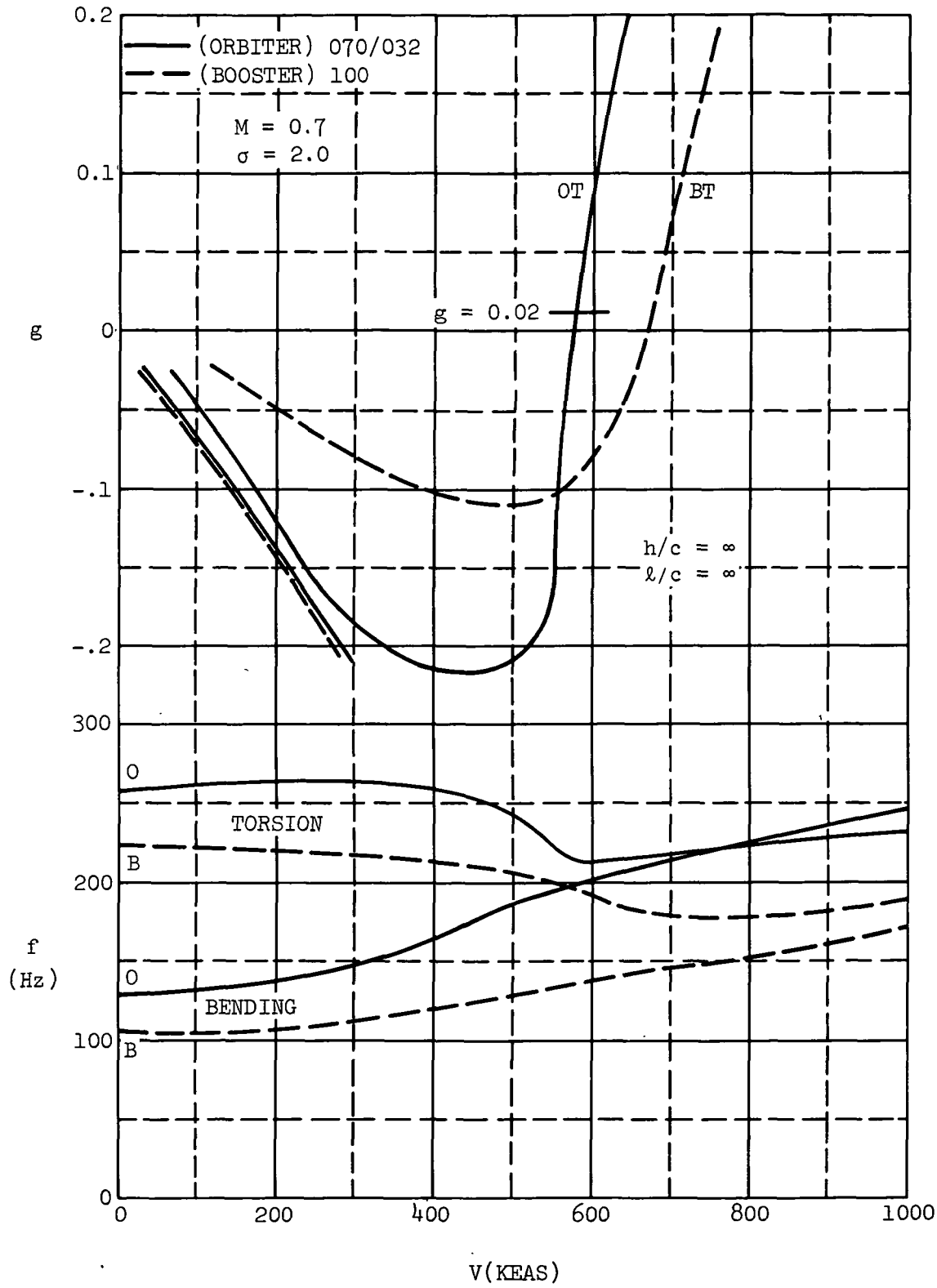

Figure 12. Damping and Frequency as a Function of Airspeed for 070/032 and 100 Wings without Aerodynamic Interference.

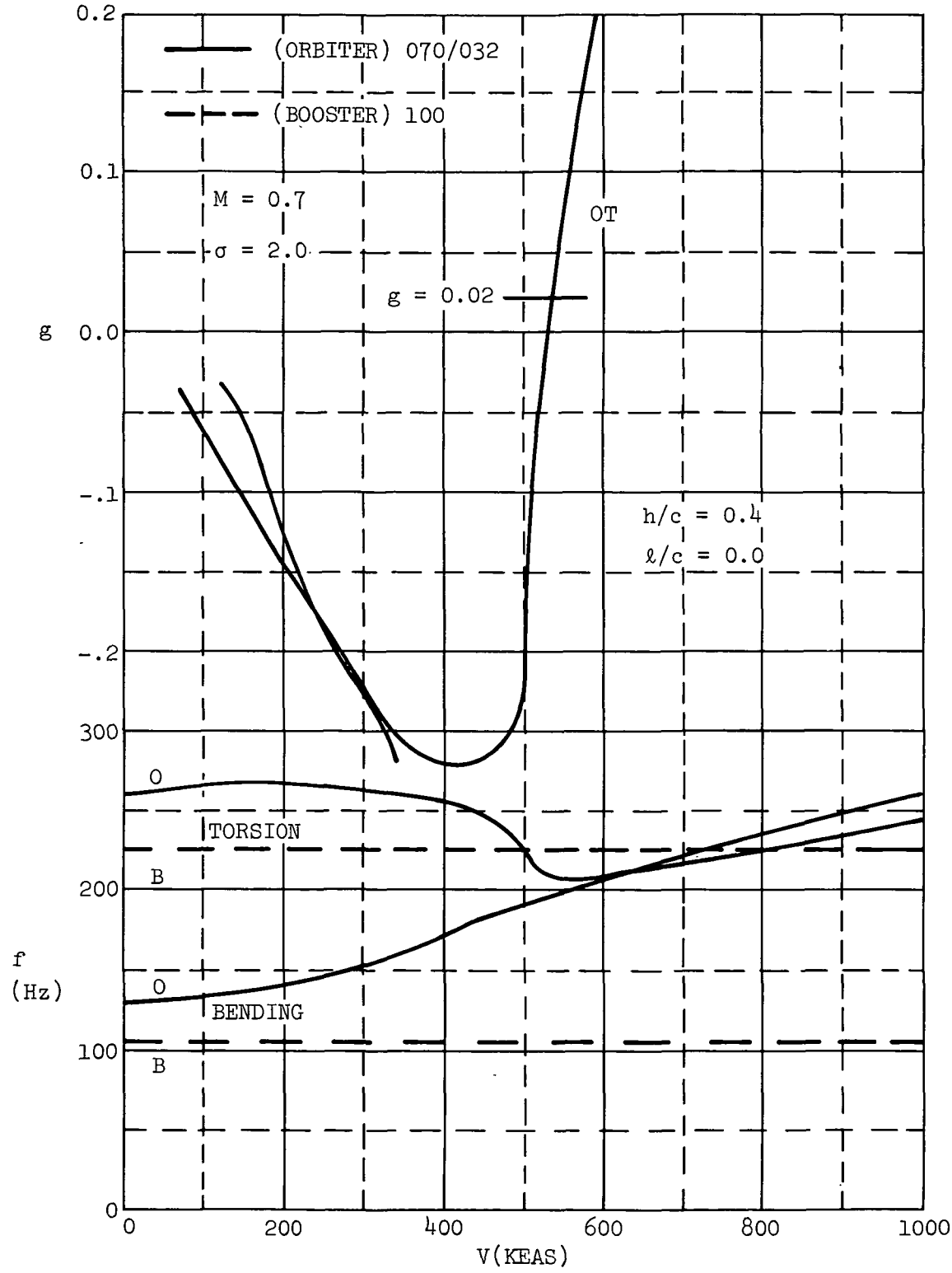

Figure 13. Damping and Frequency as a Function of Airspeed for 070/032 and a Rigid 100 Wing with Aerodynamic Interference due to Simple Reflection.

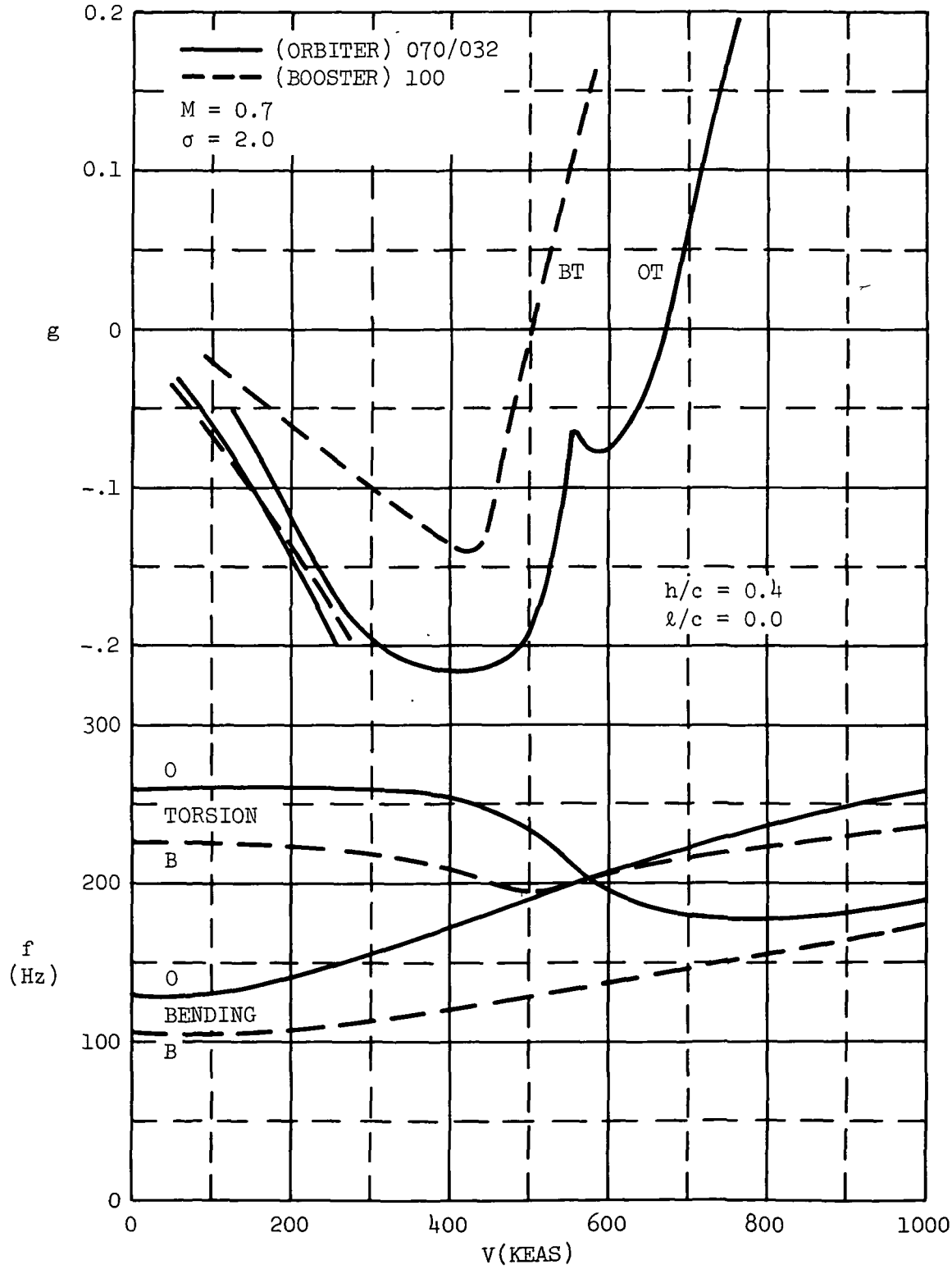

Figure 14. Damping and Frequency as a Function of Airspeed for 070/032 and 100 Wings with Aerodynamic Coupling.

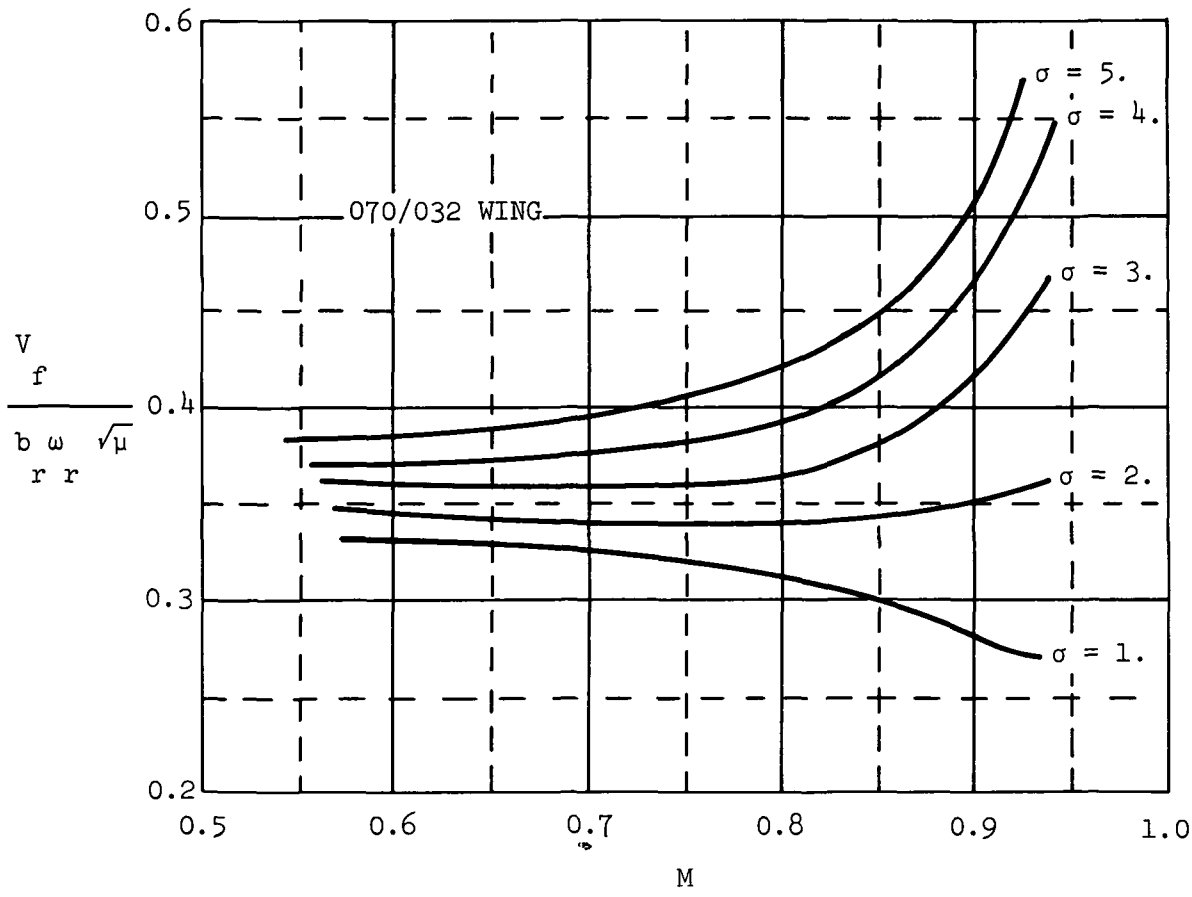

(a) Isolated 070/032 Orbiter

Figure 15. Flutter Speed Index as a Function of Mach Number and Air Density Ratio

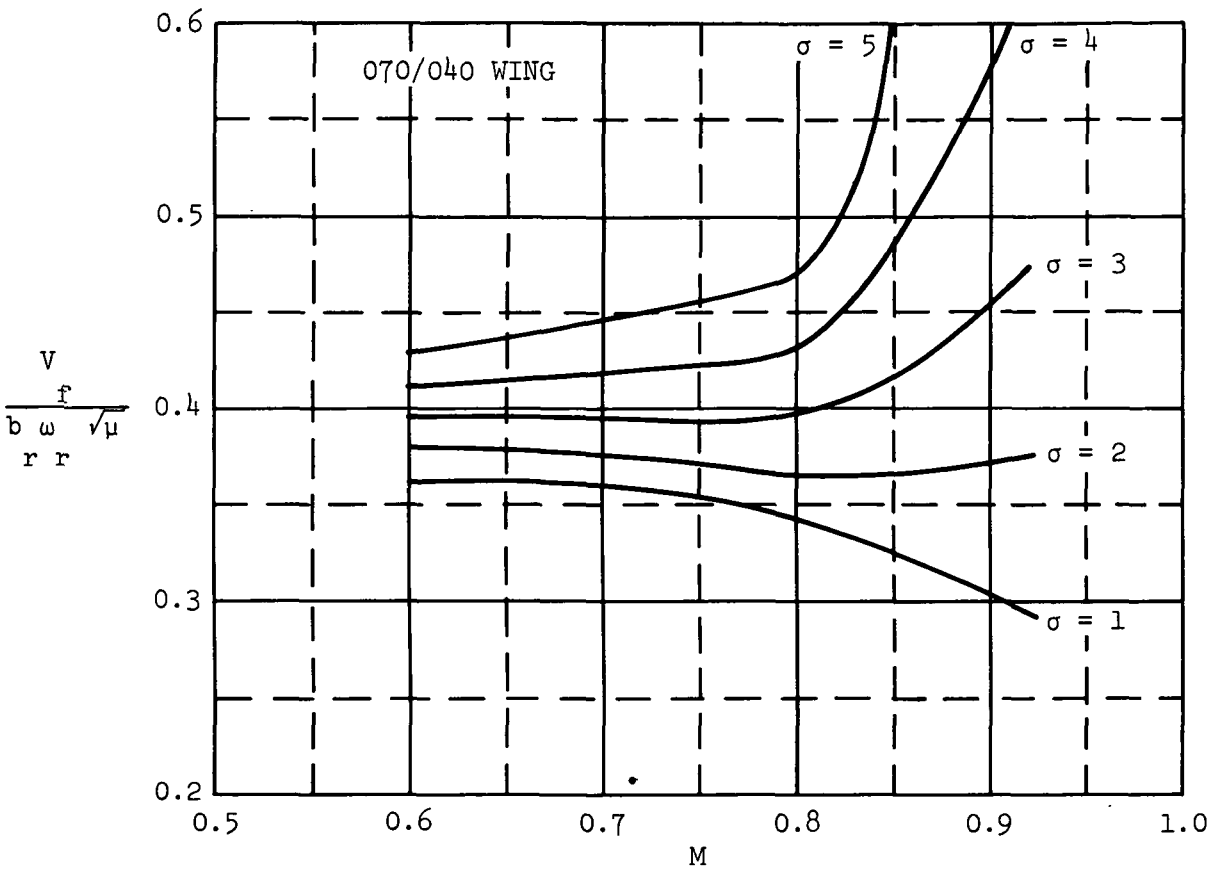

(b) Isolated 070/040 Orbiter

Fig. 15 - Continued

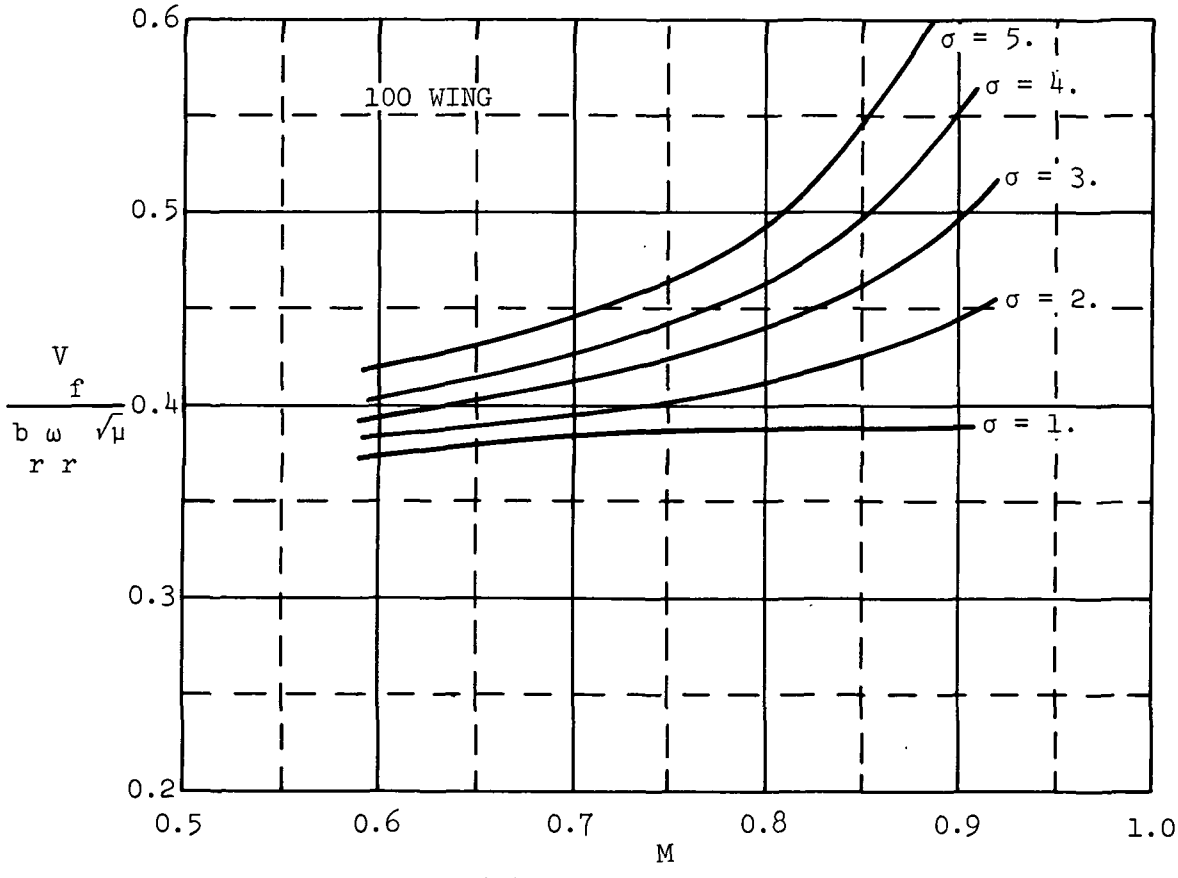

(c) Isolated 100 Booster

Fig. 15 - Concluded

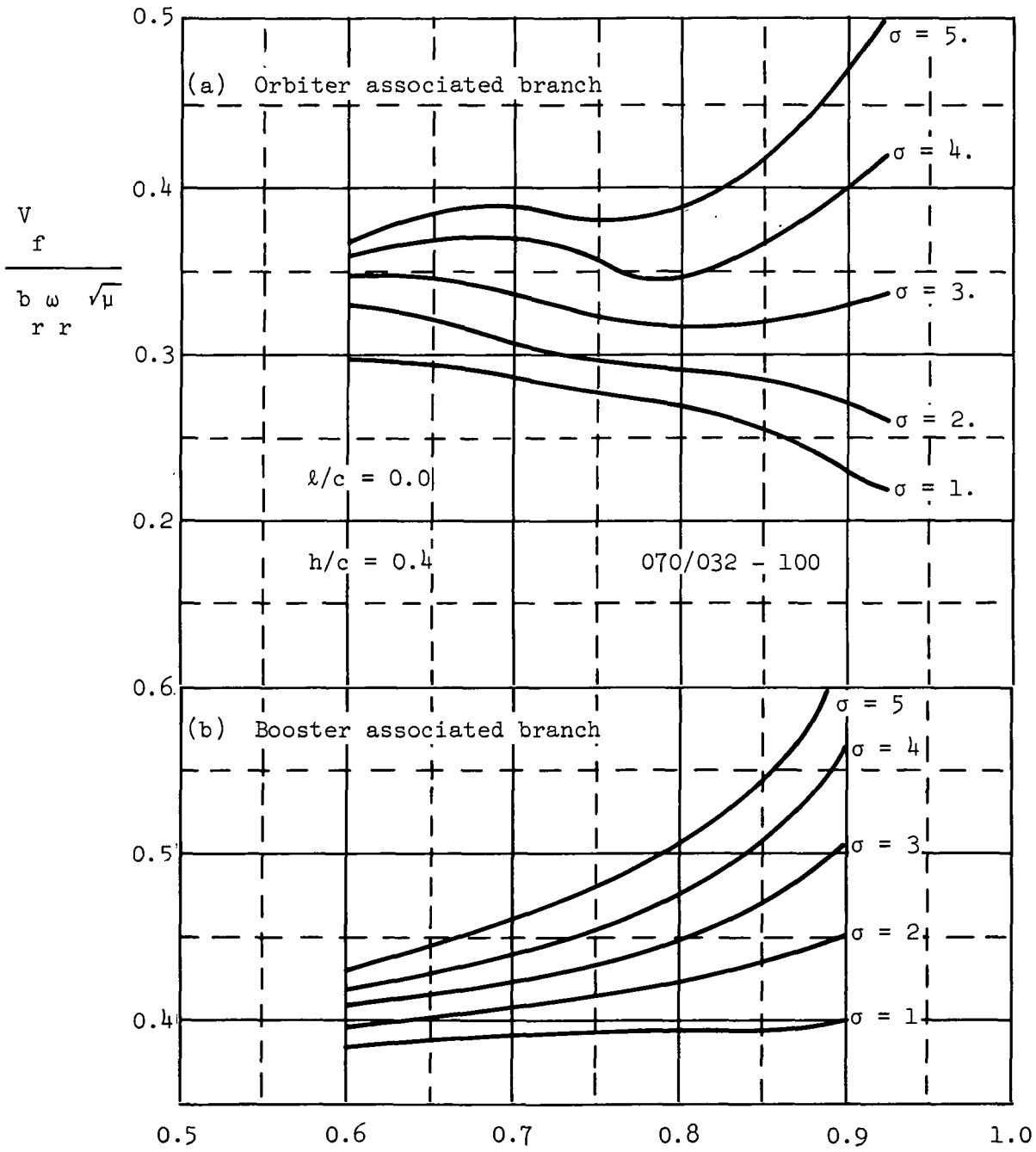

Figure 16. Flutter Speed Index as a Function of Mach Number and Air Density Ratio for the Paired 070/032 and 100 Wings.

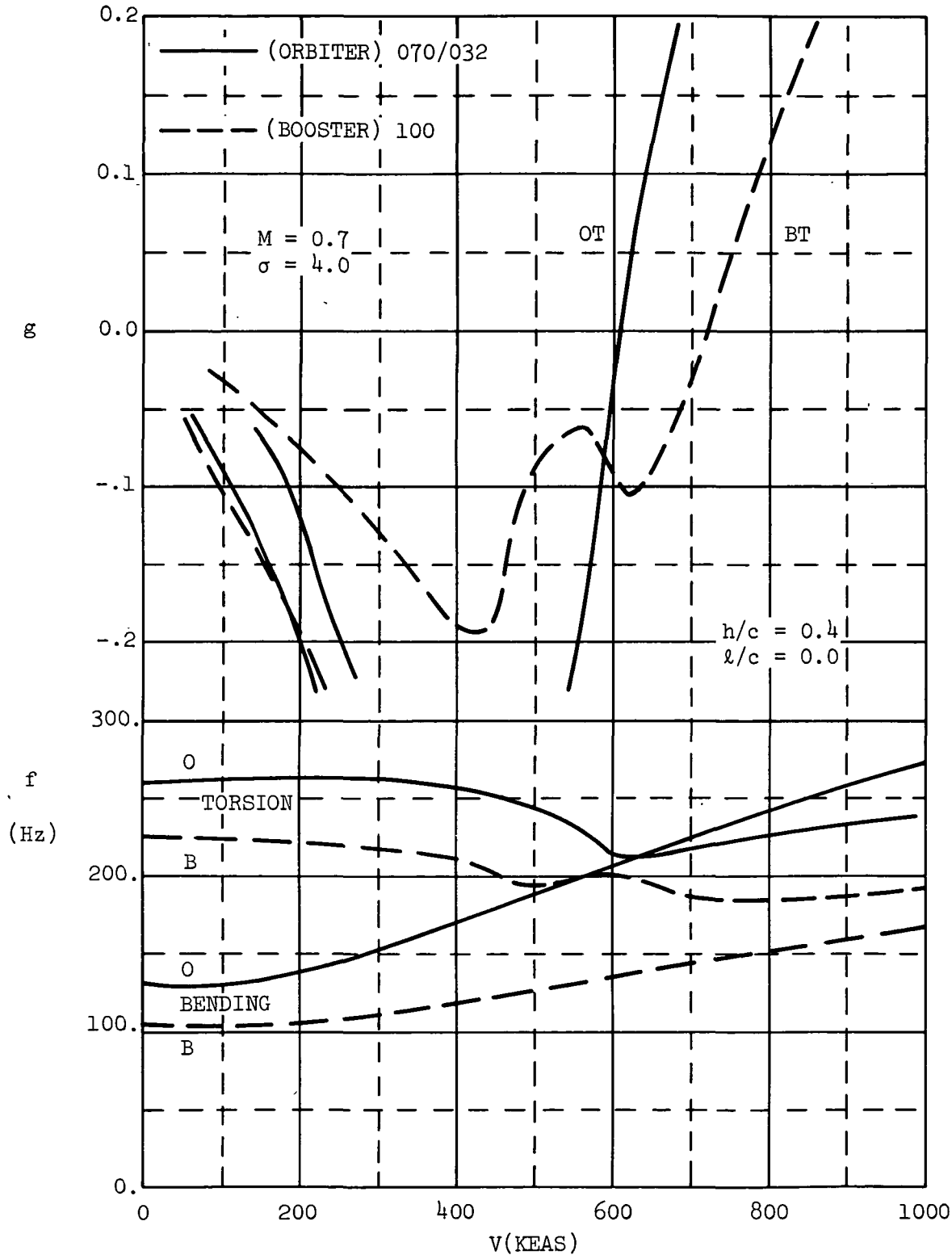

Figure 17. Damping and Frequency as a Function of Airspeed for 070/032 and 100 Wings with Aerodynamic Coupling.

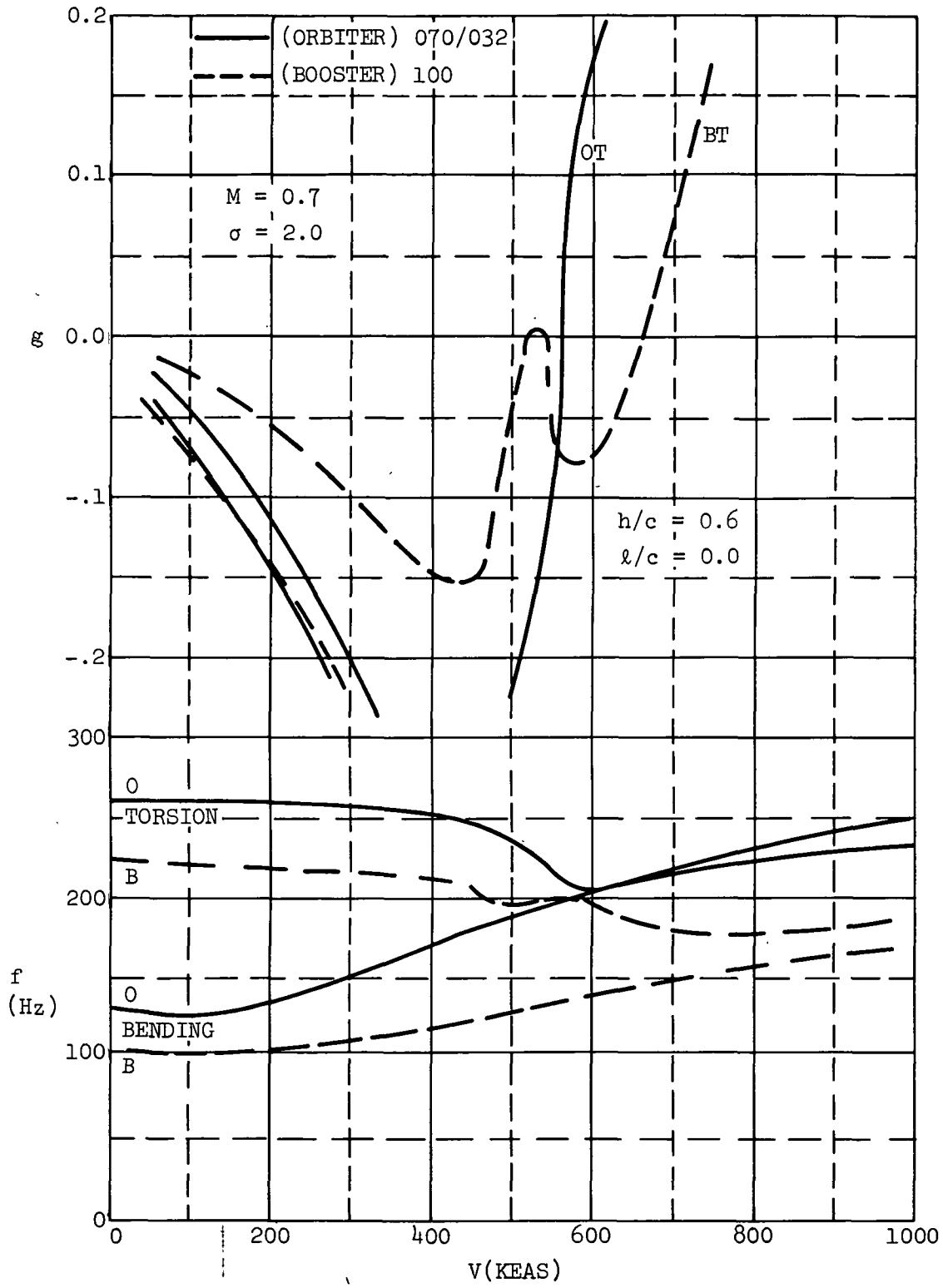

Figure 18. Damping and Frequency as a Function of Airspeed for 070/032 and 100 Wings with Aerodynamic Coupling.

NATIONAL AERONAUTICS AND SPACE ADMINISTRATION
WASHINGTON, D.C. 20546

OFFICIAL BUSINESS
PENALTY FOR PRIVATE USE $300

SPECIAL FOURTH-CLASS RATE BOOK

POSTAGE AND FEES PAID
NATIONAL AERONAUTICS AND SPACE ADMINISTRATION
451

U.S.MAIL

POSTMASTER: If Undeliverable (Section 158 Postal Manual) Do Not Return

"The aeronautical and space activities of the United States shall be conducted so as to contribute . . . to the expansion of human knowledge of phenomena in the atmosphere and space. The Administration shall provide for the widest practicable and appropriate dissemination of information concerning its activities and the results thereof."

—NATIONAL AERONAUTICS AND SPACE ACT OF 1958

NASA SCIENTIFIC AND TECHNICAL PUBLICATIONS

TECHNICAL REPORTS: Scientific and technical information considered important, complete, and a lasting contribution to existing knowledge.

TECHNICAL NOTES: Information less broad in scope but nevertheless of importance as a contribution to existing knowledge.

TECHNICAL MEMORANDUMS: Information receiving limited distribution because of preliminary data, security classification, or other reasons. Also includes conference proceedings with either limited or unlimited distribution.

CONTRACTOR REPORTS: Scientific and technical information generated under a NASA contract or grant and considered an important contribution to existing knowledge.

TECHNICAL TRANSLATIONS: Information published in a foreign language considered to merit NASA distribution in English.

SPECIAL PUBLICATIONS: Information derived from or of value to NASA activities. Publications include final reports of major projects, monographs, data compilations, handbooks, sourcebooks, and special bibliographies.

TECHNOLOGY UTILIZATION PUBLICATIONS: Information on technology used by NASA that may be of particular interest in commercial and other non-aerospace applications. Publications include Tech Briefs, Technology Utilization Reports and Technology Surveys.

Details on the availability of these publications may be obtained from:

SCIENTIFIC AND TECHNICAL INFORMATION OFFICE

NATIONAL AERONAUTICS AND SPACE ADMINISTRATION

Washington, D.C. 20546